3D modeling of internal tide generation

Cécile Le Dizes[1,2], Nicolas Grisouard[3], Olivier Thual[1] and Matthieu Mercier[1]

(3) UNIVERSITY OF TORONTO (2) Université de Toulouse (1) IMFT INSTITUT DE MECANIQUE DES FLUIDES DE TOULOUSE

Internal tides in the ocean

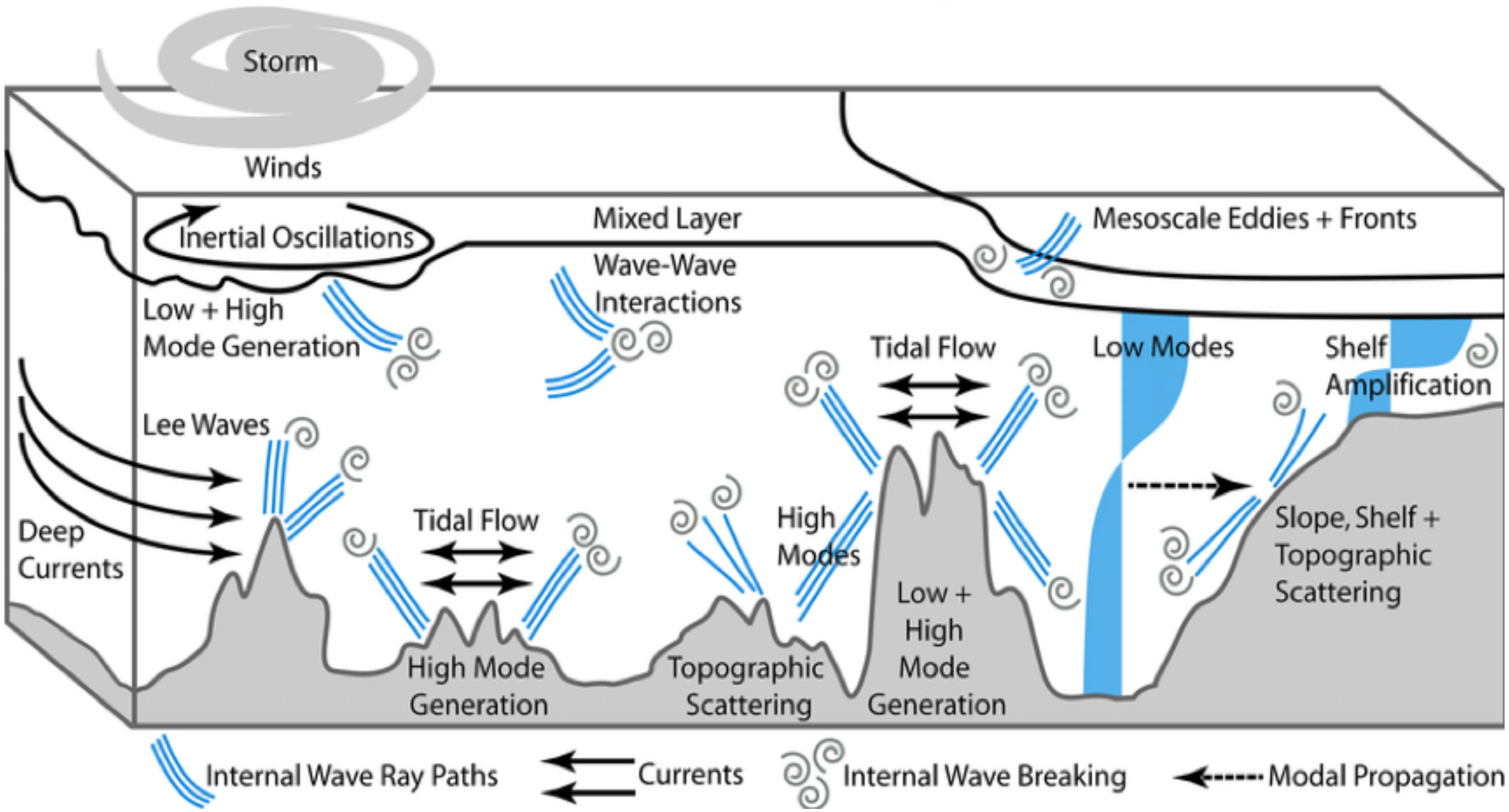

Generation and lifecycle of internal waves in the ocean (from *McKinnon et al* (2017))

Parameterizations

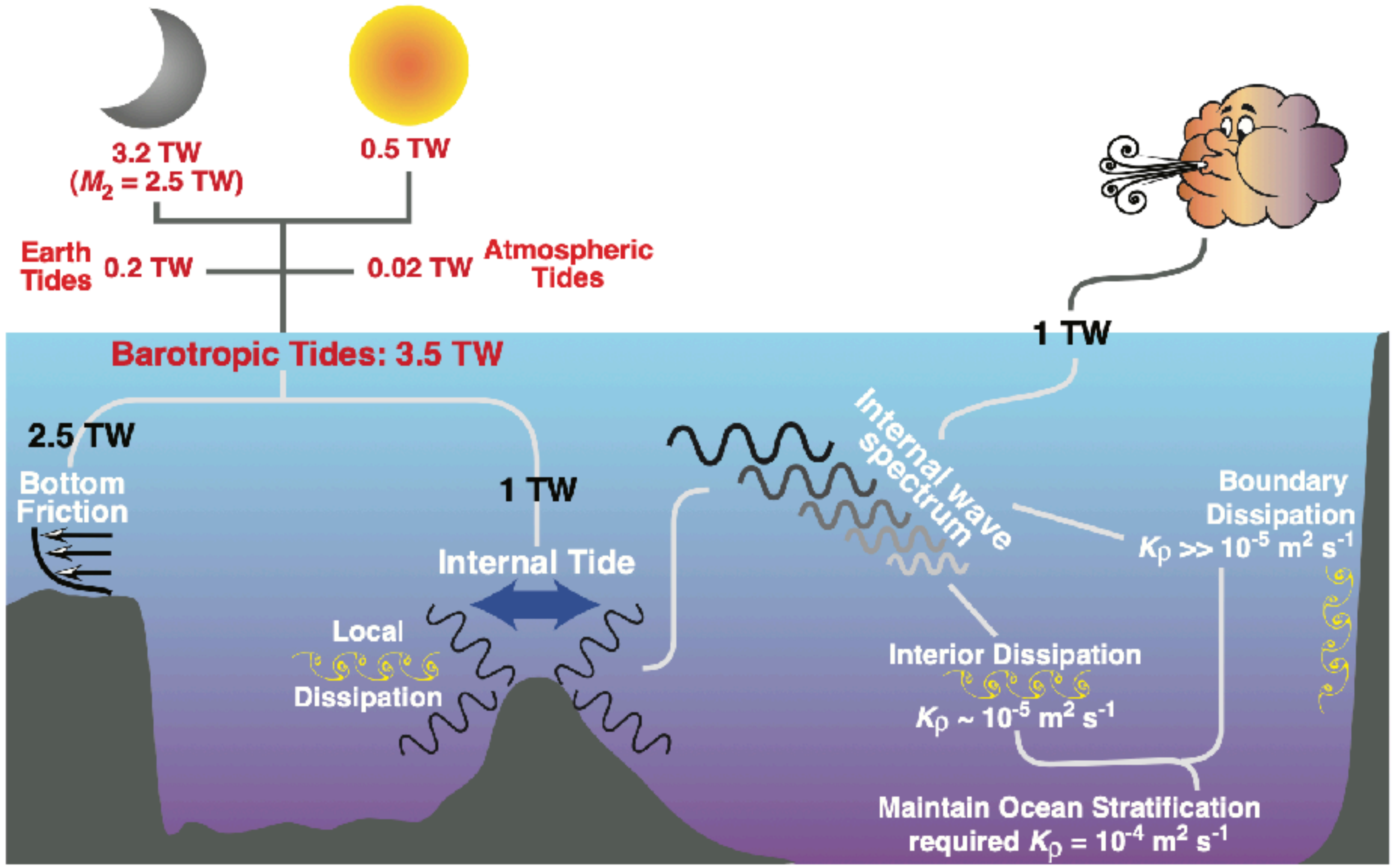

Energy budget and dissipation in the ocean (from *Carter* (2012))

- Mixing not explicitly resolved by global ocean model
- Parameterization of the diffusivity (from *St Laurent et al* (2002))

$$\kappa = \kappa_b + \frac{q\Gamma C(x,y)F(z)}{\rho N^2}$$

Parameterizations

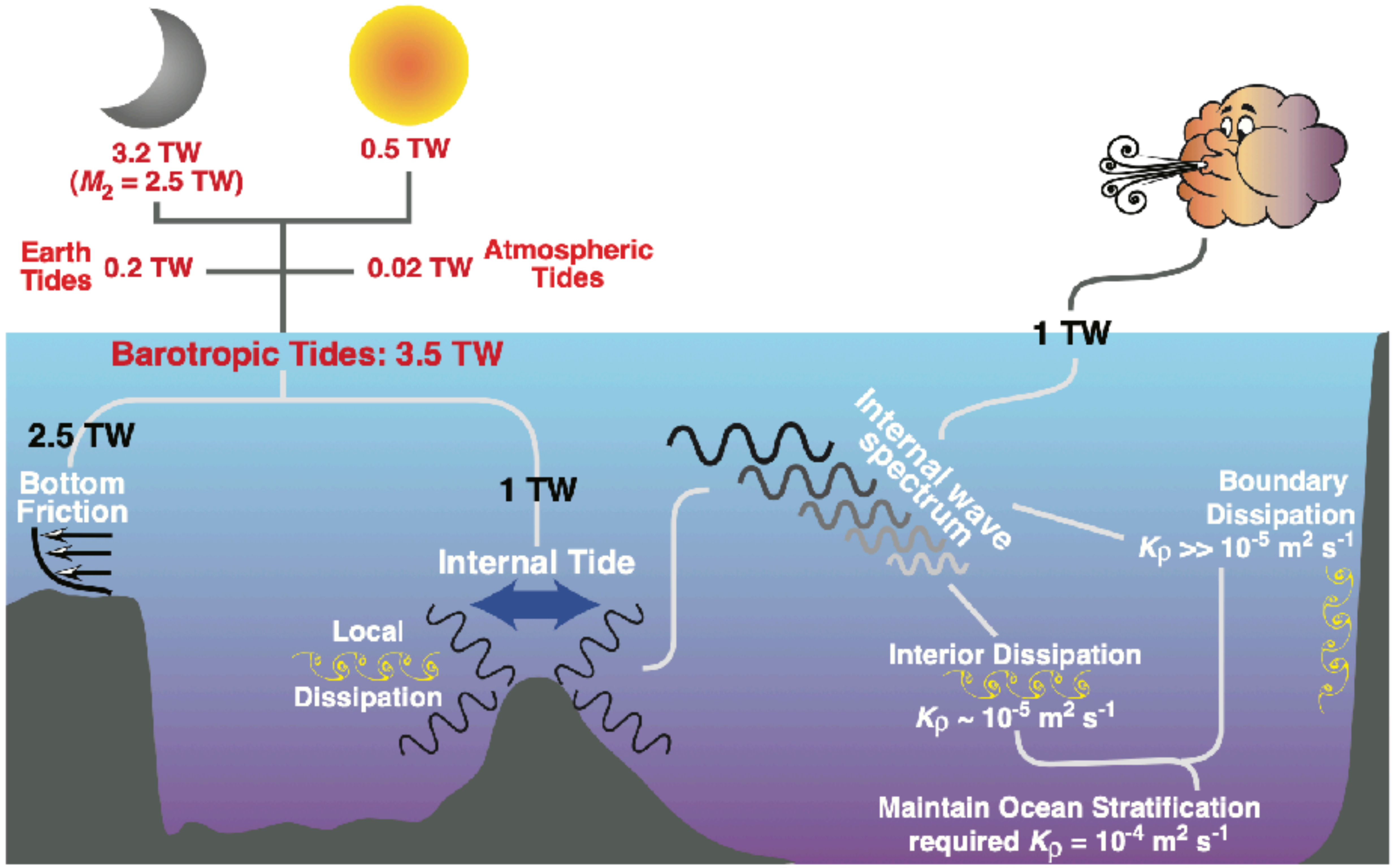

Energy budget and dissipation in the ocean (from *Carter* (2012))

- Mixing not explicitly resolved by global ocean model
- Parameterization of the diffusivity (from *St Laurent et al* (2002))

$$\kappa = \kappa_b + \frac{q\Gamma \boxed{C(x,y)} F(z)}{\rho N^2}$$

Conversion rate = energy converted from the barotropic tide to the internal waves

Traditional approximations

The Weak Topography Assumption

Steep seamounts

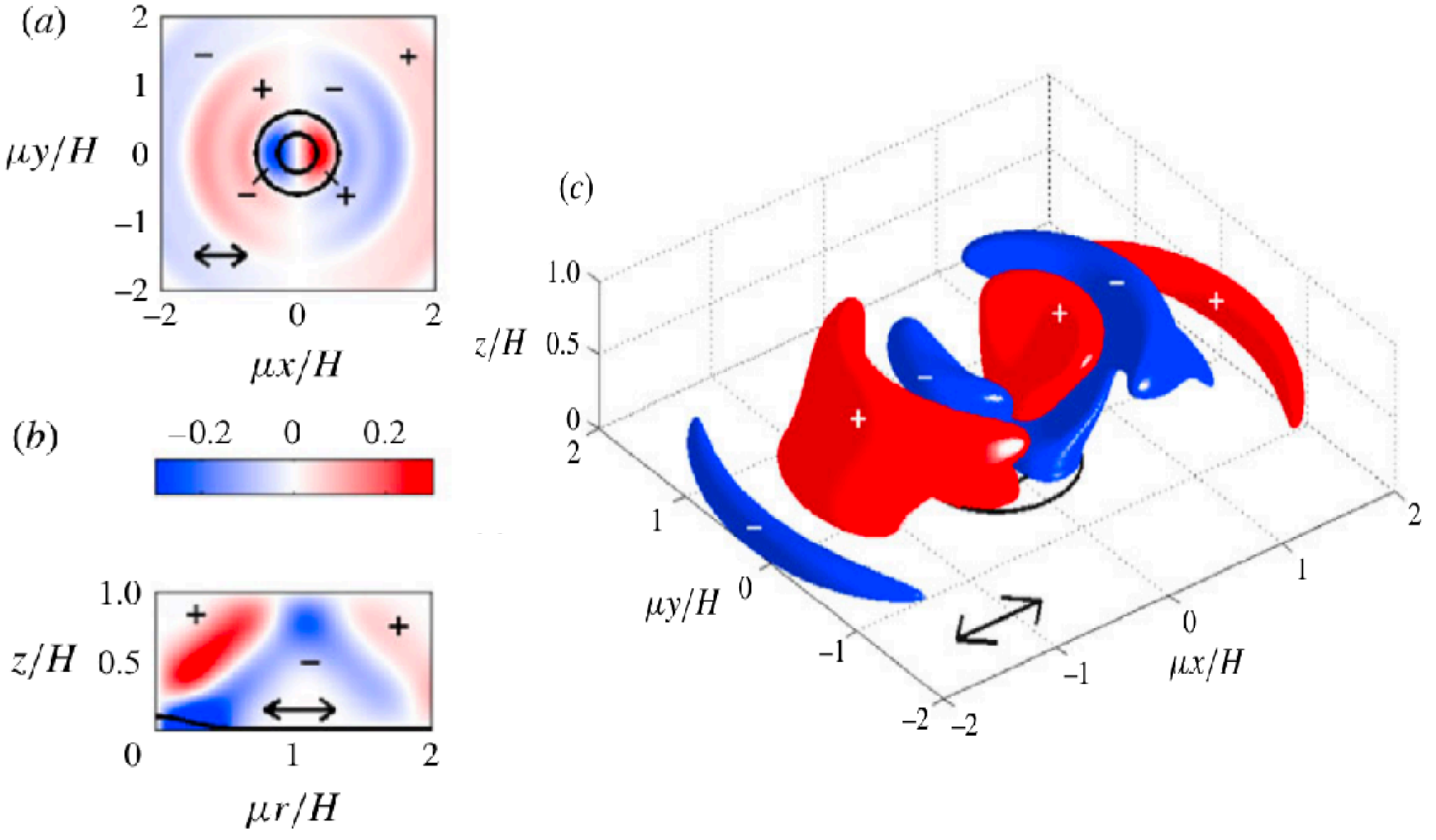

Vertical velocity (from *Grisouard and Bülher* (2012))

Bell (1975), *Llewellyn Smith and Young* (2002)

- Small and 'flat' topographies
- Linearization of the bottom boundary condition

$$w = (\mathbf{U}_0 + \cancel{\mathbf{u}_H}) \,.\, \nabla_H h$$

- Over-estimation of the conversion rate for large seamounts (*Papoutsellis et al* (2024))

Traditional approximations

The Weak Topography Assumption | Steep seamounts

- The 'pill-box' model (*Baines* (2007)) : Infinite slope limit

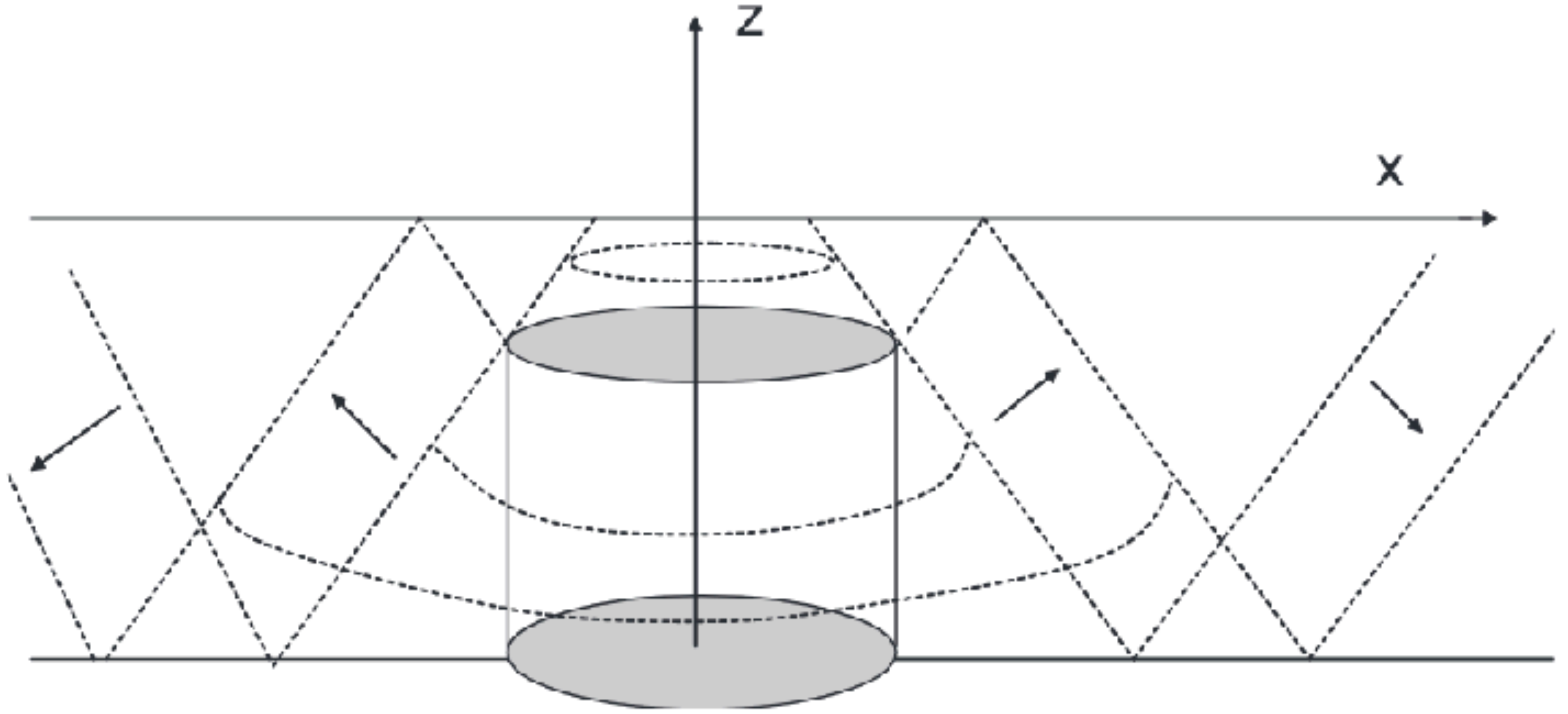

- The spheroid (*Voisin* (2024)) in a non-rotating semi-infinite ocean

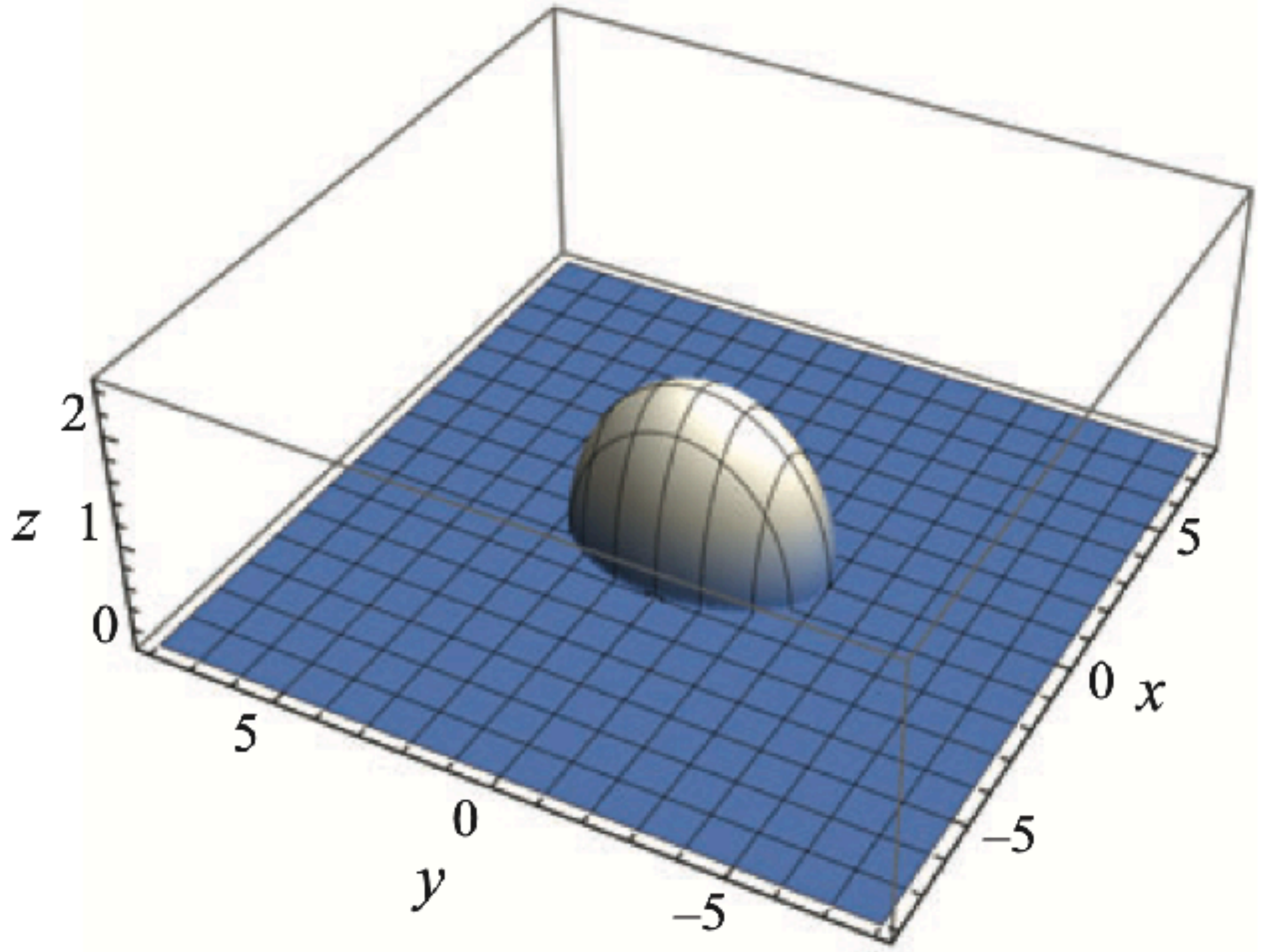

Direction of propagation

- Far-field diffusion : *Eden and Olbers* (2014)

Direction of propagation

- Far-field diffusion : *Eden and Olbers* (2014)
- Influence of the topographic shape and the tidal ellipse

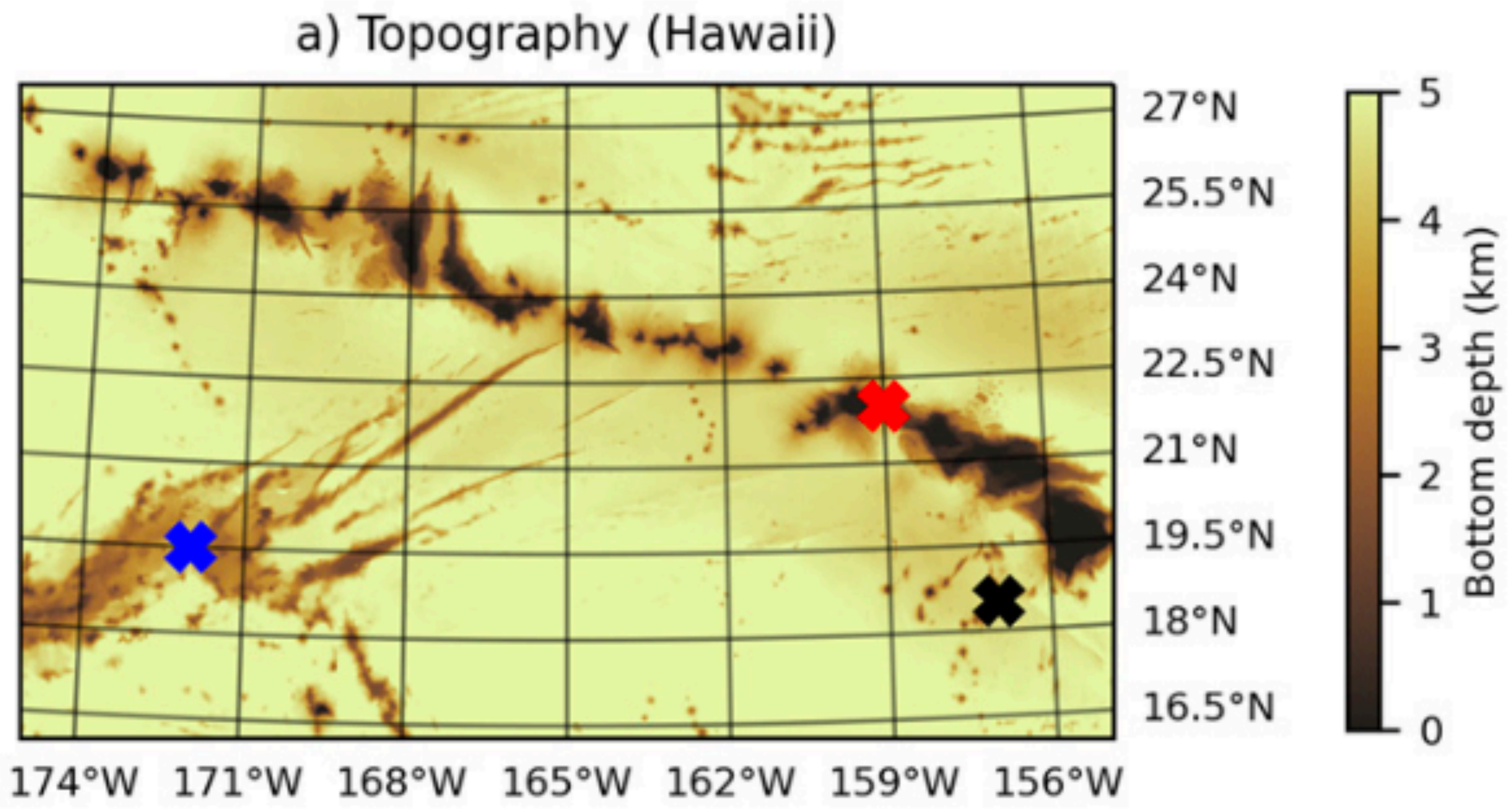

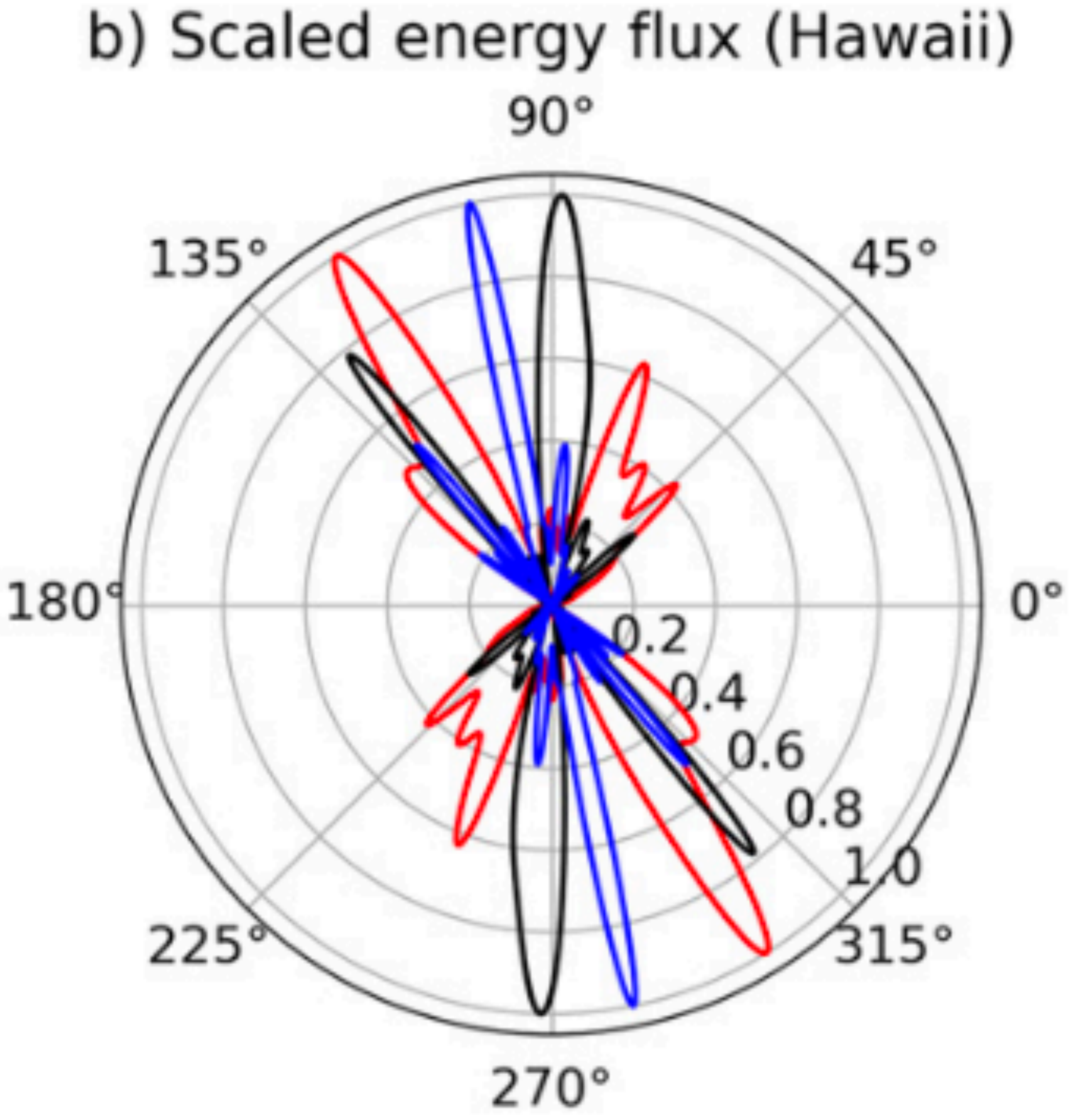

WTA model from ***Pollmann and Nycander*** (2023)

Direction of propagation

- Far-field diffusion : *Eden and Olbers* (2014)
- Influence of the topographic shape and the tidal ellipse
- Influence of the Coriolis frequency

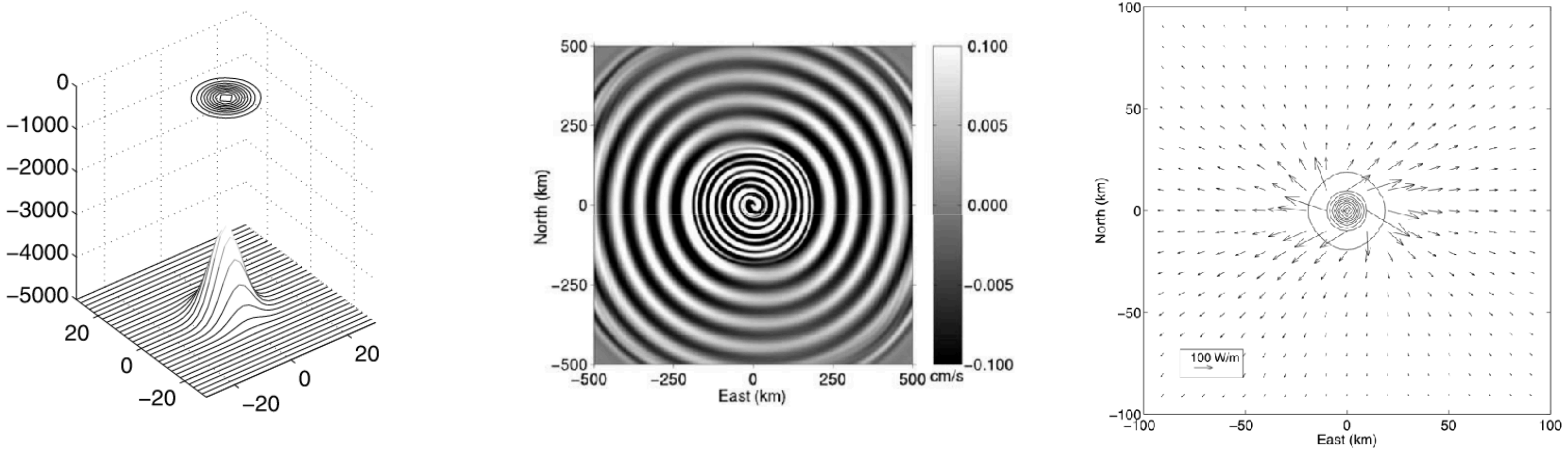

POM simulation from ***Munroe and Lamb*** (2005)

Motivation

WTA	Steep seamounts
- Limited to small and 'flat' seamount (over-estimation of the conversion rate) - No effect of the rotation on the direction	Limited to analytical topographies and specific configurations

Motivation

WTA		Steep seamounts
- Limited to small and 'flat' seamount (over-estimation of the conversion rate) - No effect of the rotation on the direction	⟷ ?	Limited to analytical topographies and specific configurations

Motivation

WTA		Steep seamounts
- Limited to small and 'flat' seamount (over-estimation of the conversion rate) - No effect of the rotation on the direction	↔ ?	Limited to analytical topographies and specific configurations

- 3D boundary element method for arbitrary topographies
- Estimates of the conversion rate and comparison with the WTA
- Influence of the Coriolis frequency on the direction of propagation

Problem definition

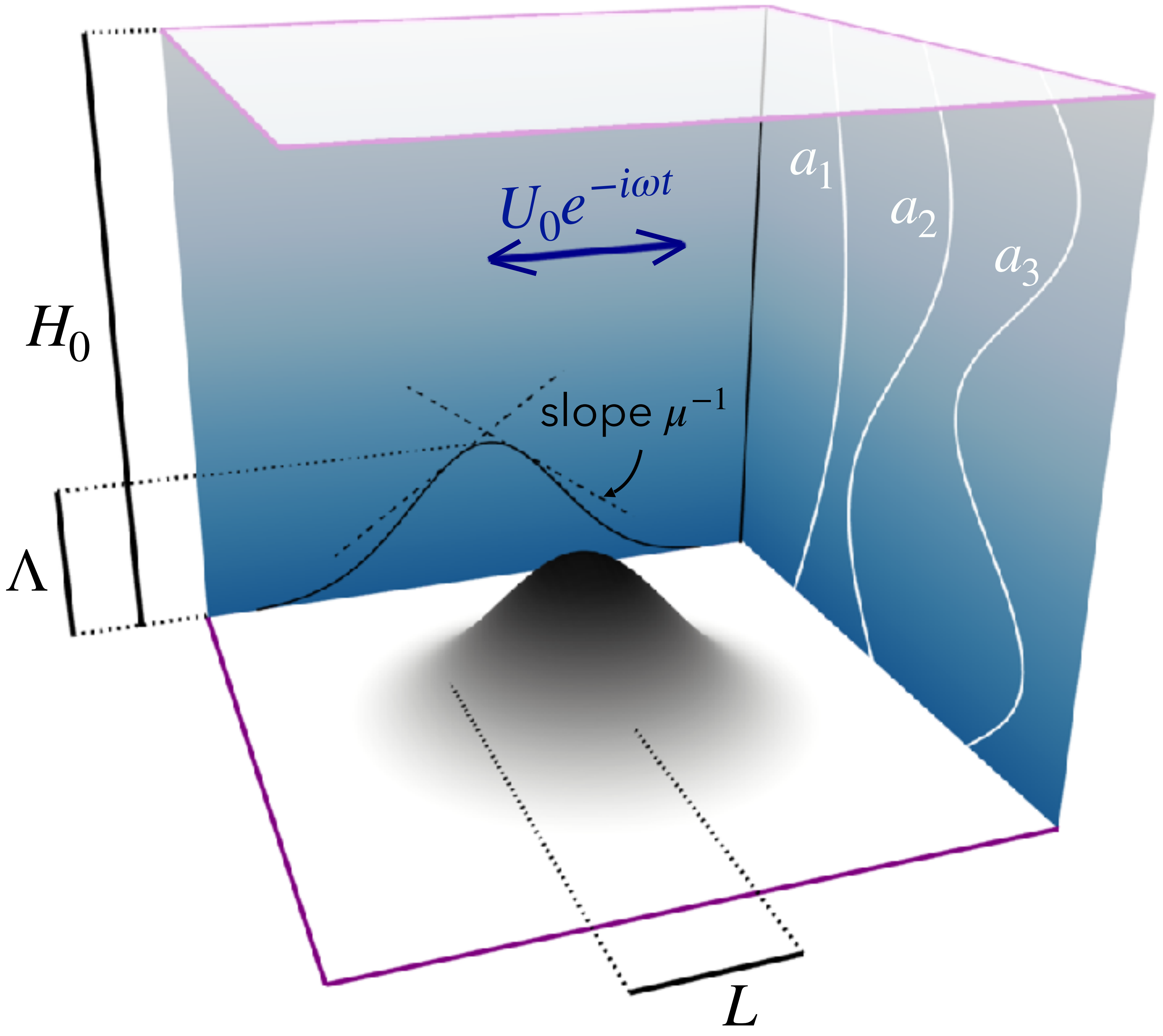

- Isolated topography of length L and height Λ
- Ocean of depth H_0 with uniform background stratification N
- Uniform barotropic tide $\mathbf{U}_0 = U_0 e^{-i\omega t} \mathbf{e_x}$
- Top-lid : $\boxed{w(z=0)=0}$
- Full bottom BC : $\boxed{w = (\mathbf{U}_0 + \mathbf{u}_H) \,.\, \nabla_H h}$

Problem definition

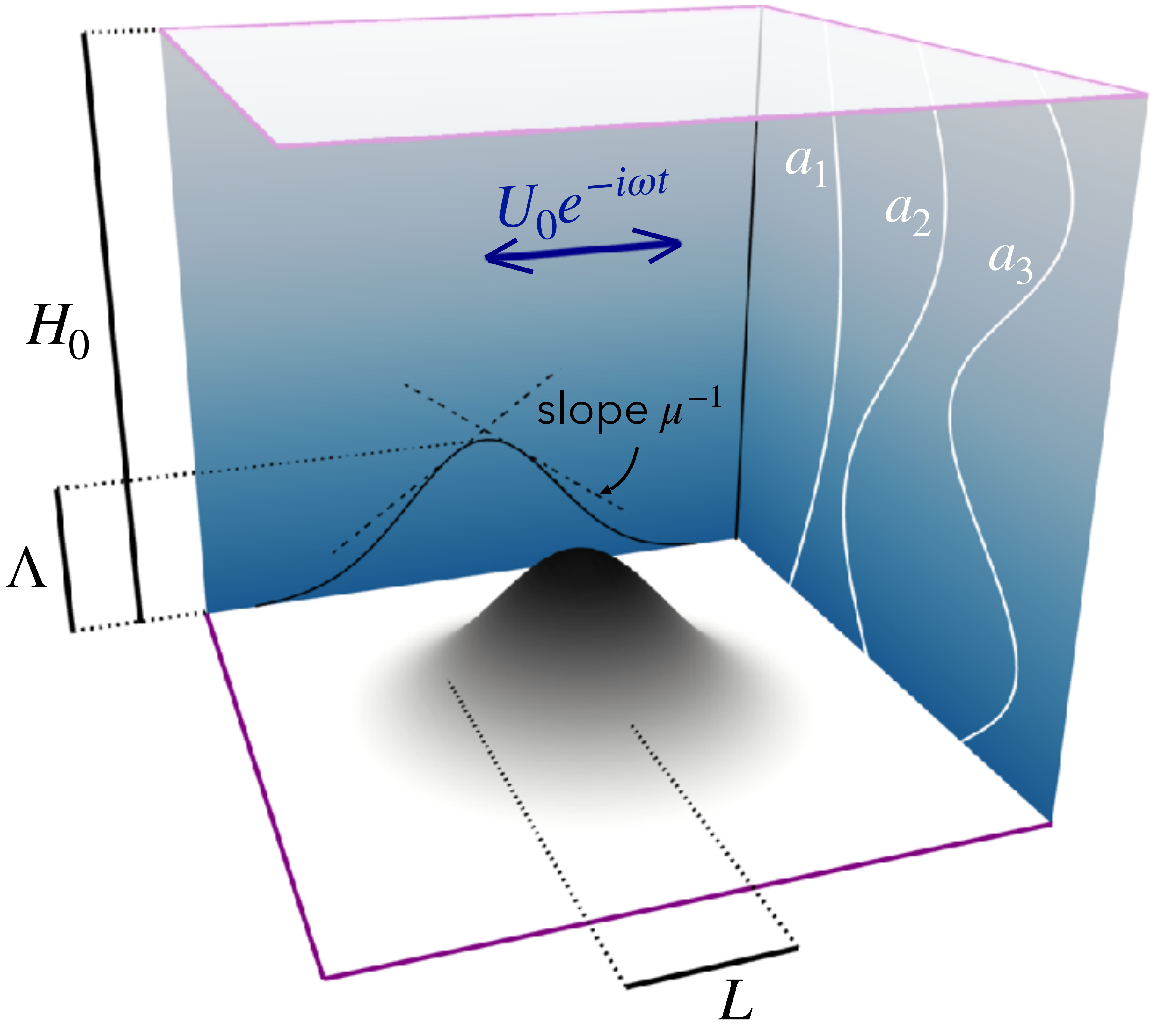

- Linear Boussinesq inviscid equations

$$u_{,t} - fv = -p_{,x}$$

$$v_{,t} + fu = -p_{,y}$$

$$w_{,t} - b = -p_{,z}$$

$$b_{,t} + N^2 w = 0$$

$$u_{,x} + v_{,y} + w_{,z} = 0$$

Problem definition

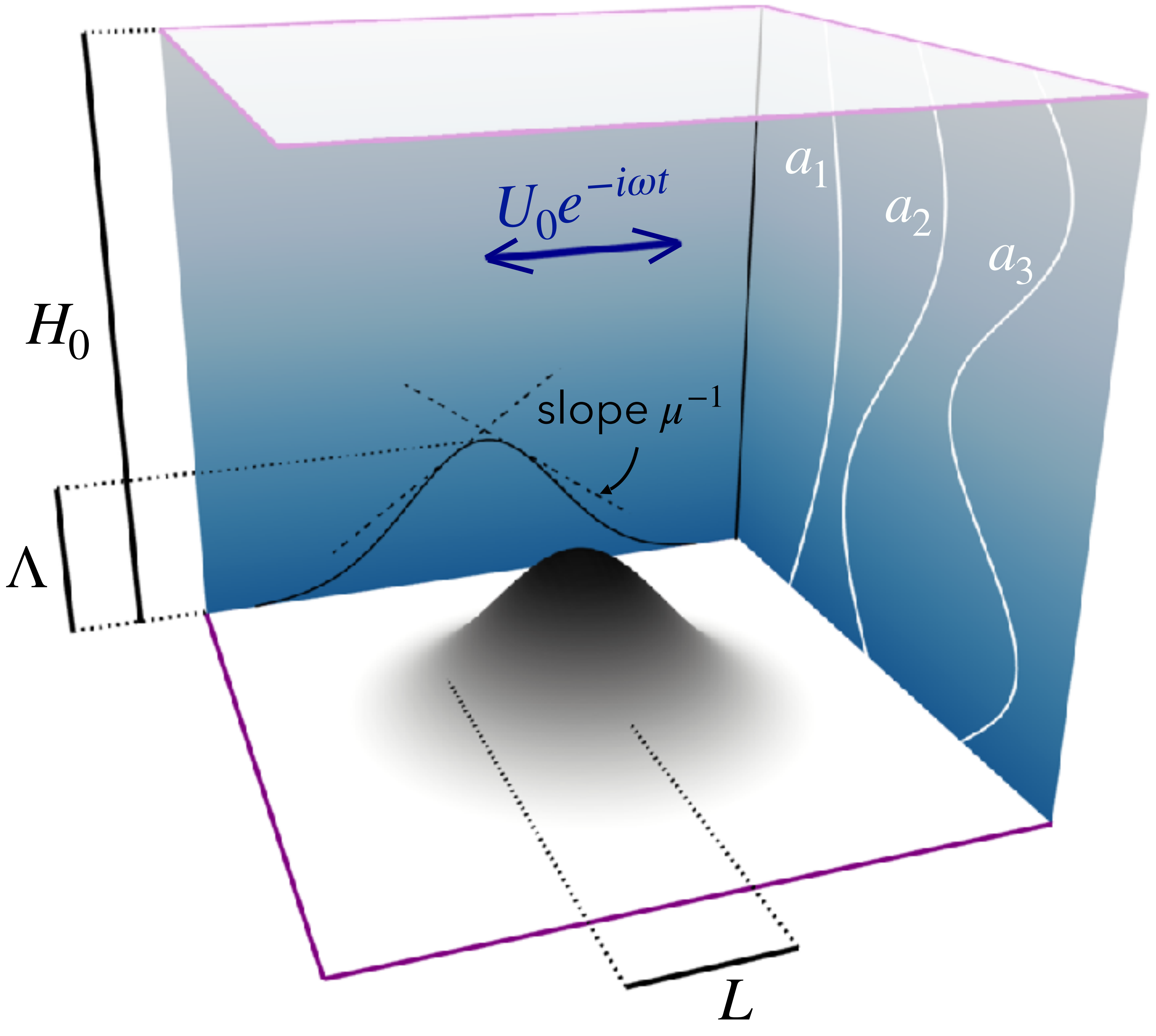

- Linear Boussinesq inviscid equations

$$-i\omega u - fv = -p_{,x}$$

$$-i\omega v + fu = -p_{,y}$$

$$-i\omega w - b = -p_{,z}$$

$$-i\omega b + N^2 w = 0$$

$$u_{,x} + v_{,y} + w_{,z} = 0$$

$$\Rightarrow \left(\frac{N^2-\omega^2}{\omega^2-f^2}\right)\nabla_H^2 w - w_{,zz} = 0$$

Dimensionless parameters

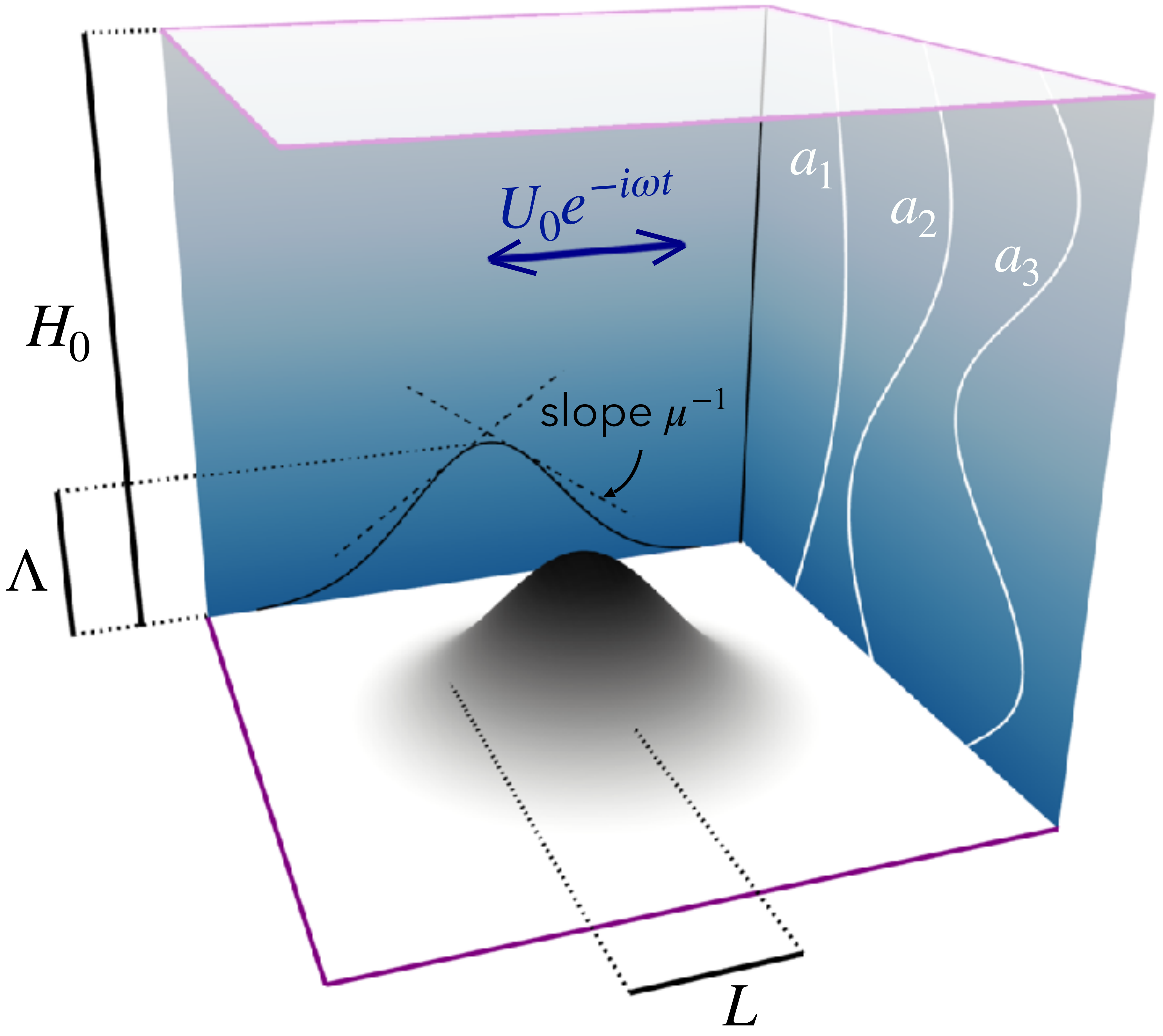

- Slope of the wave beams : $\mu^{-1} = \sqrt{\dfrac{\omega^2 - f^2}{N^2 - \omega^2}}$
- Frequency ratios : $\beta = f/\omega$ and N/ω
- Excursion parameter : $\alpha = \dfrac{U_0 L}{\omega} \ll 1$
- Height ratio : $\delta = \dfrac{\Lambda}{H_0}$
- Criticality parameter : $\epsilon = \mu max(\partial_x h)$

Dimensionless parameters

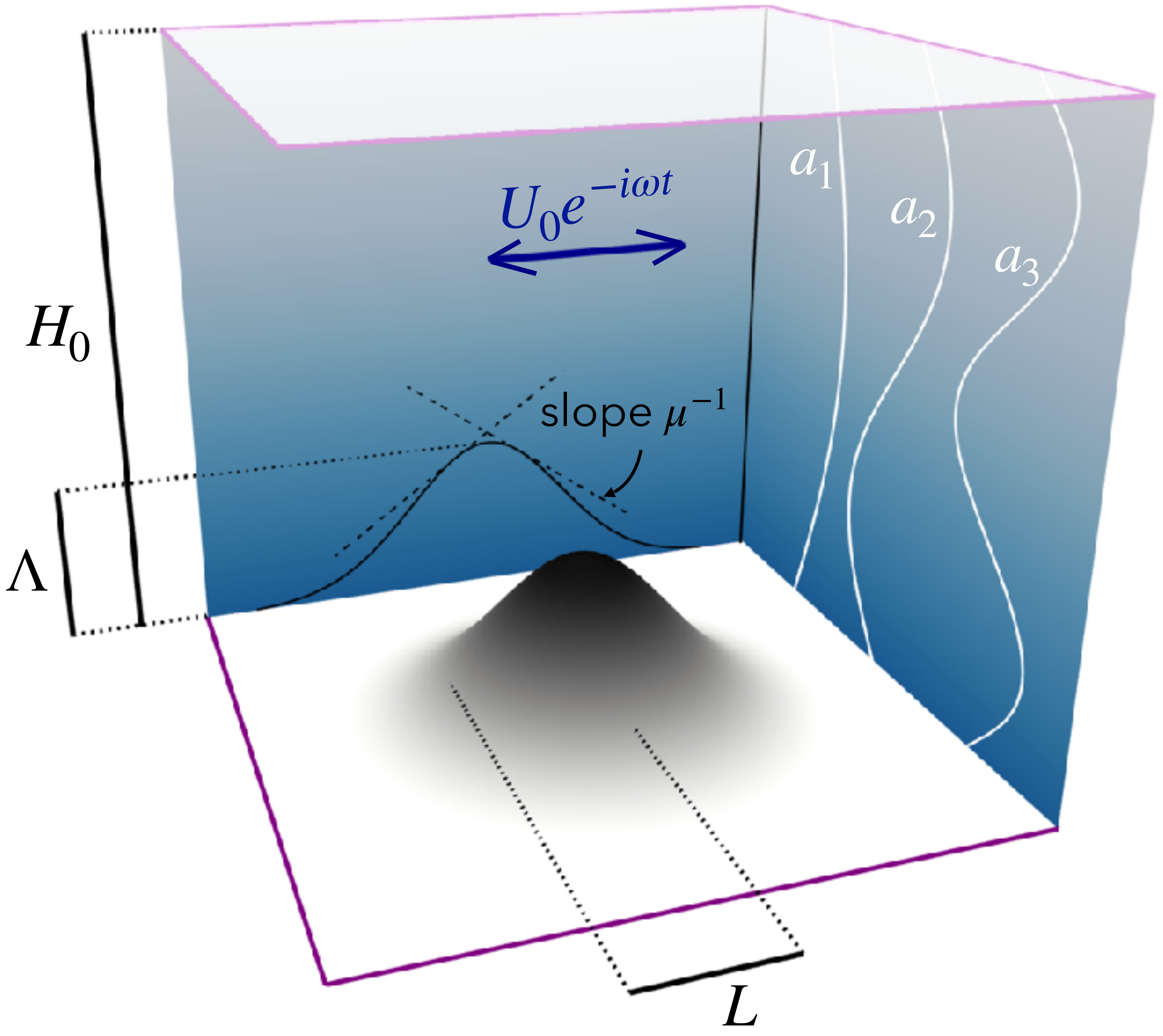

- Slope of the wave beams : $\mu^{-1} = \sqrt{\dfrac{\omega^2 - f^2}{N^2 - \omega^2}}$
- Frequency ratios : $\boxed{\beta = f/\omega}$ and N/ω
- Excursion parameter : $\alpha = \dfrac{U_0 L}{\omega} \ll 1$
- Height ratio : $\boxed{\delta = \dfrac{\Lambda}{H_0}}$
- Criticality parameter : $\boxed{\epsilon = \mu max(\partial_x h)}$

Dimensionless equations

- We introduce the scaling :

$$[\widehat{x}, \widehat{y}] = \frac{\pi[x, y]}{\mu H_0}, \widehat{z} = \frac{\pi z}{H_0}; [\widehat{u}, \widehat{v}] = \frac{[u, v]}{U_0}, \widehat{w} = \frac{\mu w}{U_0};$$

$$\widehat{p} = \frac{\pi p}{\omega U_0 \mu (1 - \beta^2) H_0}; \widehat{b} = \frac{b \mu \omega}{N^2 U_0}$$

- This leads to the following equations

$$u = -i(p_{,x} + i\beta p_{,y})$$

$$v = -i(p_{,y} - i\beta p_{,x})$$

$$w = ip_{,z}$$

$$b = -iw$$

$$u_{,x} + v_{,y} + w_{,z} = 0$$

Dimensionless equations

- We introduce the scaling :

$$[\hat{x},\hat{y}] = \frac{\pi[x,y]}{\mu H_0},\ \hat{z} = \frac{\pi z}{H_0};[\hat{u},\hat{v}] = \frac{[u,v]}{U_0},\ \hat{w} = \frac{\mu w}{U_0};$$

$$\hat{p} = \frac{\pi p}{\omega U_0 \mu (1-\beta^2) H_0};\ \hat{b} = \frac{b\mu\omega}{N^2 U_0}$$

- And the vertical modes decomposition:

$$[w,b] = \sum_n [w_n, b_n](x,y)\sin(nz)$$

$$[u,v,p] = \sum_n [u_n, v_n, p_n](x,y)\cos(nz)$$

- This leads to the following equations

$$u_n = n^{-1}(w_{n,x} + i\beta w_{n,y})$$

$$v_n = n^{-1}(w_{n,y} - i\beta w_{n,x})$$

$$w_n = -inp_n$$

$$b_n = -iw_n$$

$\Rightarrow$ all quantities (u_n, v_n, b_n, p_n) can be expressed using w_n

Boundary integral equation

Echeverri and Peacock (2010)

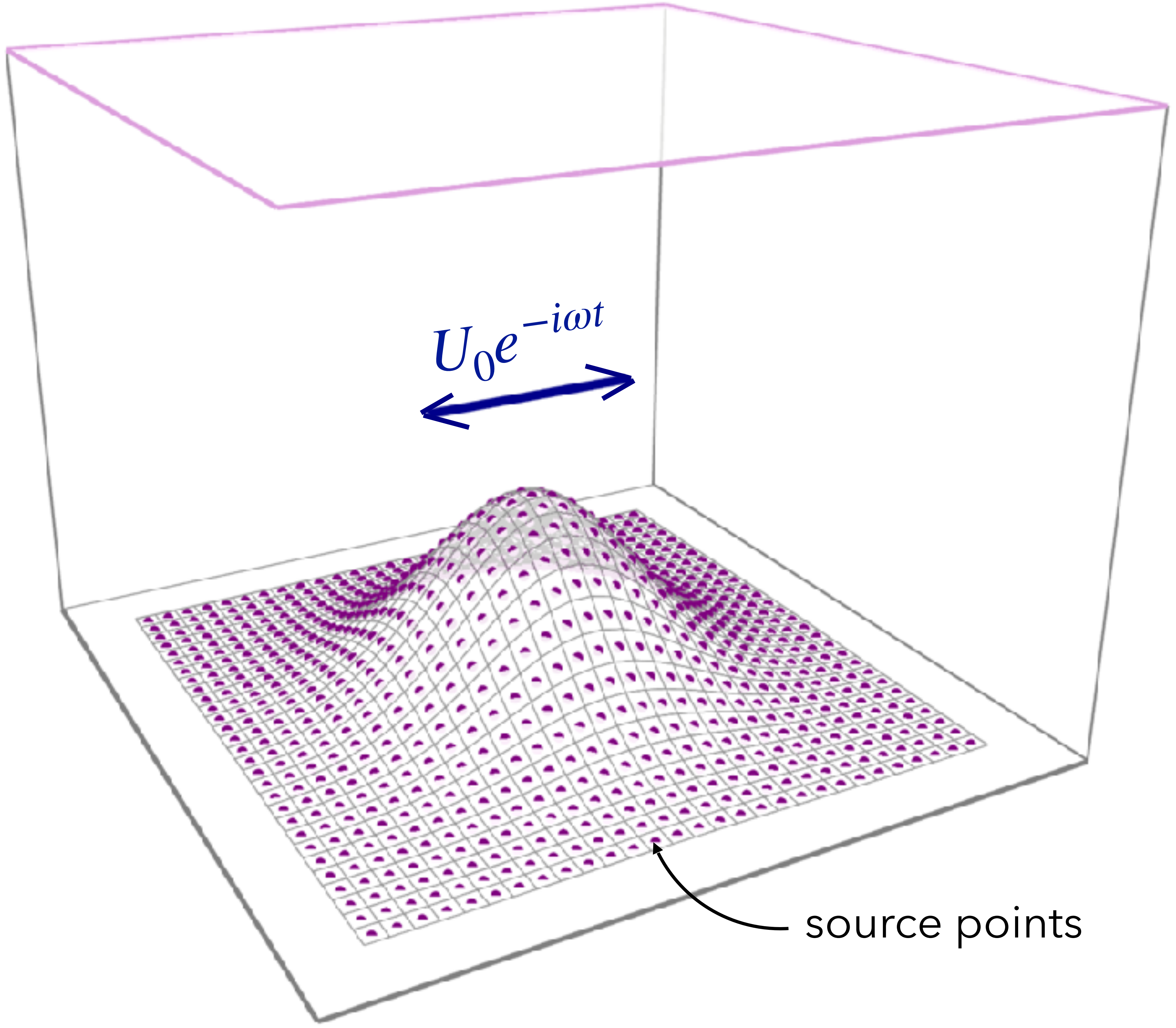

- We introduce the source distribution

$$\nabla_H^2 w - w_{,zz} = S$$

- Green's function associated with the point source $(\mathbf{r}', h(\mathbf{r}'))$

$$\nabla_H^2 \mathscr{G} - \mathscr{G}_{,zz} = \delta(\boldsymbol{r} - \boldsymbol{r}')\delta(z - h(\boldsymbol{r}'))$$

Boundary integral equation

Echeverri and Peacock (2010)

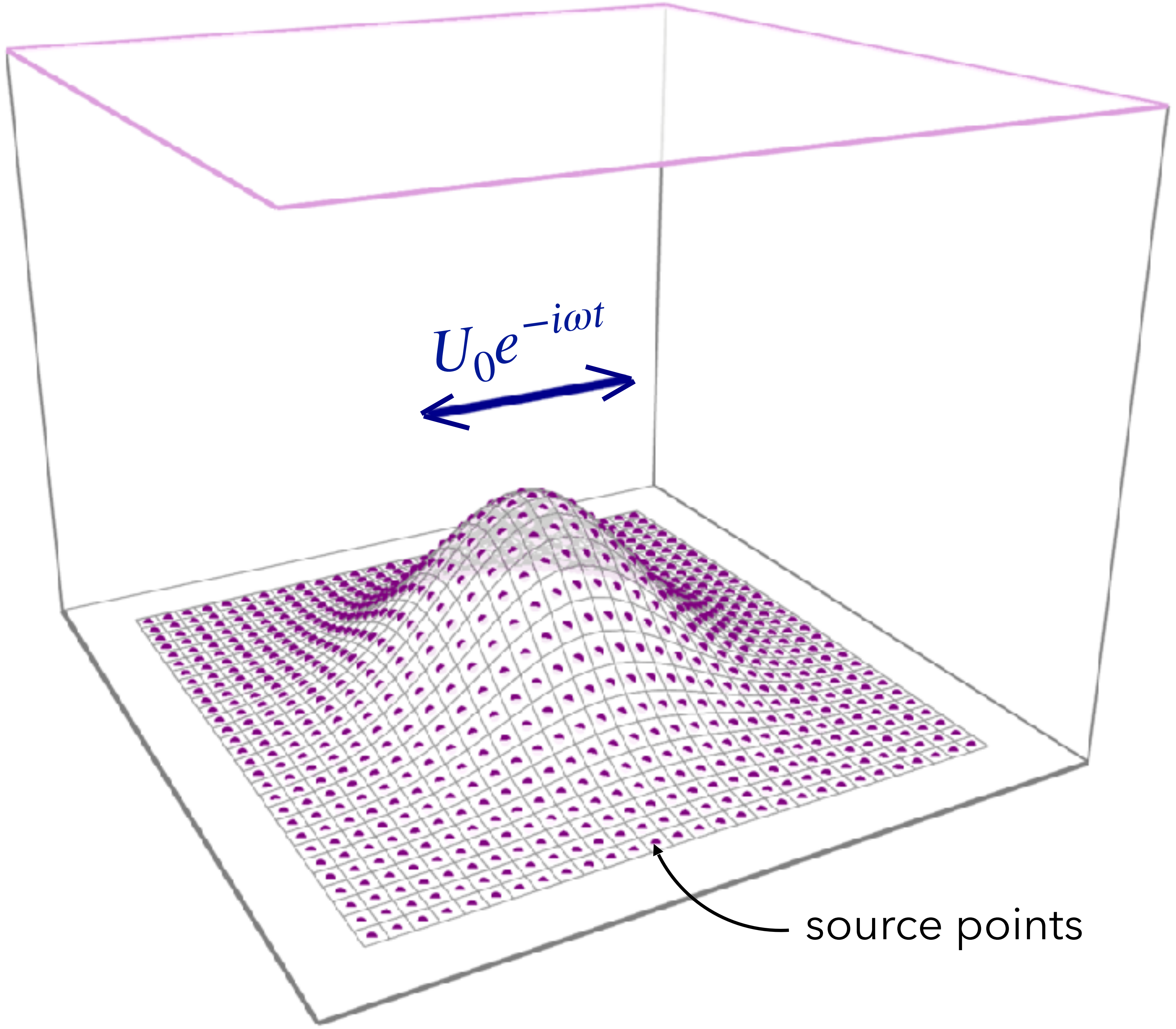

- We introduce the source distribution

$$\nabla_H^2 w - w_{,zz} = S$$

- Green's function associated with the point source $(\mathbf{r}', h(\mathbf{r}'))$

$$\mathcal{G}(\boldsymbol{r}, z; \boldsymbol{r}', h(\boldsymbol{r}')) = \sum_{m=1}^{\infty} g_m(\boldsymbol{r}, \boldsymbol{r}')\sin(mz)$$

with $g_m(\boldsymbol{r}; \boldsymbol{r}') = \dfrac{\sin(mh(\boldsymbol{r}'))}{2i\pi}\mathcal{H}_0^{(1)}(m \parallel \boldsymbol{r} - \boldsymbol{r}' \parallel)$

Boundary integral equation

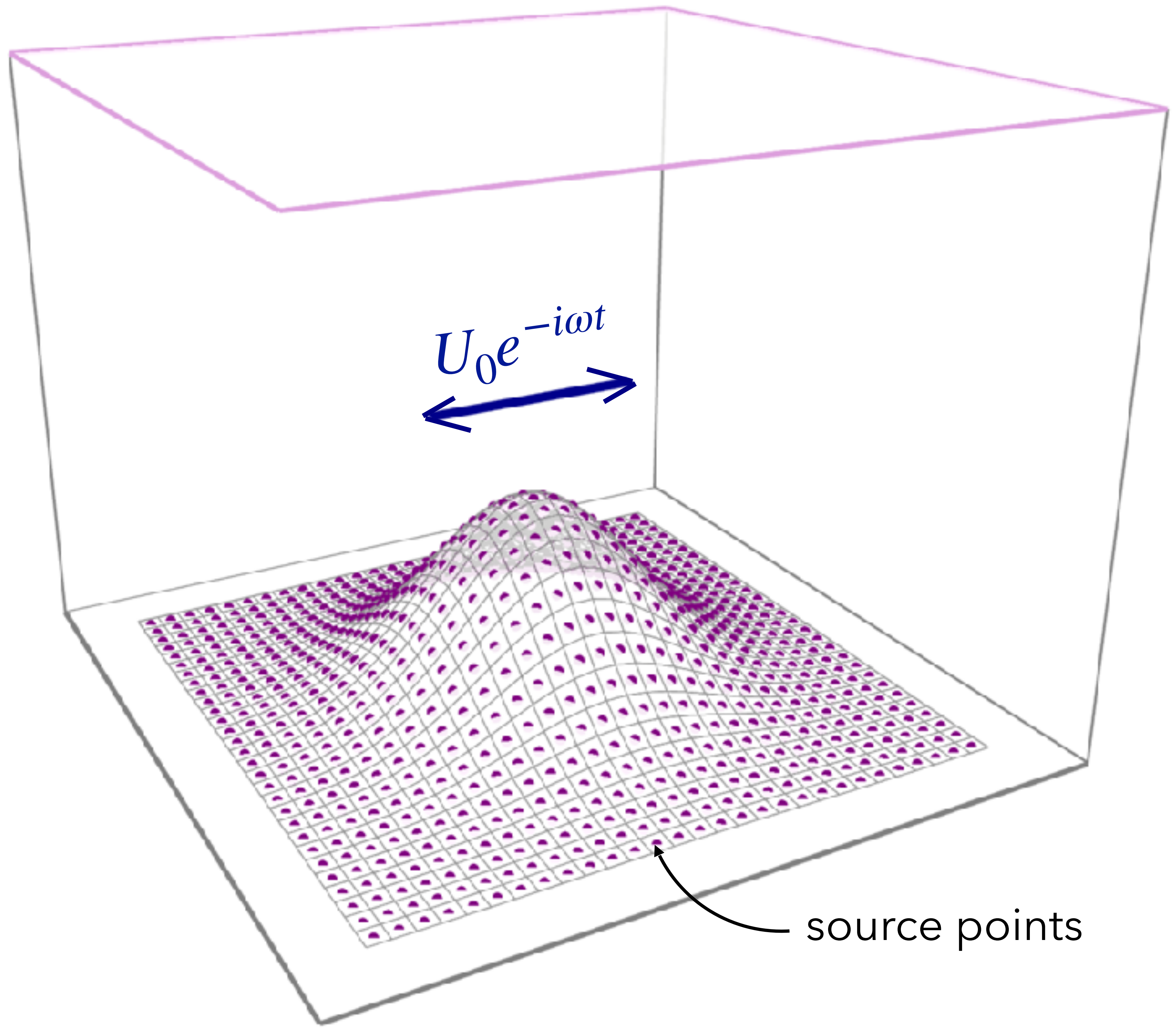

- We can then write

$$w = \mathscr{G} * S$$

$*$ convolution operator

Boundary integral equation

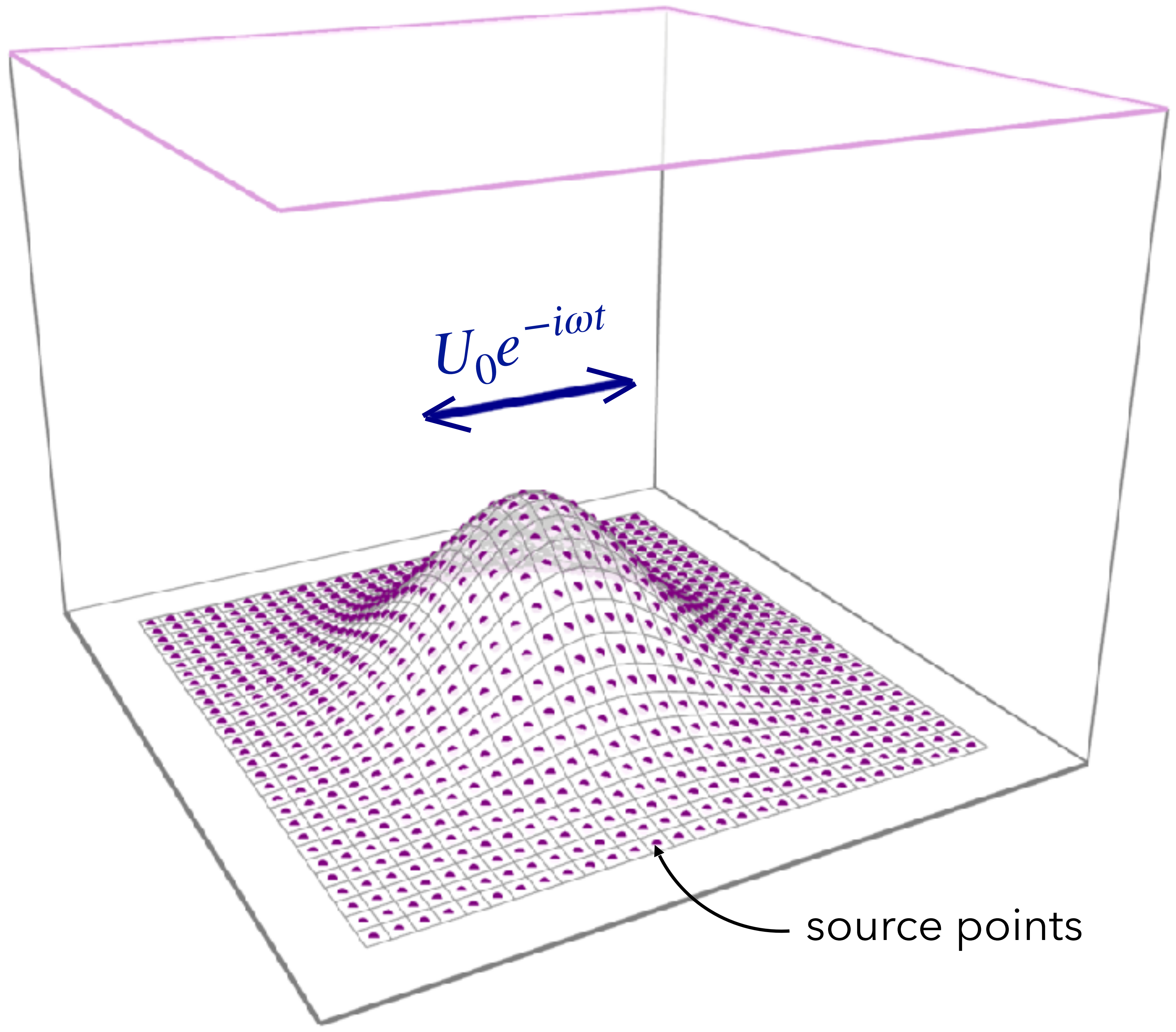

- We can then write

$$w = \mathcal{G} * S$$

$$[u, v, p, b] = [\mathcal{G}_u, \mathcal{G}_v, \mathcal{G}_p, \mathcal{G}_p] * S$$

* convolution operator

Boundary integral equation

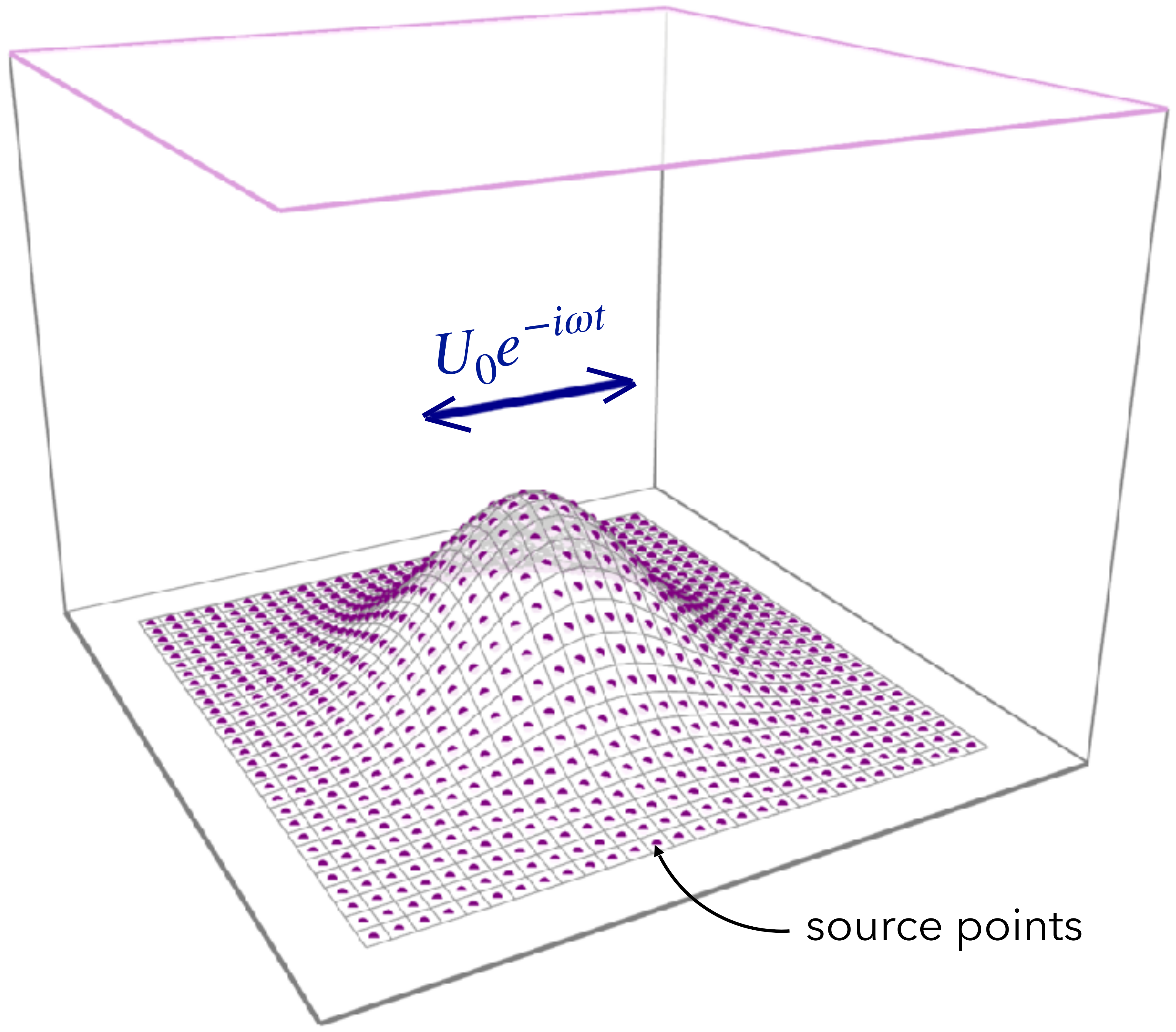

- We can then write

$$w = \mathcal{G} * S$$

$$[u, v, p, b] = [\mathcal{G}_u, \mathcal{G}_v, \mathcal{G}_p, \mathcal{G}_p] * S$$

- Bottom boundary condition

$$\boldsymbol{U}_0 \cdot \nabla_H h = w - \boldsymbol{u}_H \cdot \nabla_H h$$

* convolution operator

Boundary integral equation

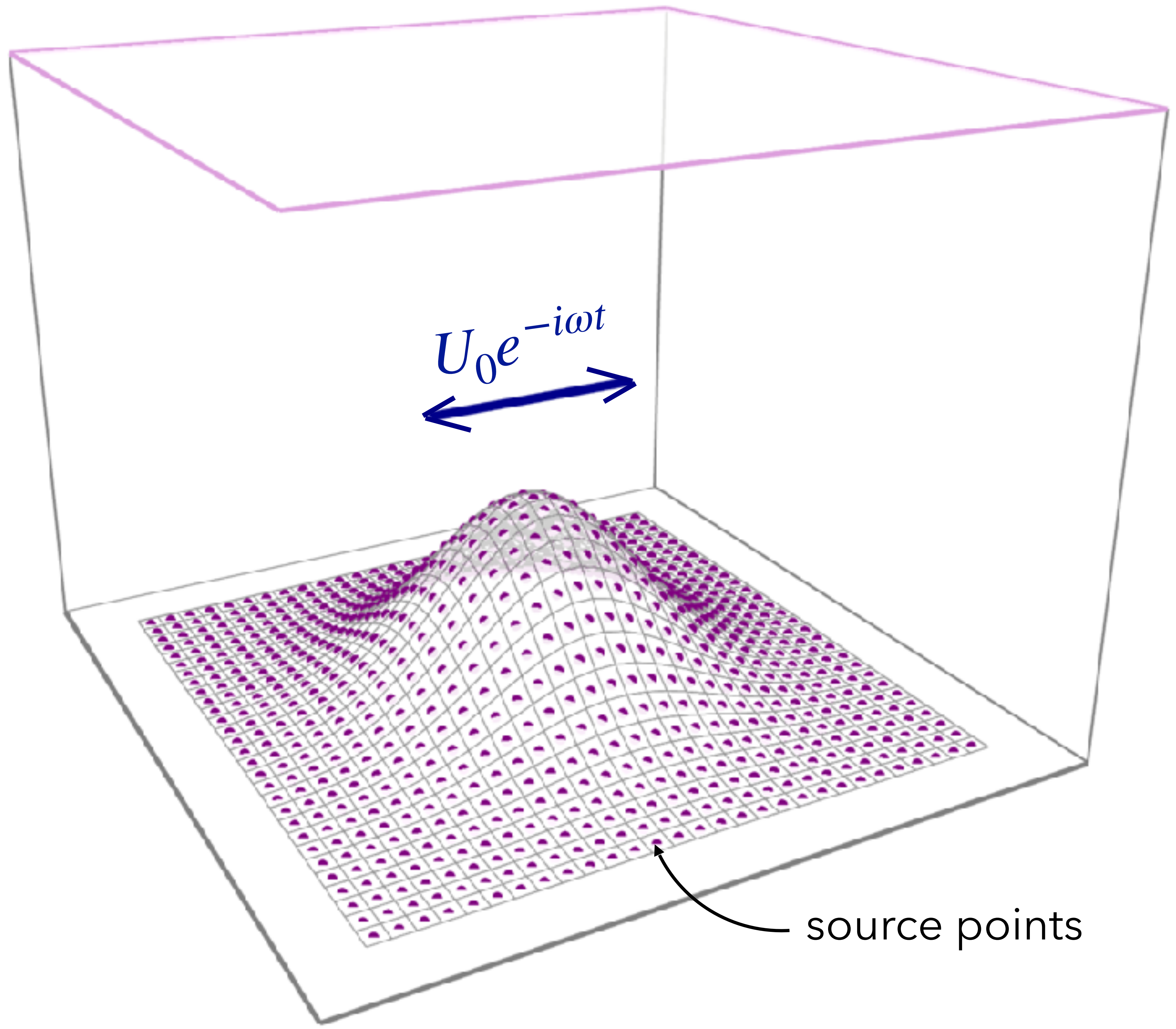

- We can then write

$$w = \mathscr{G} * S$$
$$[u, v, p, b] = [\mathscr{G}_u, \mathscr{G}_v, \mathscr{G}_p, \mathscr{G}_p] * S$$

- Bottom boundary condition

$$\boldsymbol{U}_0 \cdot \nabla_H h = w - \boldsymbol{u}_H \cdot \nabla_H h$$
$$= \left(\mathscr{G} - \partial_x h \mathscr{G}_u - \partial_y h \mathscr{G}_v\right) * S$$

* convolution operator

Boundary integral equation

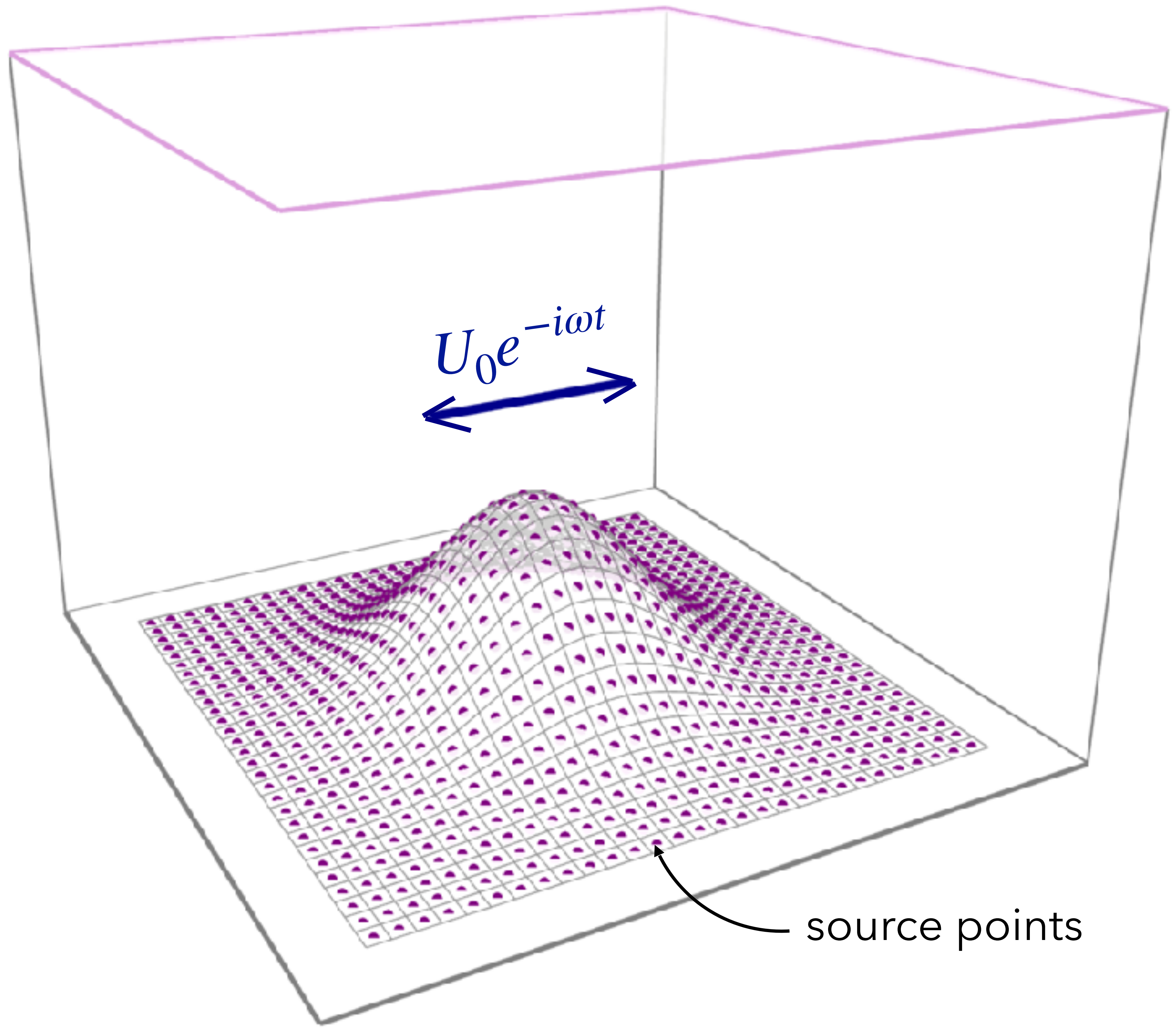

- We can then write

$$w = \mathscr{G} * S$$

$$[u, v, p, b] = [\mathscr{G}_u, \mathscr{G}_v, \mathscr{G}_p, \mathscr{G}_p] * S$$

- Bottom boundary condition

$$\begin{aligned} \boldsymbol{U}_0 \cdot \nabla_H h &= w - \boldsymbol{u}_H \cdot \nabla_H h \\ &= \Big(\underbrace{\mathscr{G} - \partial_x h \mathscr{G}_u - \partial_y h \mathscr{G}_v}_{\mathscr{F}} \Big) * S \end{aligned}$$

* convolution operator

Boundary integral equation

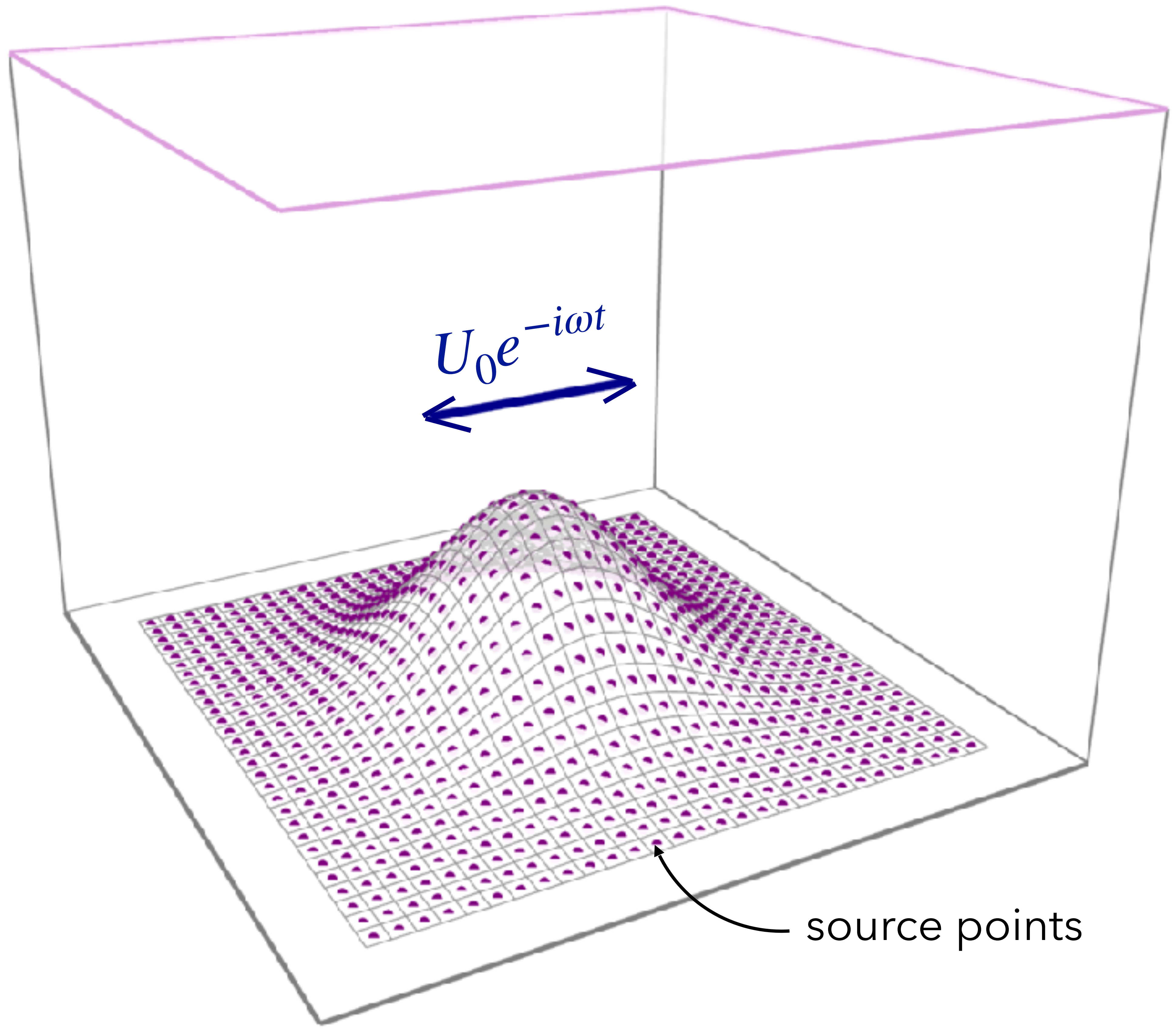

- We can then write

$$w = \mathscr{G} * S$$
$$[u, v, p, b] = [\mathscr{G}_u, \mathscr{G}_v, \mathscr{G}_p, \mathscr{G}_p] * S$$

- Bottom boundary condition

$$\begin{aligned} \boldsymbol{U}_0 \cdot \nabla_H h &= w - \boldsymbol{u}_H \cdot \nabla_H h \\ &= \left(\mathscr{G} - \partial_x h \mathscr{G}_u - \partial_y h \mathscr{G}_v\right) * S \\ &= \mathscr{F} * S \end{aligned}$$

* convolution operator

Boundary integral equation

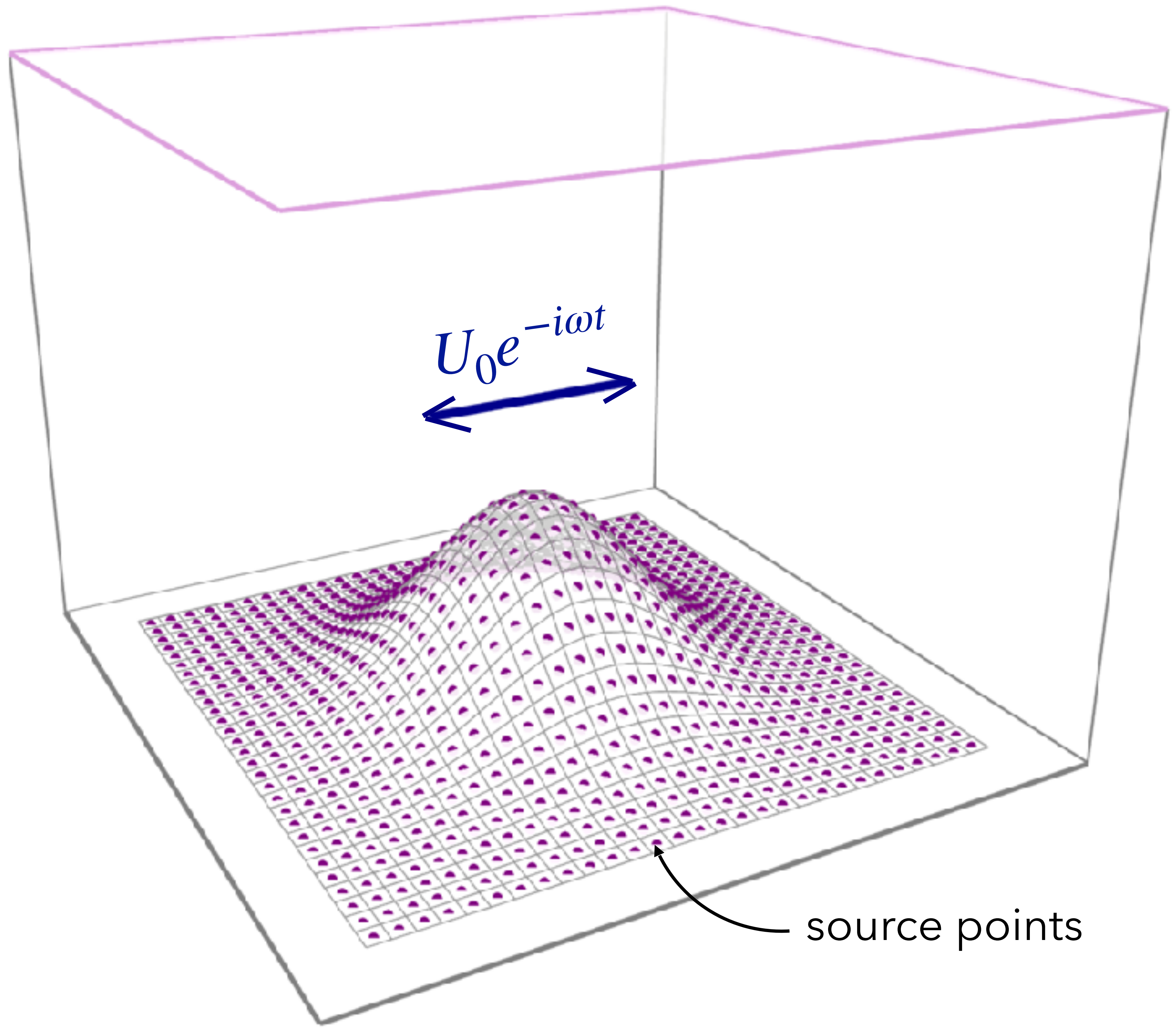

- We can then write

$$w = \mathscr{G} * S$$

$$[u, v, p, b] = [\mathscr{G}_u, \mathscr{G}_v, \mathscr{G}_p, \mathscr{G}_p] * S$$

- Bottom boundary condition

$$\boldsymbol{U}_0 \cdot \nabla_H h = \mathscr{F} * S$$

* convolution operator

Boundary integral equation

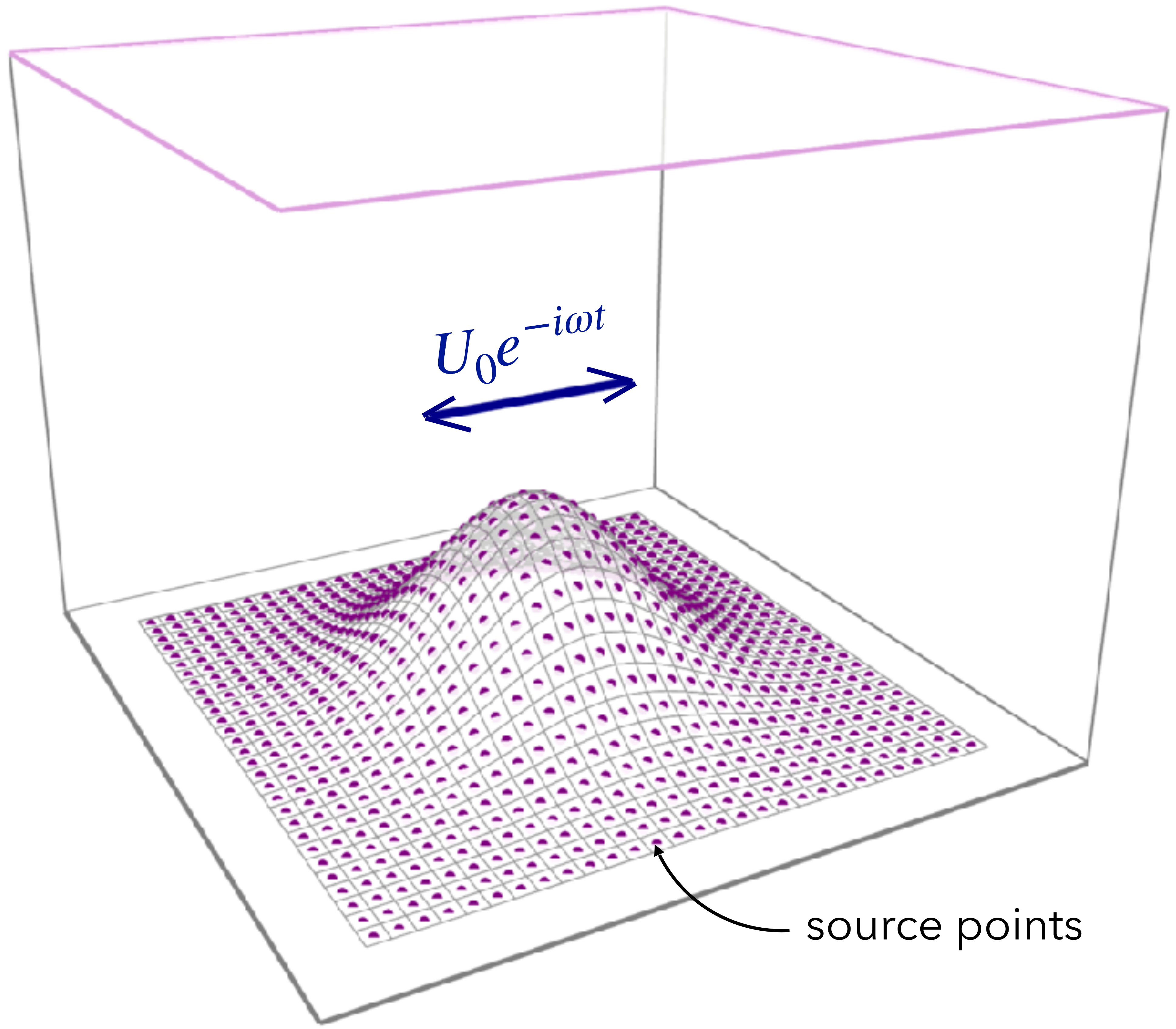

- We can then write

$$w = \mathcal{G} * S$$

$$[u, v, p, b] = [\mathcal{G}_u, \mathcal{G}_v, \mathcal{G}_p, \mathcal{G}_p] * S$$

- Bottom boundary condition

$$\boxed{\boldsymbol{U}_0 \cdot \nabla_H h = \mathcal{F} * S}$$

Integral equation of unknown S

* convolution operator

Boundary integral equation

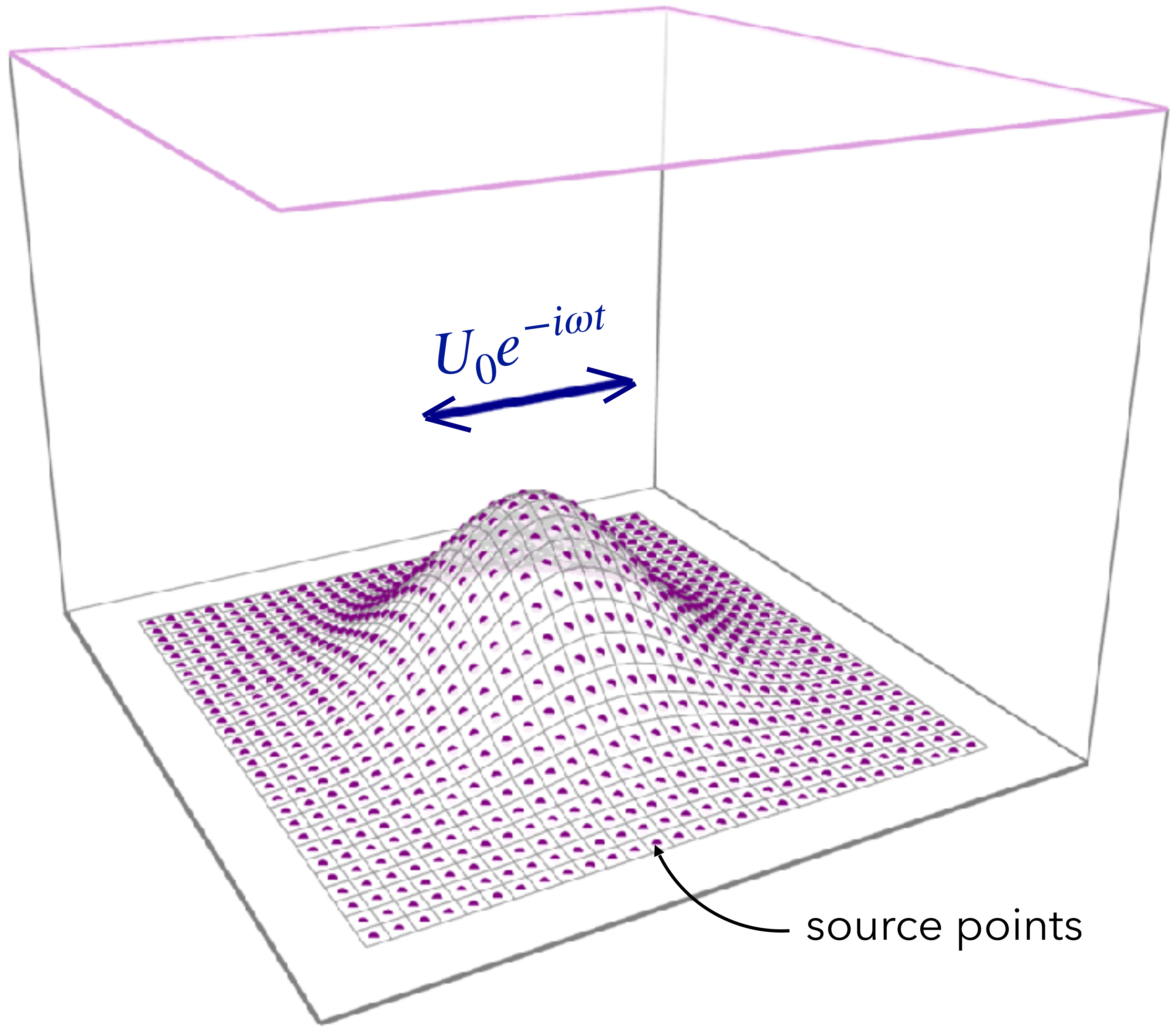

$$\boxed{U_0 \cdot \nabla_H h = \mathcal{F} * S}$$

Numerical strategy

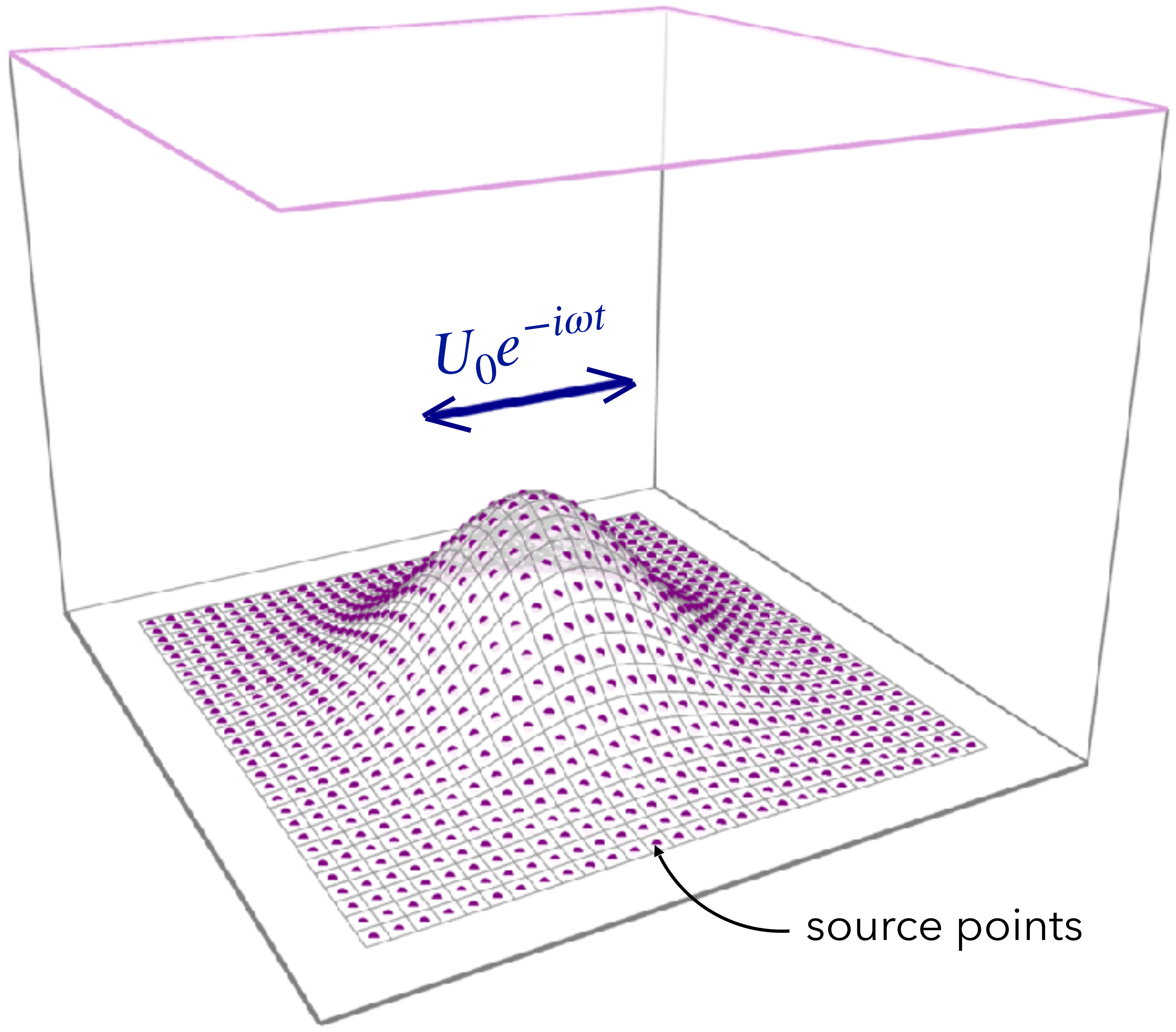

$$\boxed{U_0 \cdot \nabla_H h = \mathscr{F} * S}$$

Numerical strategy

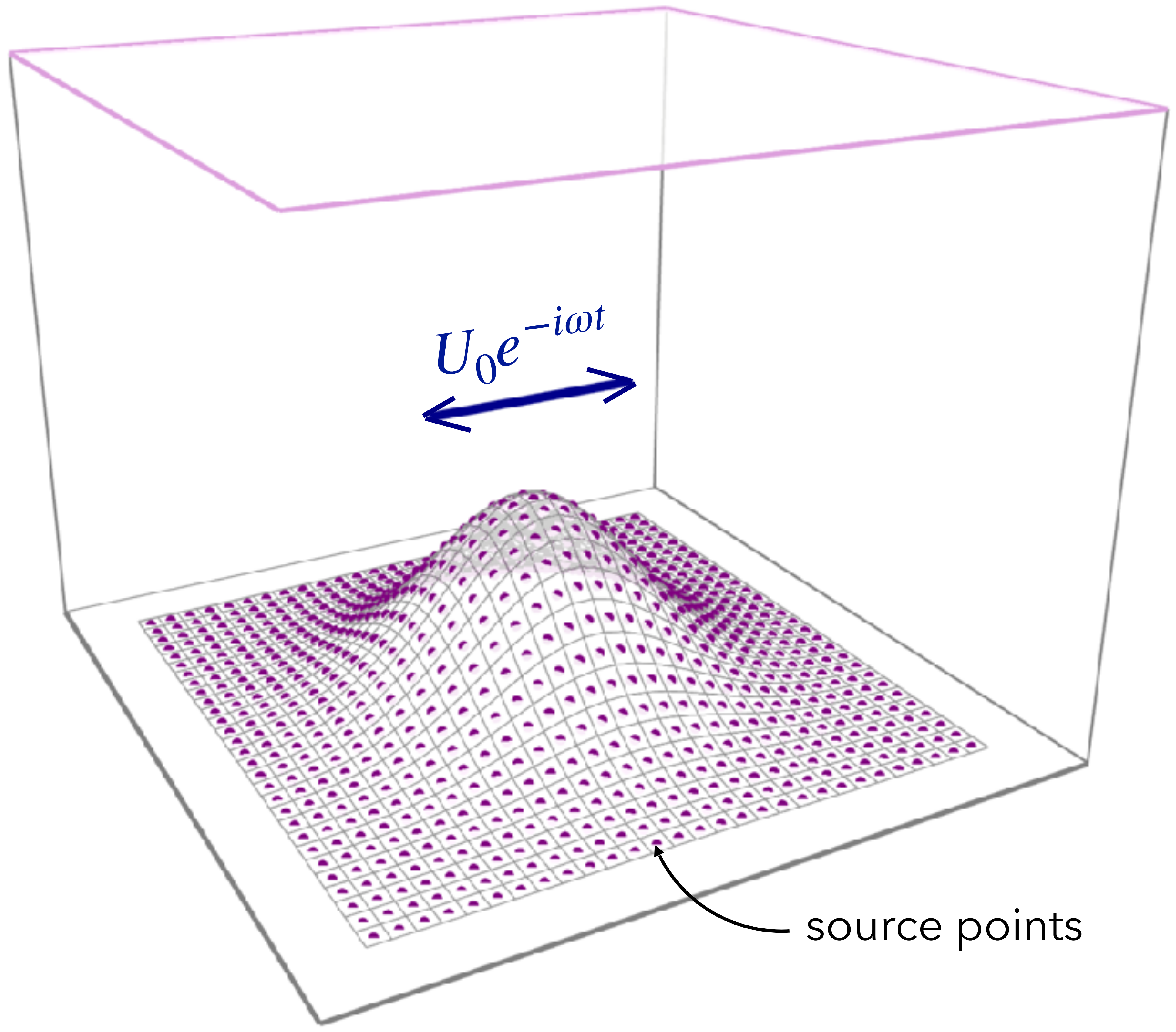

$$\boxed{U_0 \cdot \nabla_H h = \mathscr{F} * S}$$

- We discretize the seamount into square cells C_k

Numerical strategy

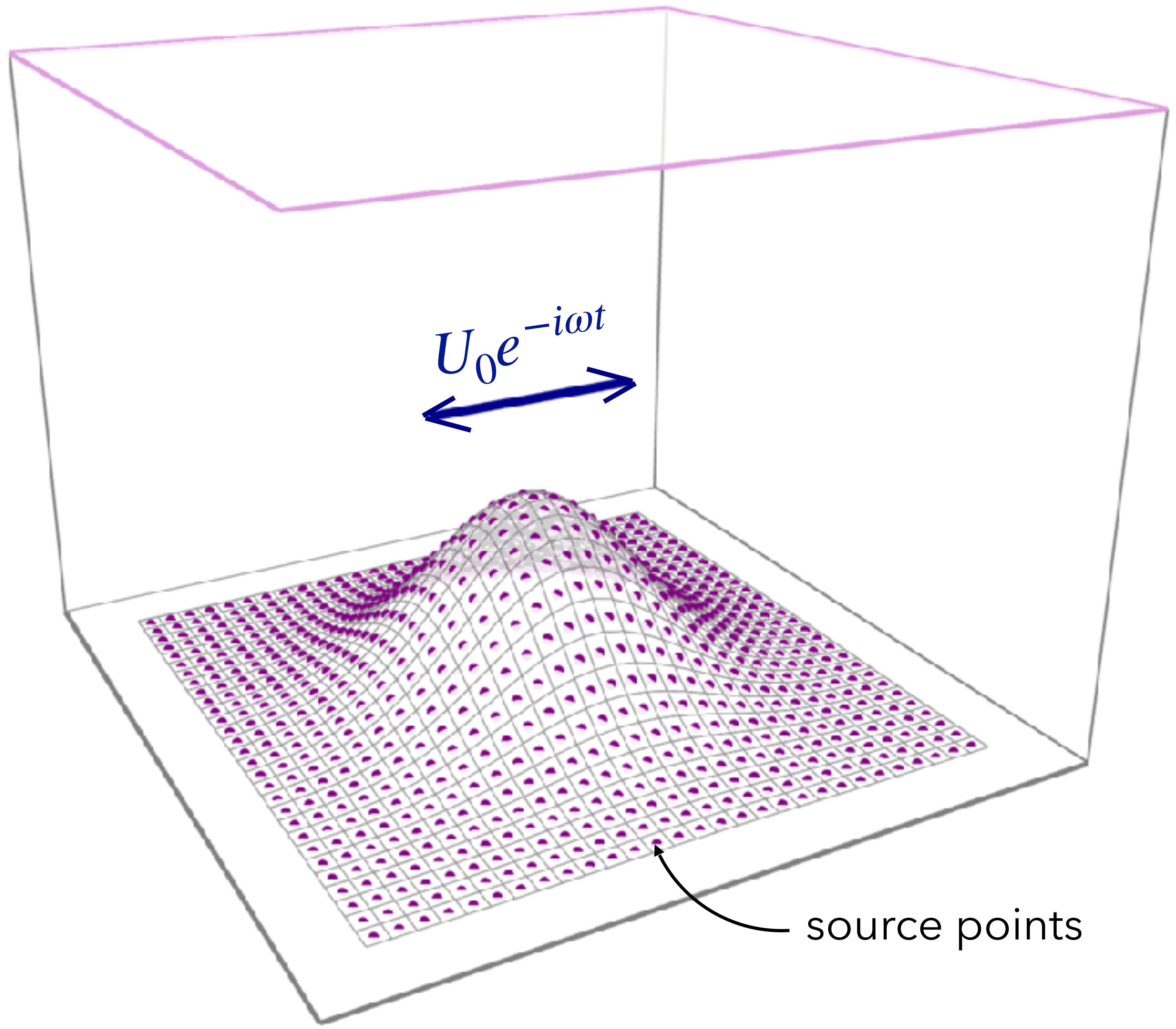

$$\boxed{\boldsymbol{U}_0 \cdot \nabla_H h = \mathscr{F} * S}$$

- We discretize the seamount into square cells C_k

$$\boldsymbol{U}_0 \cdot \nabla_H h = \sum_k S_k \iint_{C_k} \mathscr{F}\, dx' dy'$$

Numerical strategy

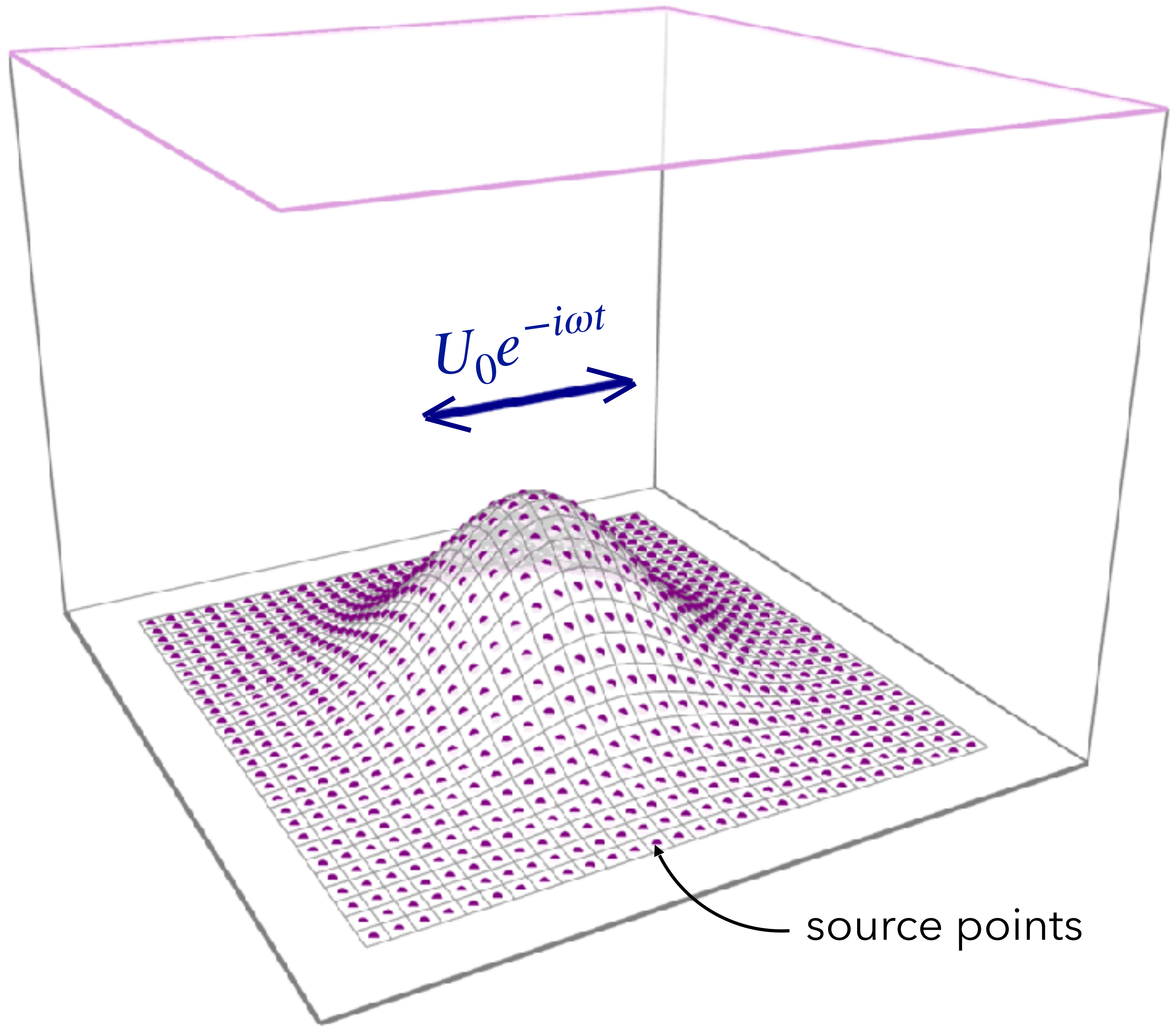

$$\boxed{U_0 \cdot \nabla_H h = \mathcal{F} * S}$$

- We discretize the seamount into square cells C_k
- Integrating over a cell C_l

$$U_0 \cdot \nabla_H h = \sum_k S_k \iint_{C_k} \mathcal{F}\, dx' dy'$$

Numerical strategy

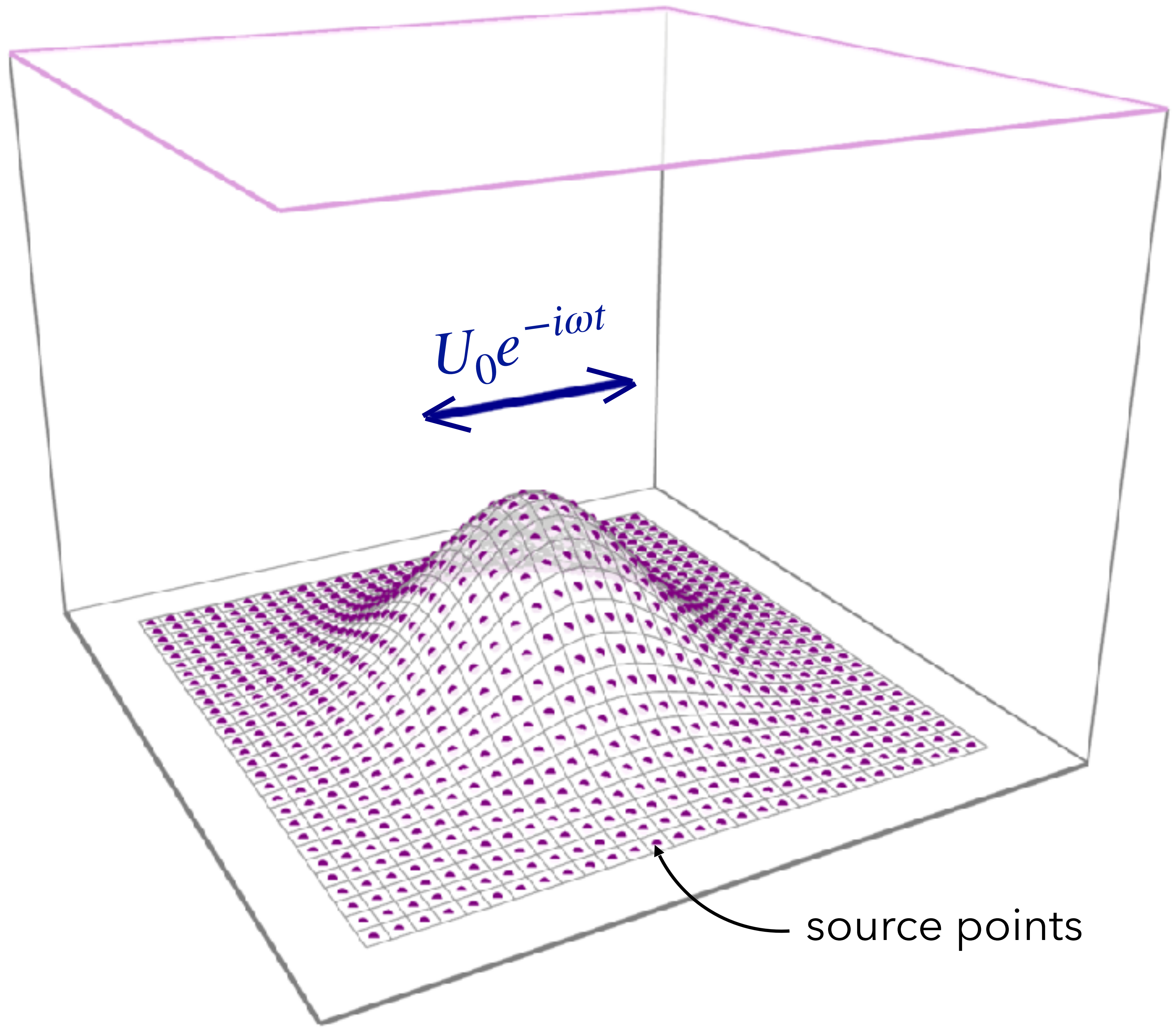

$$\boxed{\boldsymbol{U}_0 \cdot \nabla_H h = \mathcal{F} * S}$$

- We discretize the seamount into square cells C_k
- Integrating over a cell C_l

$$\iint_{C_l} \boldsymbol{U}_0 \cdot \nabla_H h dxdy = \sum_k S_k \iint_{C_l} \iint_{C_k} \mathcal{F} dx'dy'dxdy$$

Numerical strategy

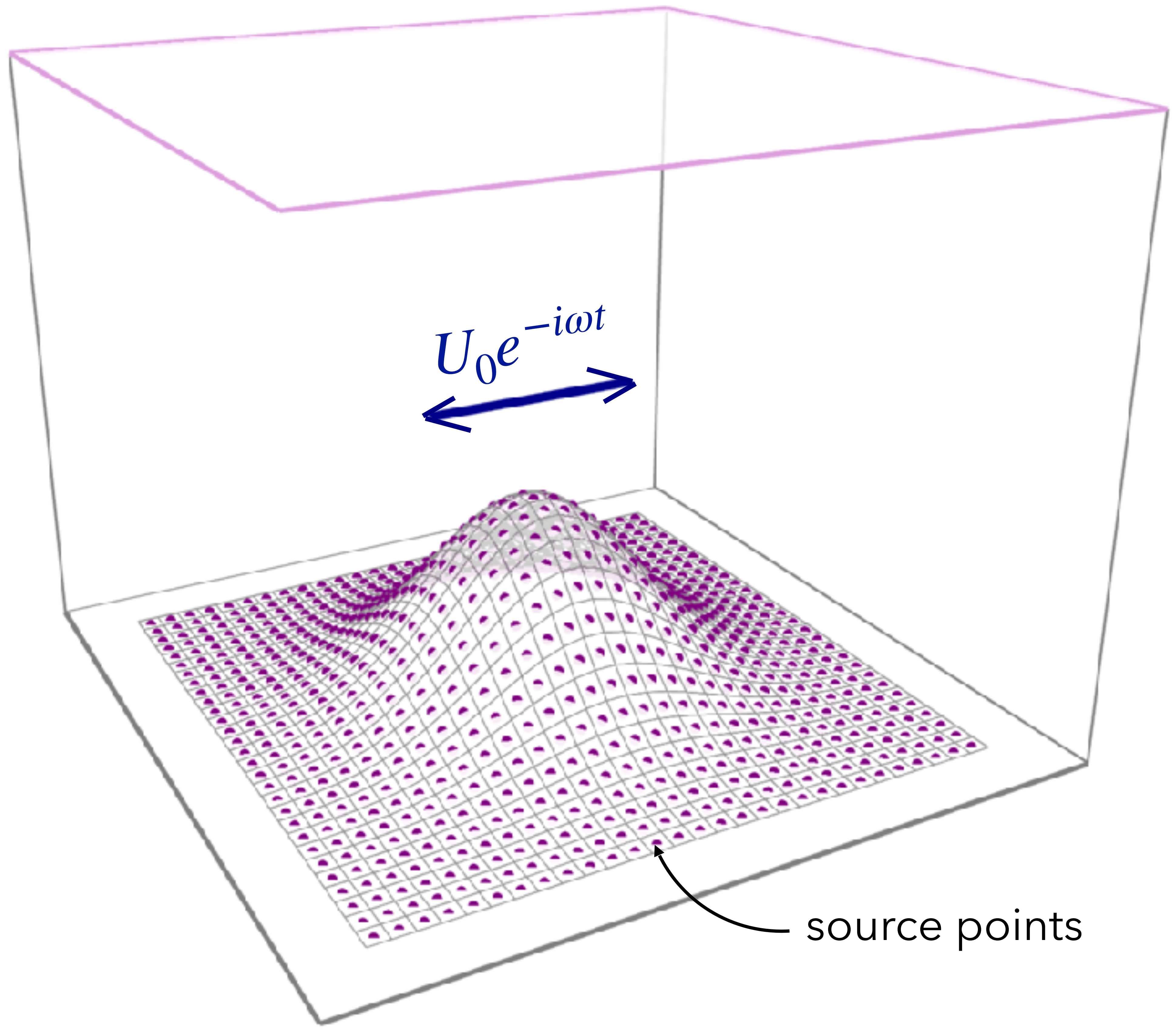

$$\boxed{U_0 \cdot \nabla_H h = \mathcal{F} * S}$$

- We discretize the seamount into square cells C_k
- Integrating over a cell C_l

$$A_l = \sum_k S_k M_{l,k}$$

Wavefield and energetics

- Velocity, pressure, buoyancy

$$w = \mathcal{G} * S$$

$$[u, v, p, b] = [\mathcal{G}_u, \mathcal{G}_v, \mathcal{G}_p, \mathcal{G}_p] * S$$

Wavefield and energetics

- Velocity, pressure, buoyancy

$$w = \mathcal{G} * S$$
$$[u, v, p, b] = [\mathcal{G}_u, \mathcal{G}_v, \mathcal{G}_p, \mathcal{G}_p] * S$$

- Depth-integrated energy flux :

$$\boldsymbol{J} = \int_z \left\langle p\boldsymbol{u} \right\rangle dz = \sum_n \boldsymbol{J}_n \text{with} \boldsymbol{J}_n = \mathrm{Re}\left(\frac{\pi}{4} p_n^* \boldsymbol{u}_n\right)$$

Wavefield and energetics

- Velocity, pressure, buoyancy

$$w = \mathcal{G} * S$$
$$[u, v, p, b] = [\mathcal{G}_u, \mathcal{G}_v, \mathcal{G}_p, \mathcal{G}_p] * S$$

- Depth-integrated energy flux :

$$\boldsymbol{J} = \int_z \left\langle p\boldsymbol{u} \right\rangle dz = \sum_n \boldsymbol{J}_n \text{with} \boldsymbol{J}_n = \mathrm{Re}\left(\frac{\pi}{4} p_n^* \boldsymbol{u}_n\right)$$

- Conversion rate

$$C = \iint \left\langle p\boldsymbol{u} \right\rangle \cdot \boldsymbol{\eta} dS = \sum_n C_n \text{with} C_n = \int \boldsymbol{J}_n \cdot \boldsymbol{\eta} dl$$

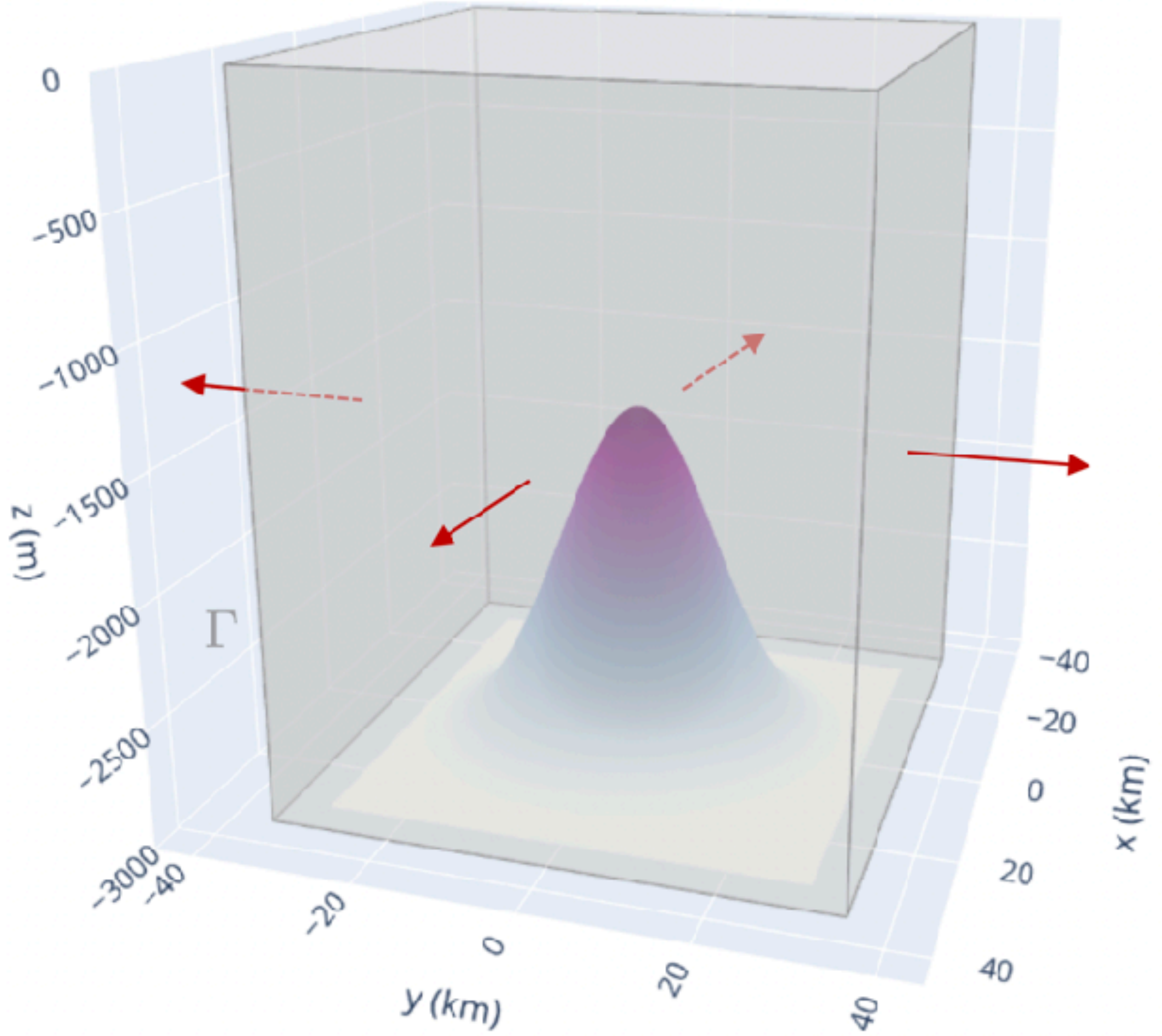

Parameters

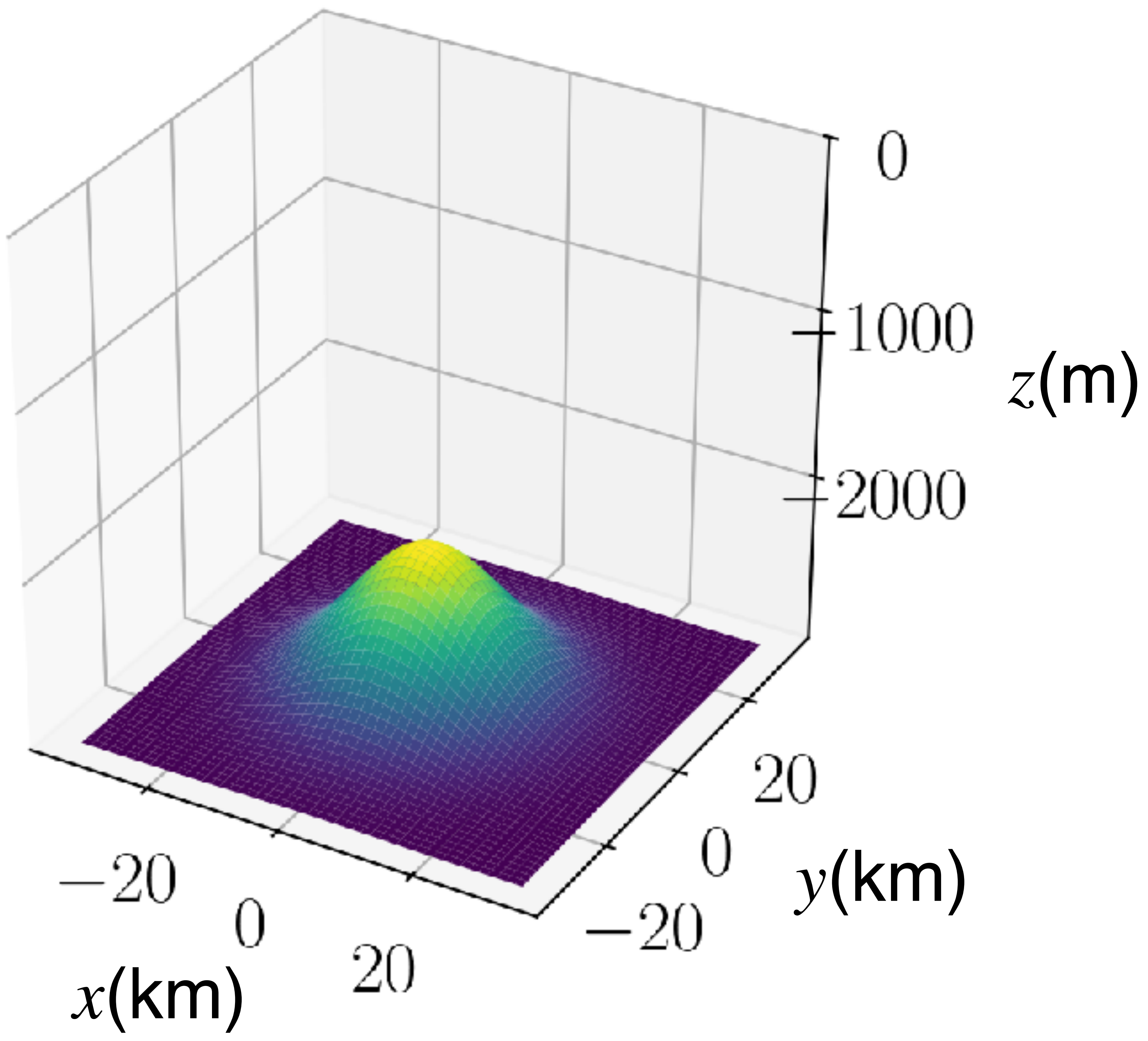

- Frequencies
  $N = 2 \times 10^{-3}\mathrm{s}^{-1}; \omega = 1.4 \times 10^{-4}\mathrm{s}^{-1}$
  Non rotating : $f = 0$

- Gaussian topography

$$h(\boldsymbol{r}) = \Lambda \exp\left(-\frac{\| \boldsymbol{r} \|^2}{2L^2}\right) \text{if } |x|, |y| < 3L$$

with $\Lambda = 900\mathrm{m}; L = 11\mathrm{km}$ and $H_0 = 3$ km.

Parameters

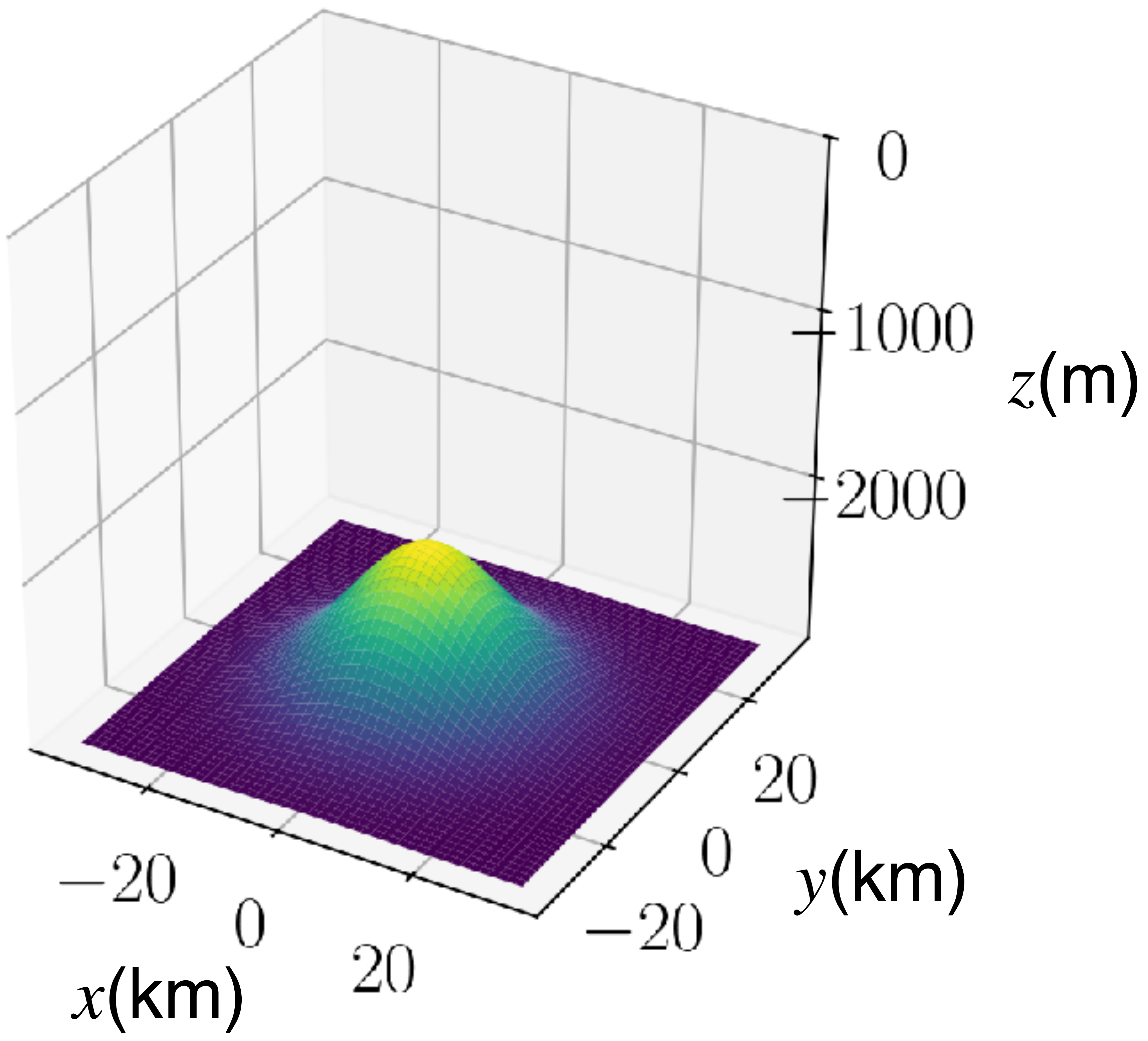

- Frequencies
  $N = 2 \times 10^{-3}\mathrm{s}^{-1}; \omega = 1.4 \times 10^{-4}\mathrm{s}^{-1}$
  Non rotating : $f = 0$

- Gaussian topography

$$h(\boldsymbol{r}) = \Lambda \exp\left(-\frac{\| \boldsymbol{r} \|^2}{2L^2}\right) \text{if } |x|, |y| < 3L$$

with $\Lambda = 900\mathrm{m}; L = 11\mathrm{km}$ and $H_0 = 3$ km.

$$\Rightarrow \boxed{\delta = 0.3; \epsilon = 0.7; \beta = 0}$$

Source distribution S

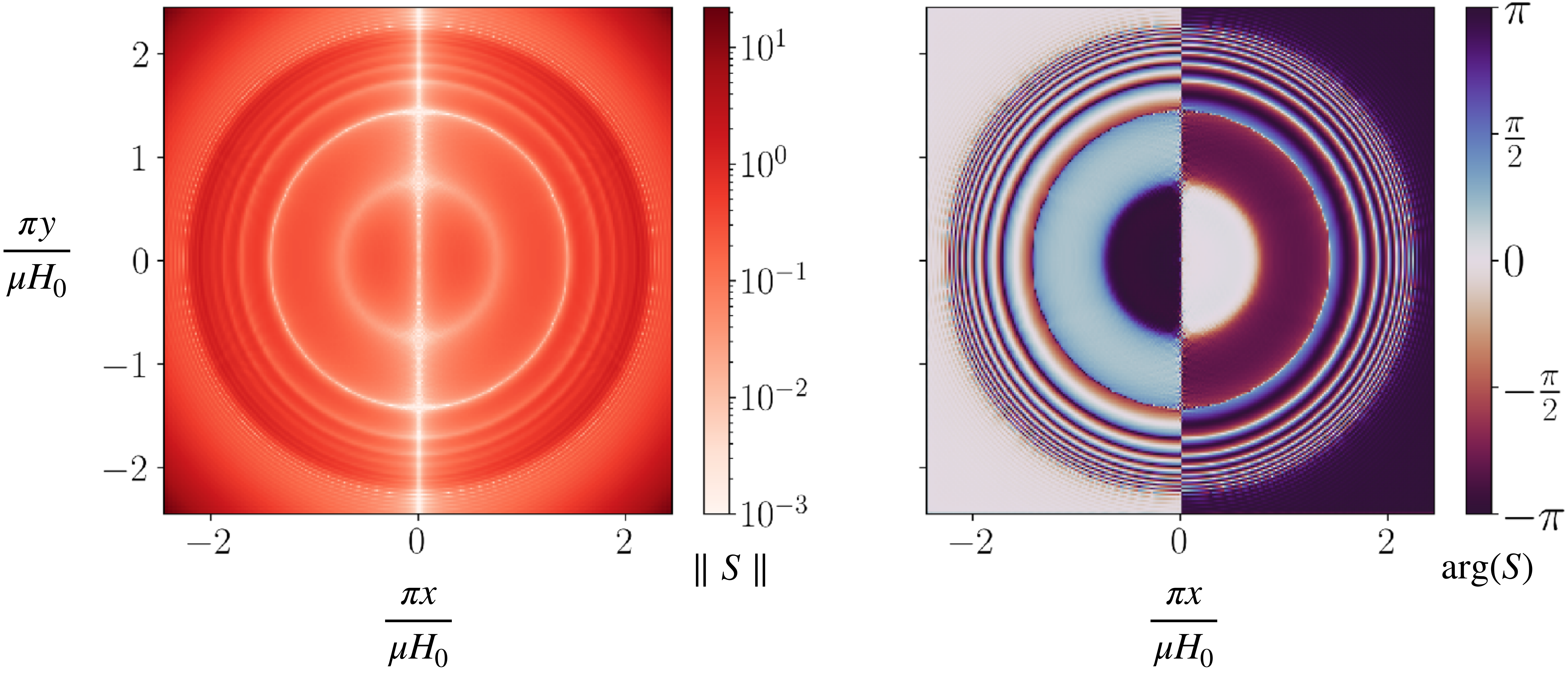

Vertical velocity

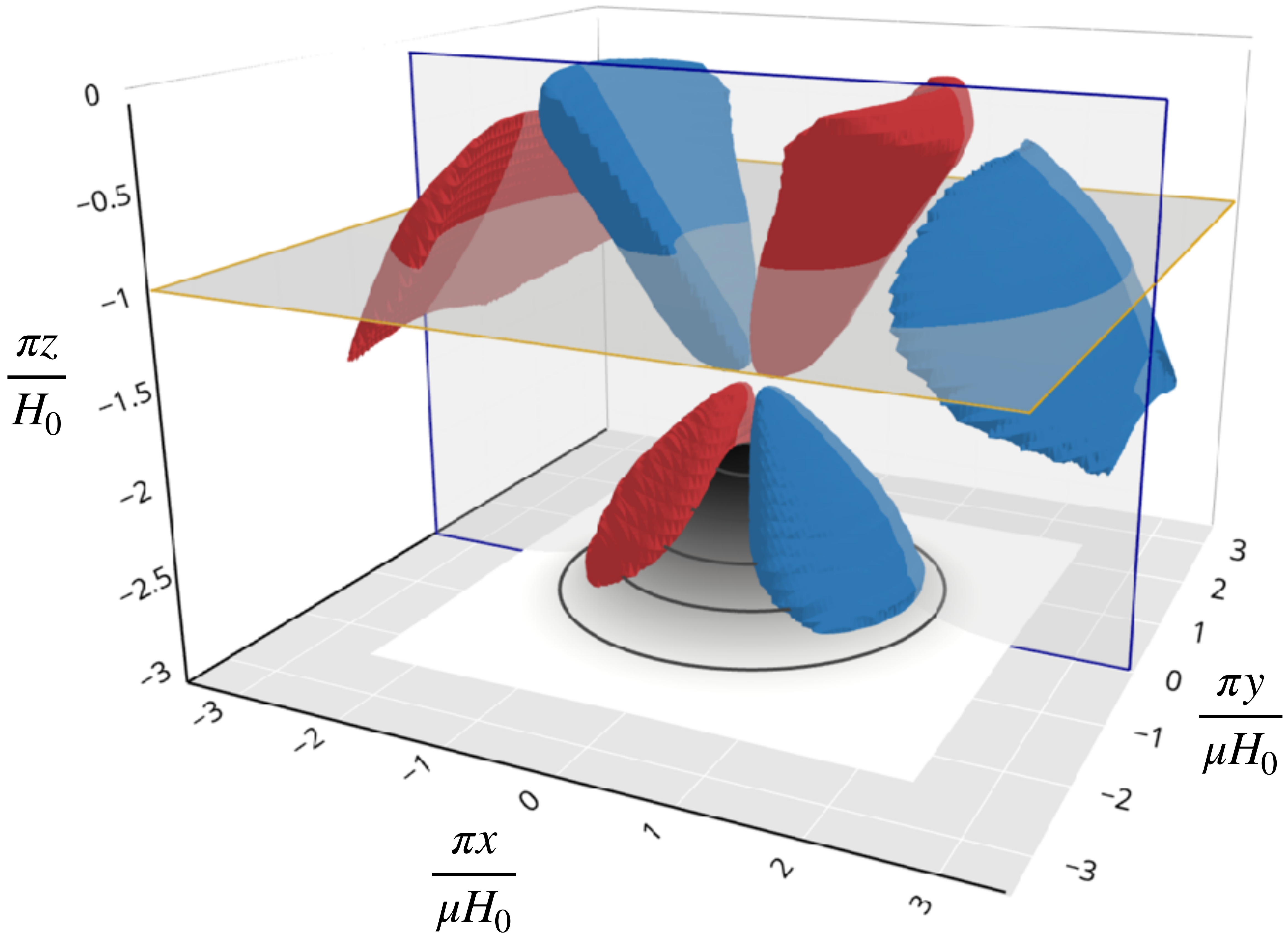

Isocontours $\mu w/U_0 = \pm 0.5$

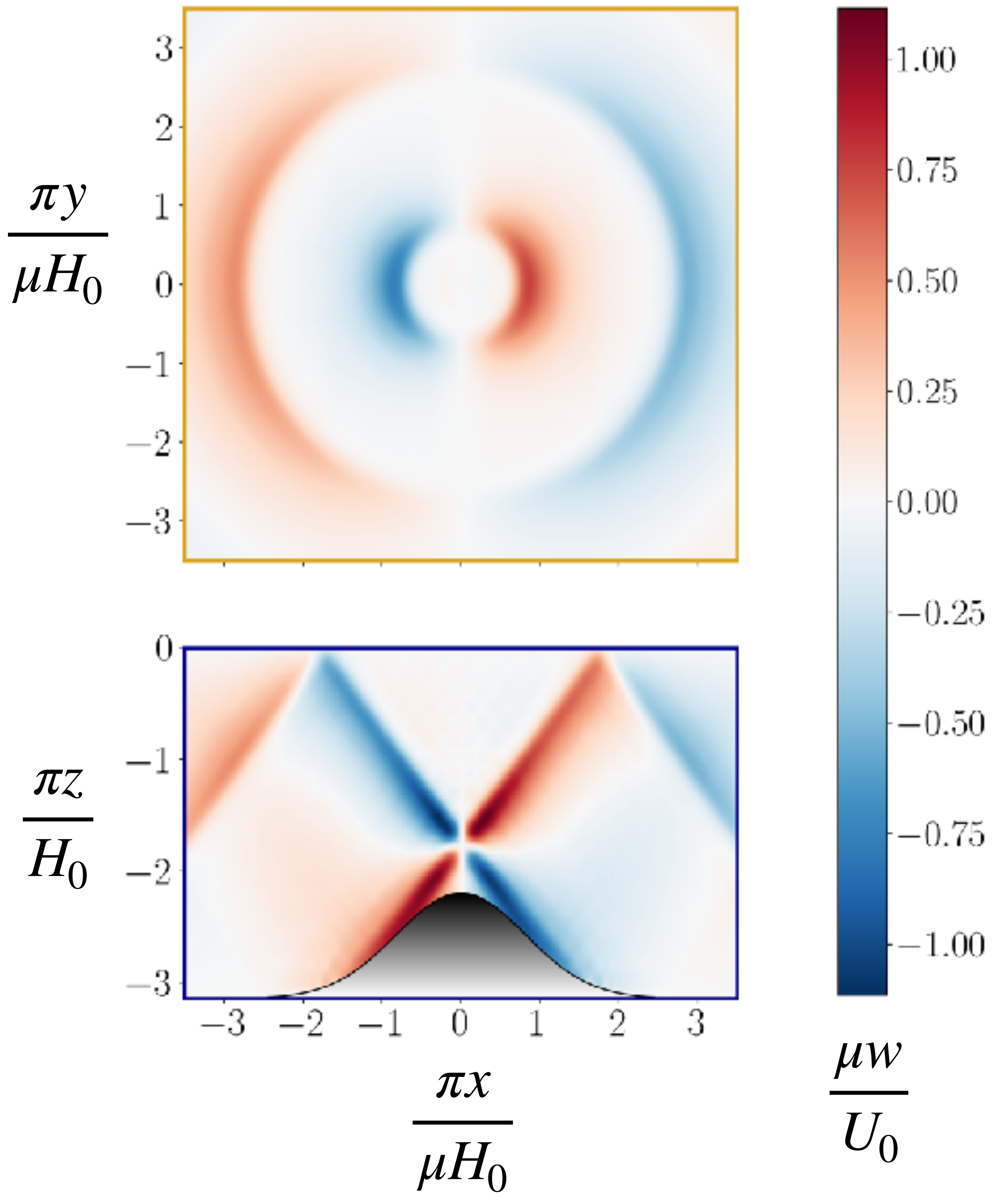

Horizontal and vertical cuts

Energy conversion rate

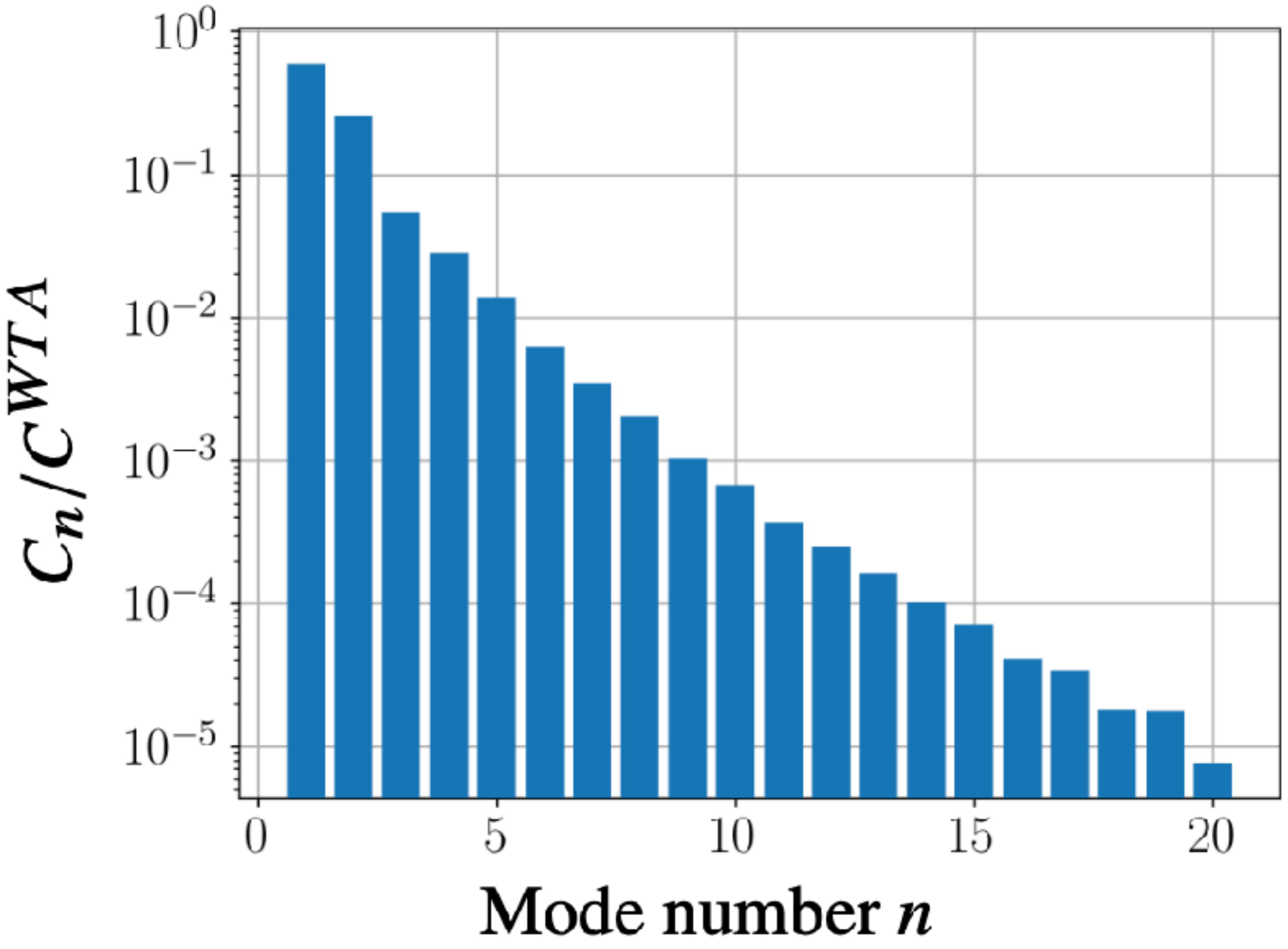

- C_n decrease exponentially with mode number.
- Most of the energy contained in the first 5 modes.

Energy conversion rate

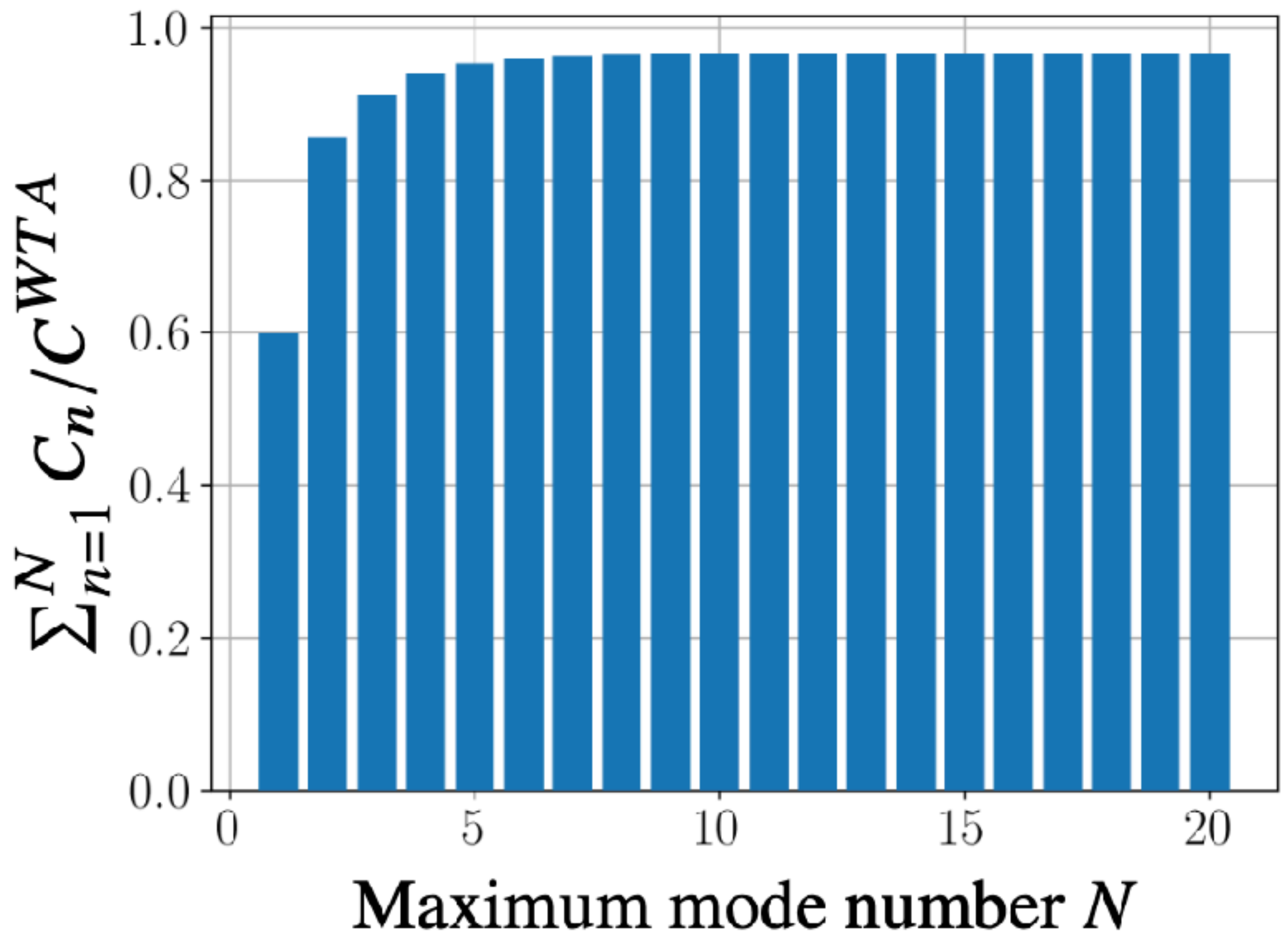

- C_n decrease exponentially with mode number.
- Most of the energy contained in the first 5 modes.
- Total conversion rate C close to the WTA estimate.

Energy conversion rate

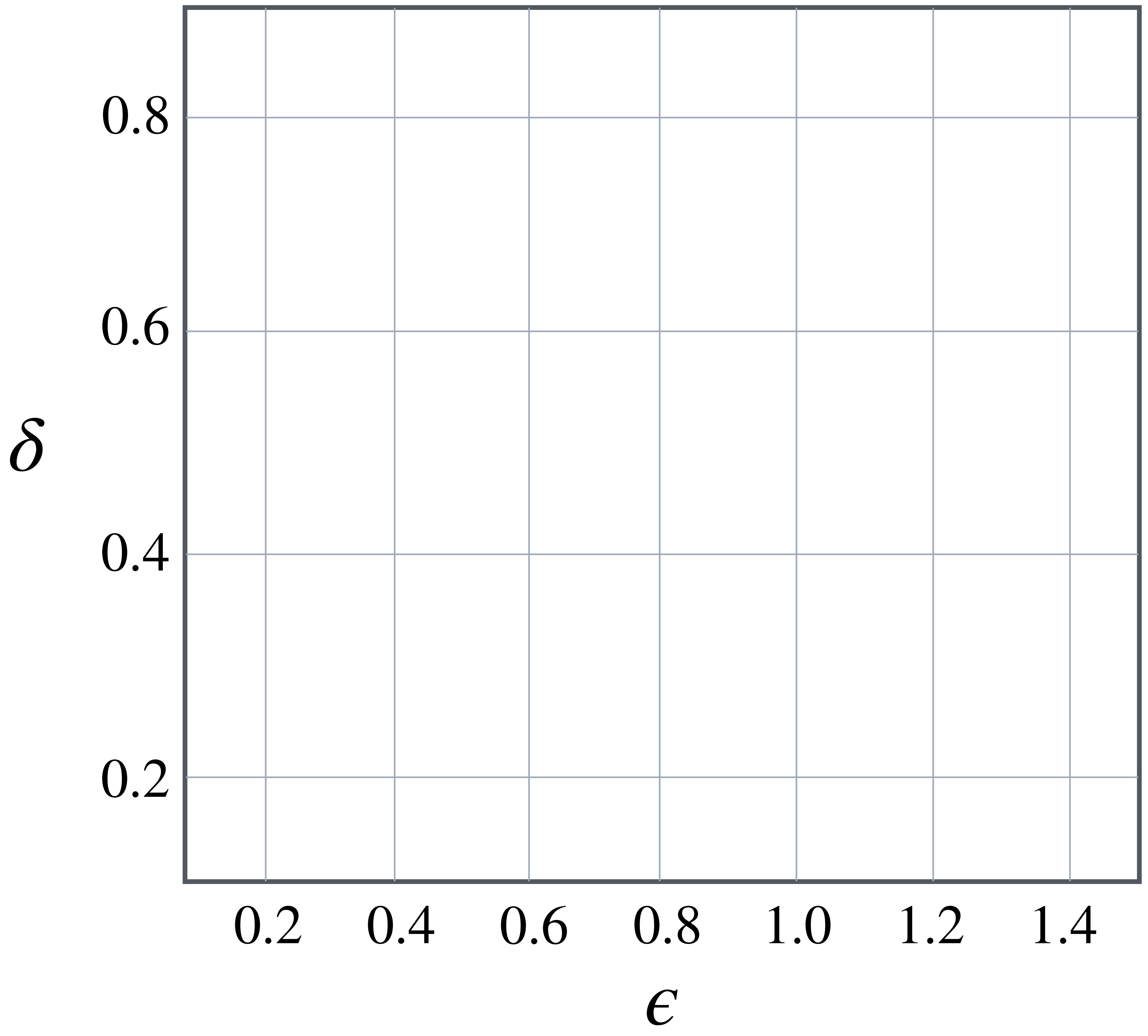

Energy conversion rate

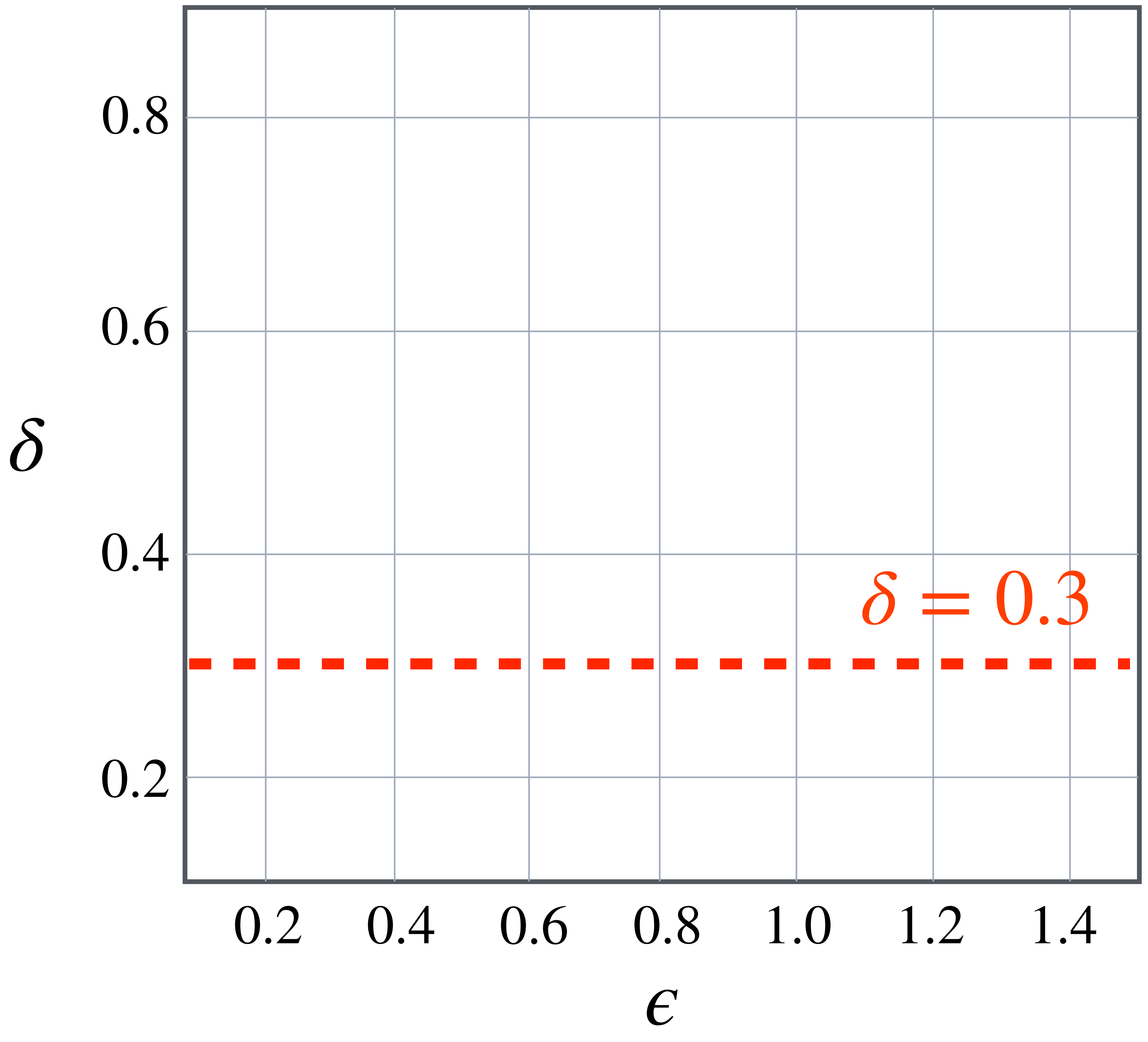

Energy conversion rate

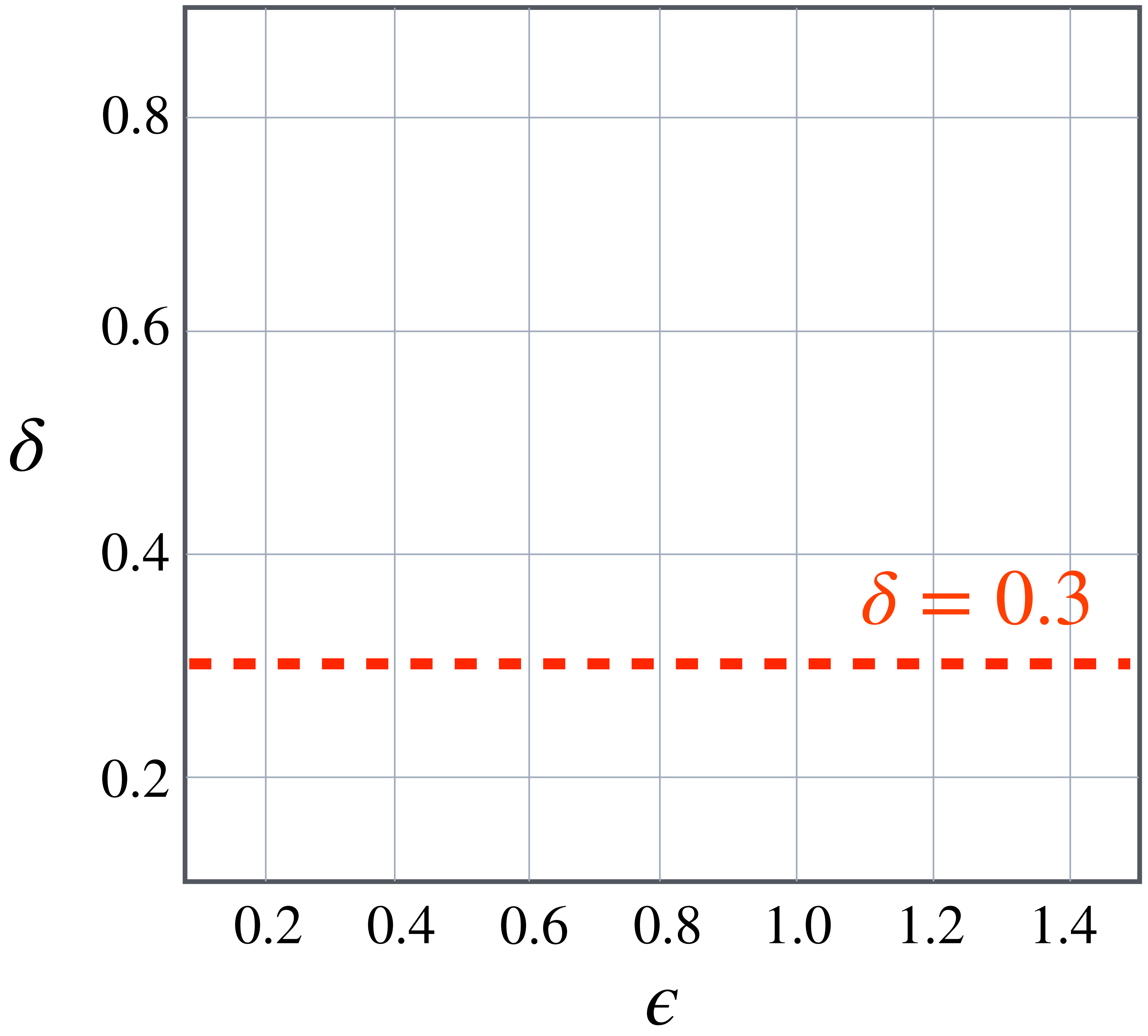

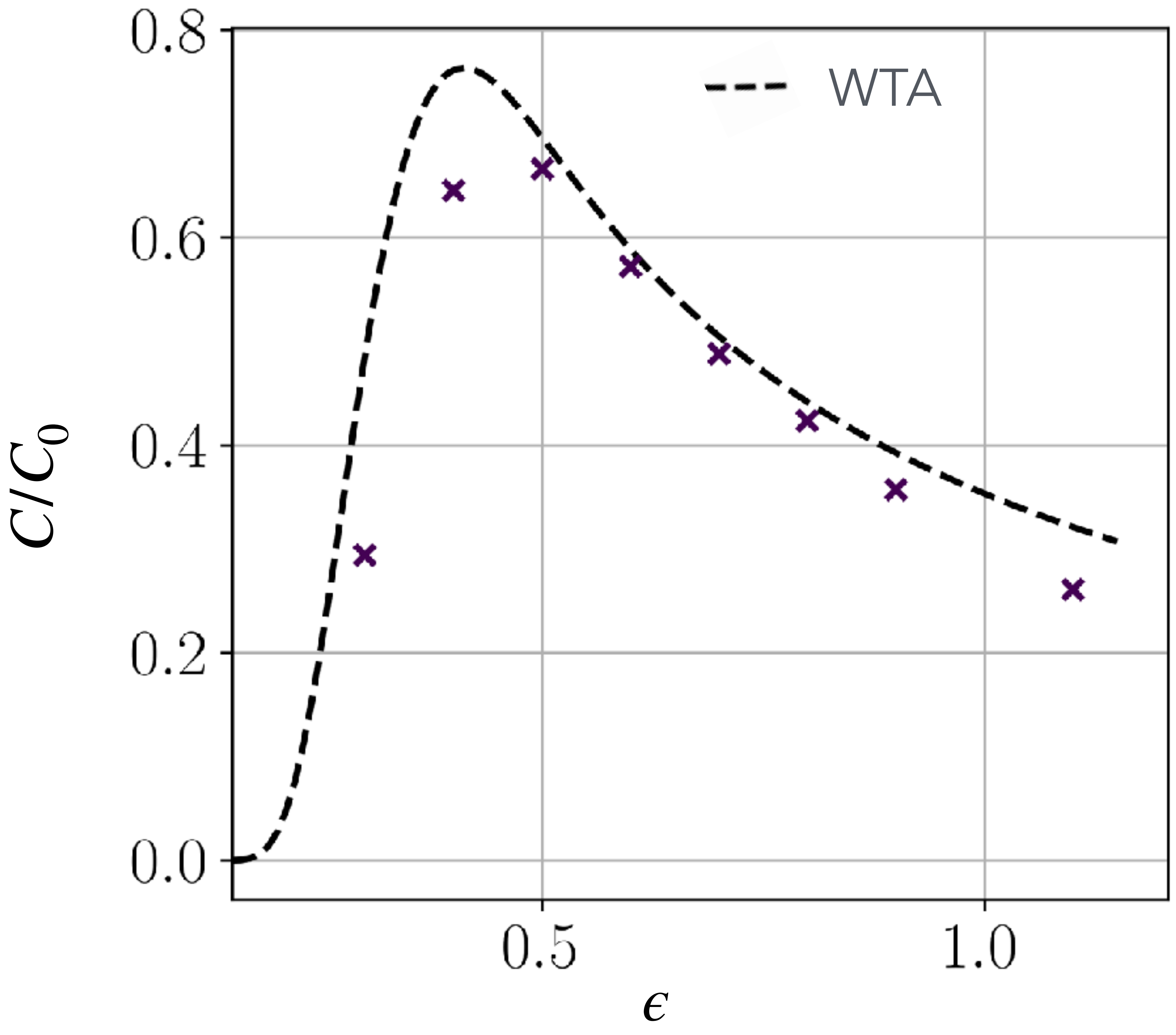

Energy conversion rate

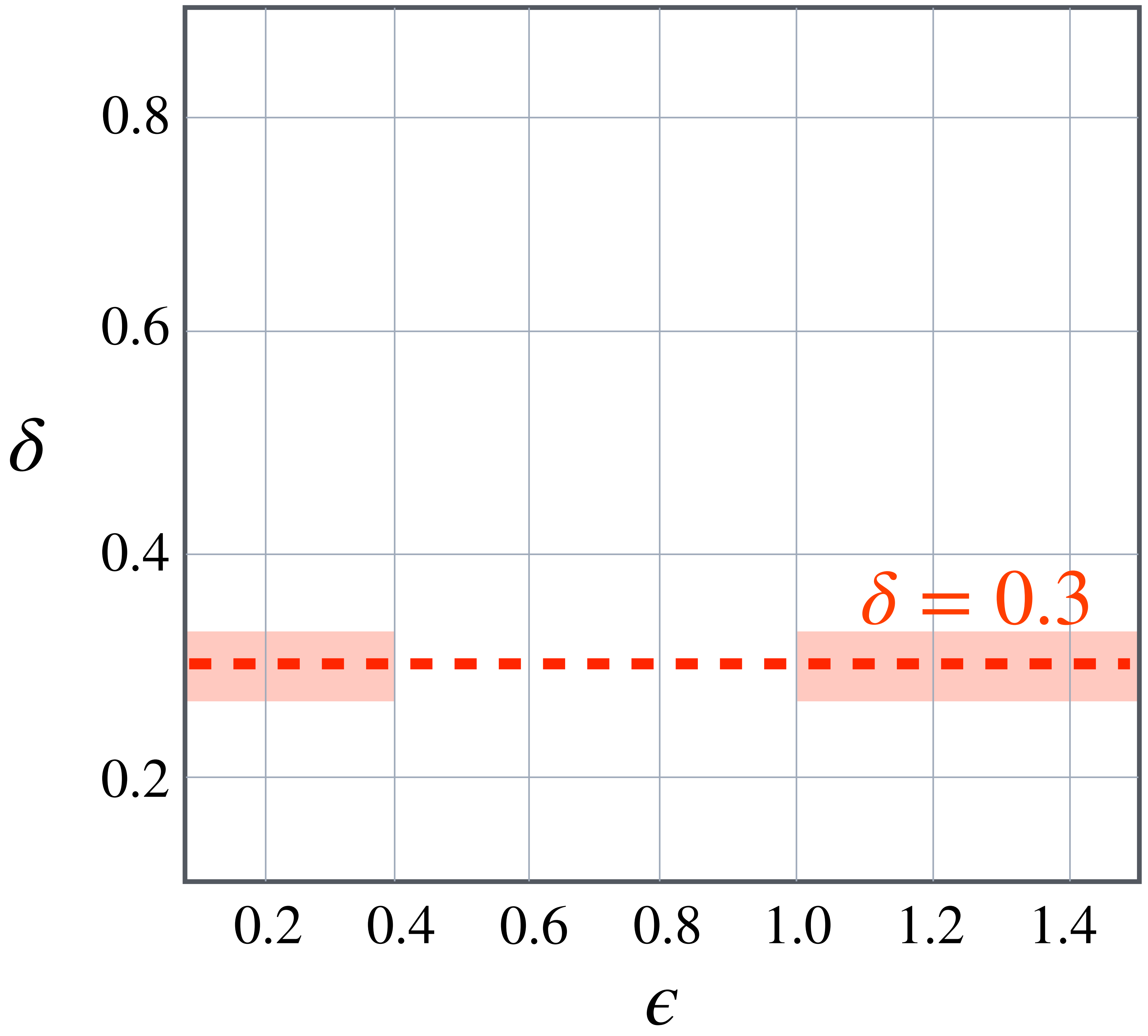

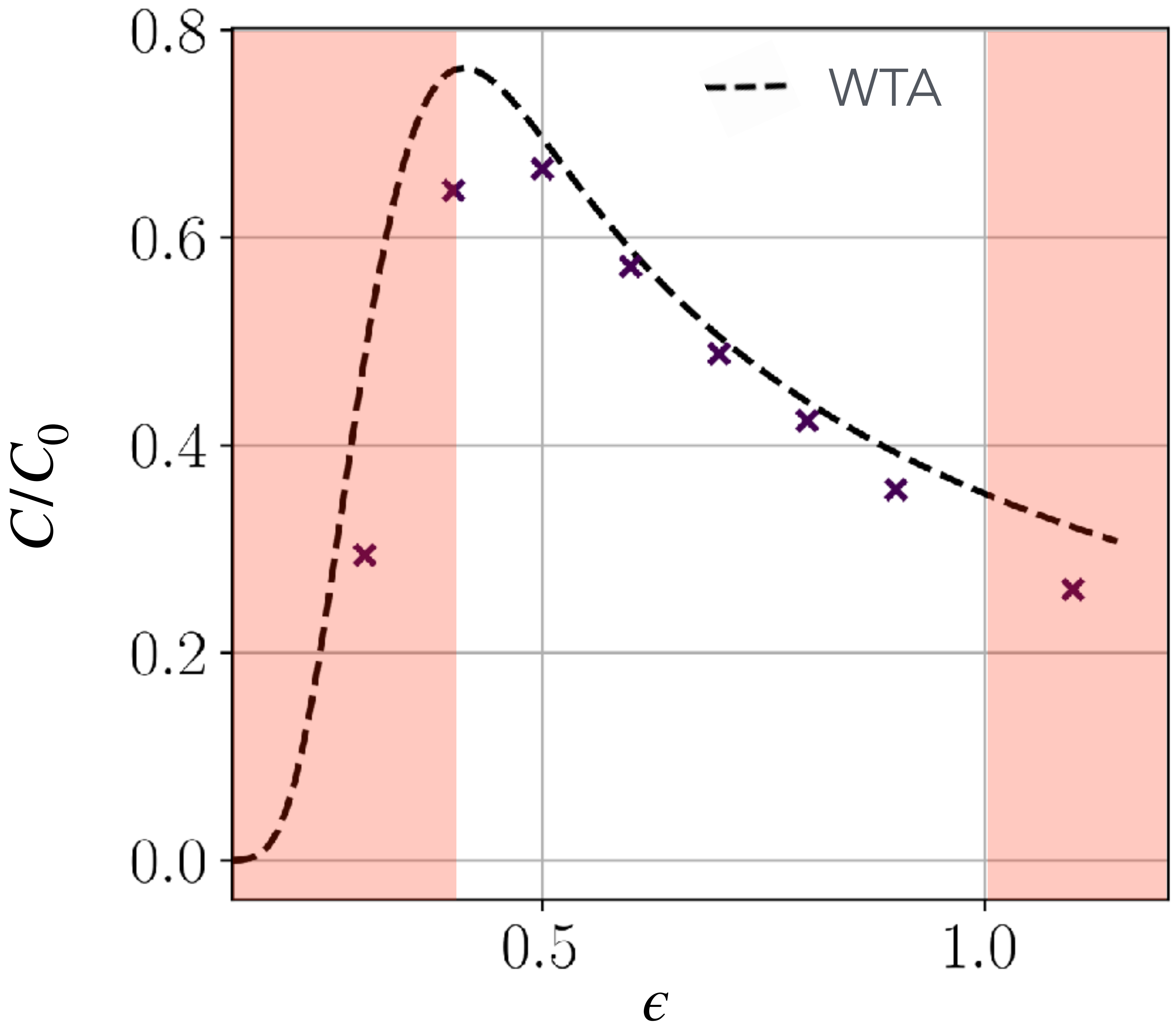

Energy conversion rate

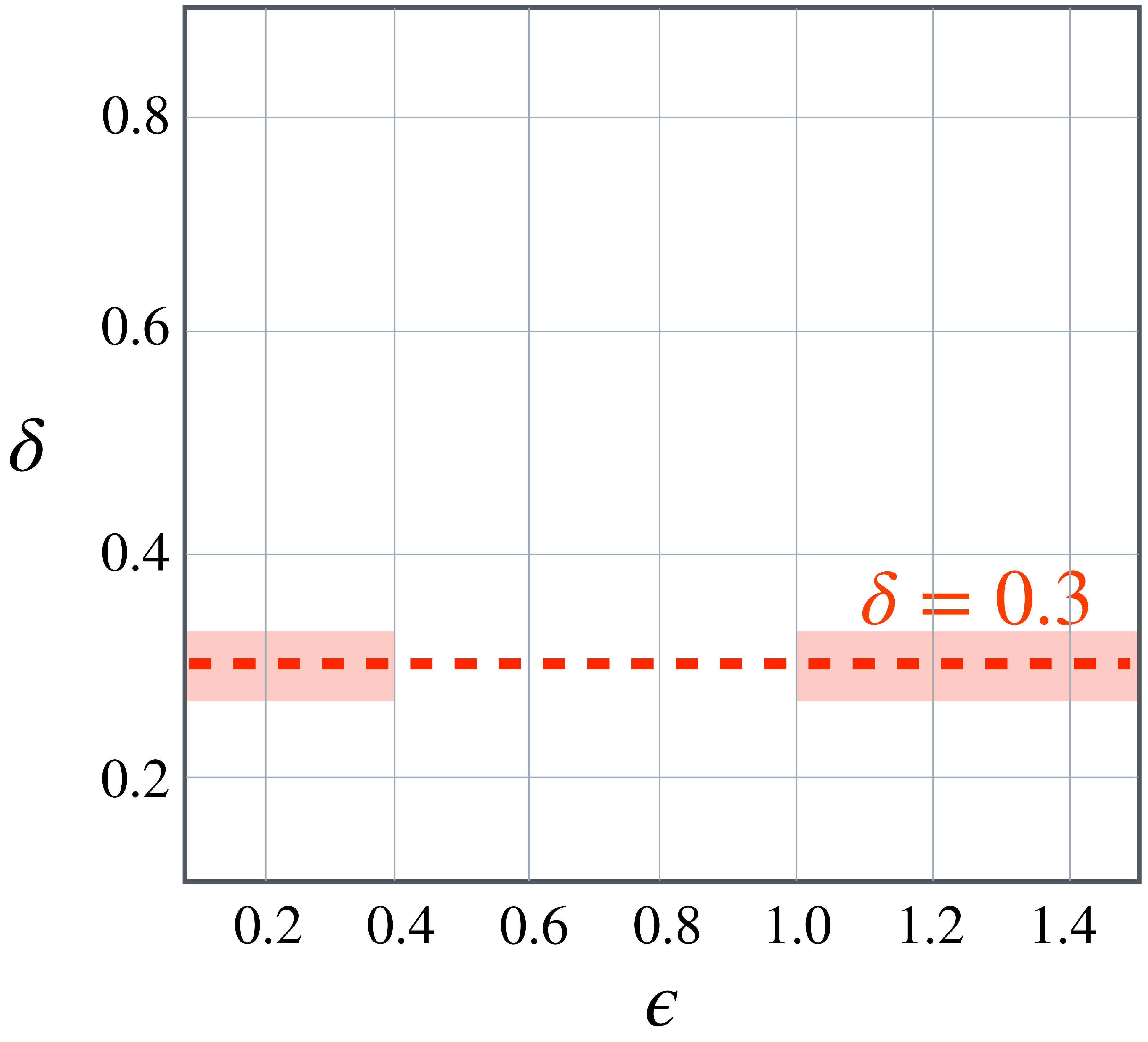

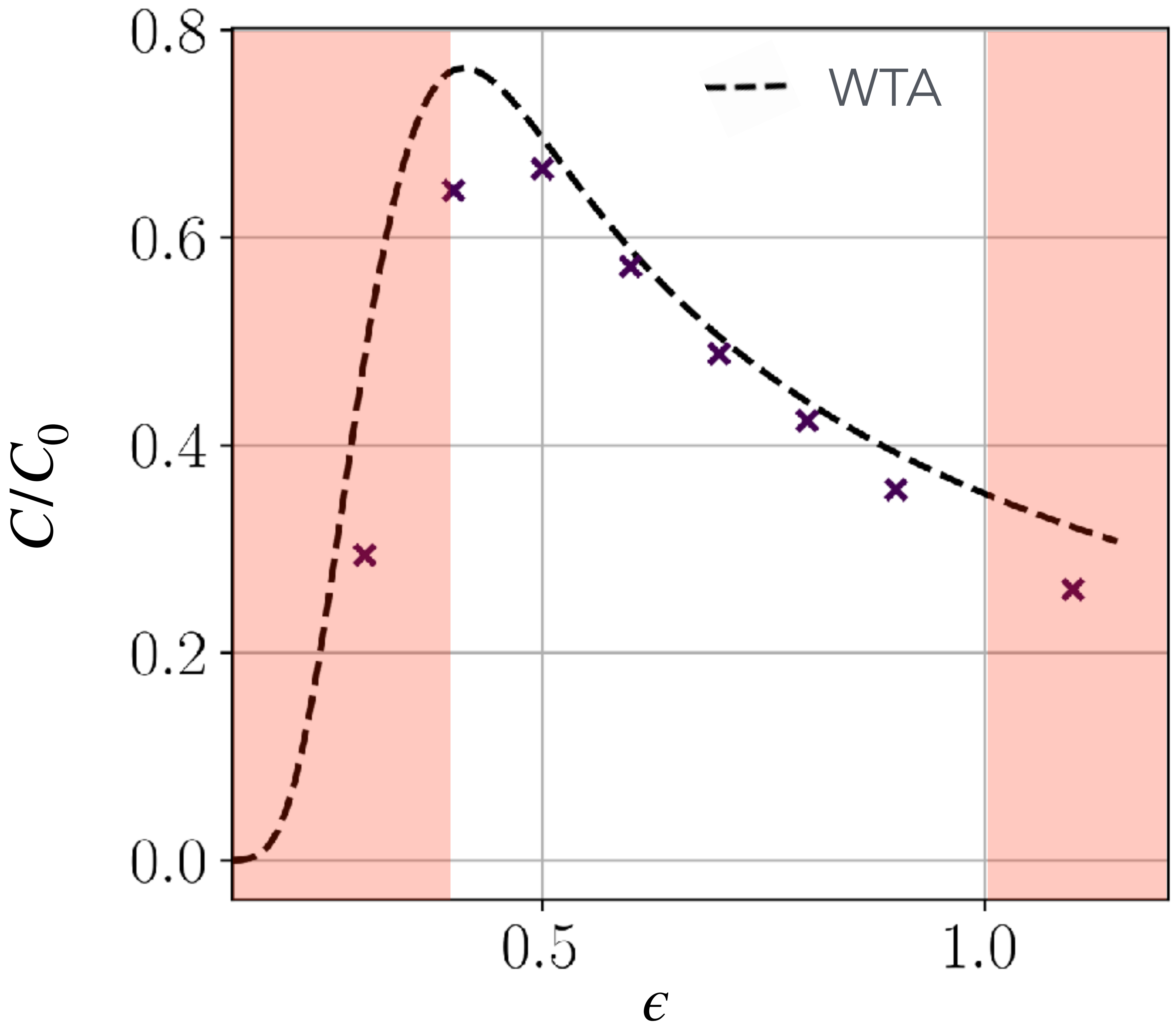

Energy conversion rate

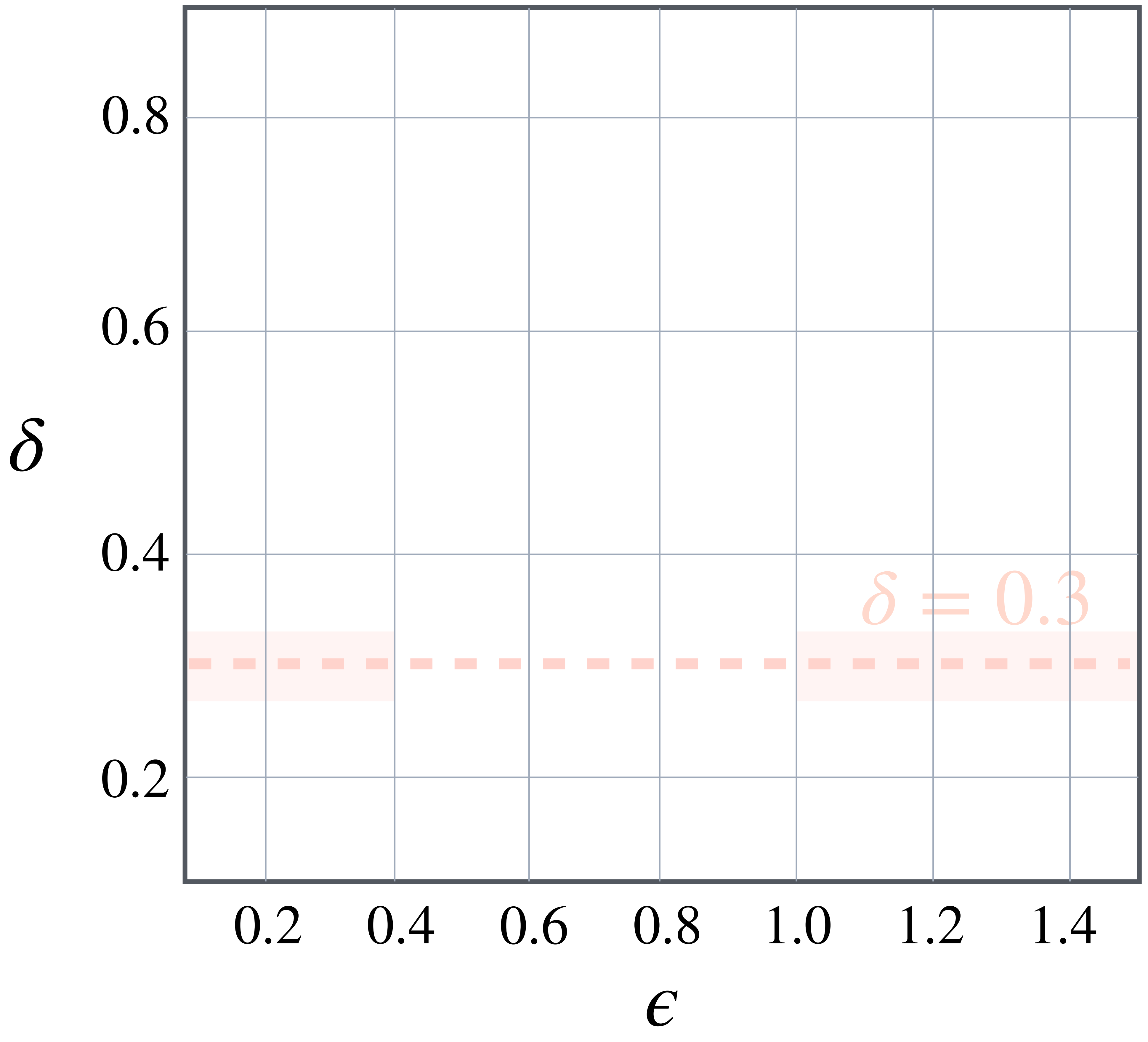

Energy conversion rate

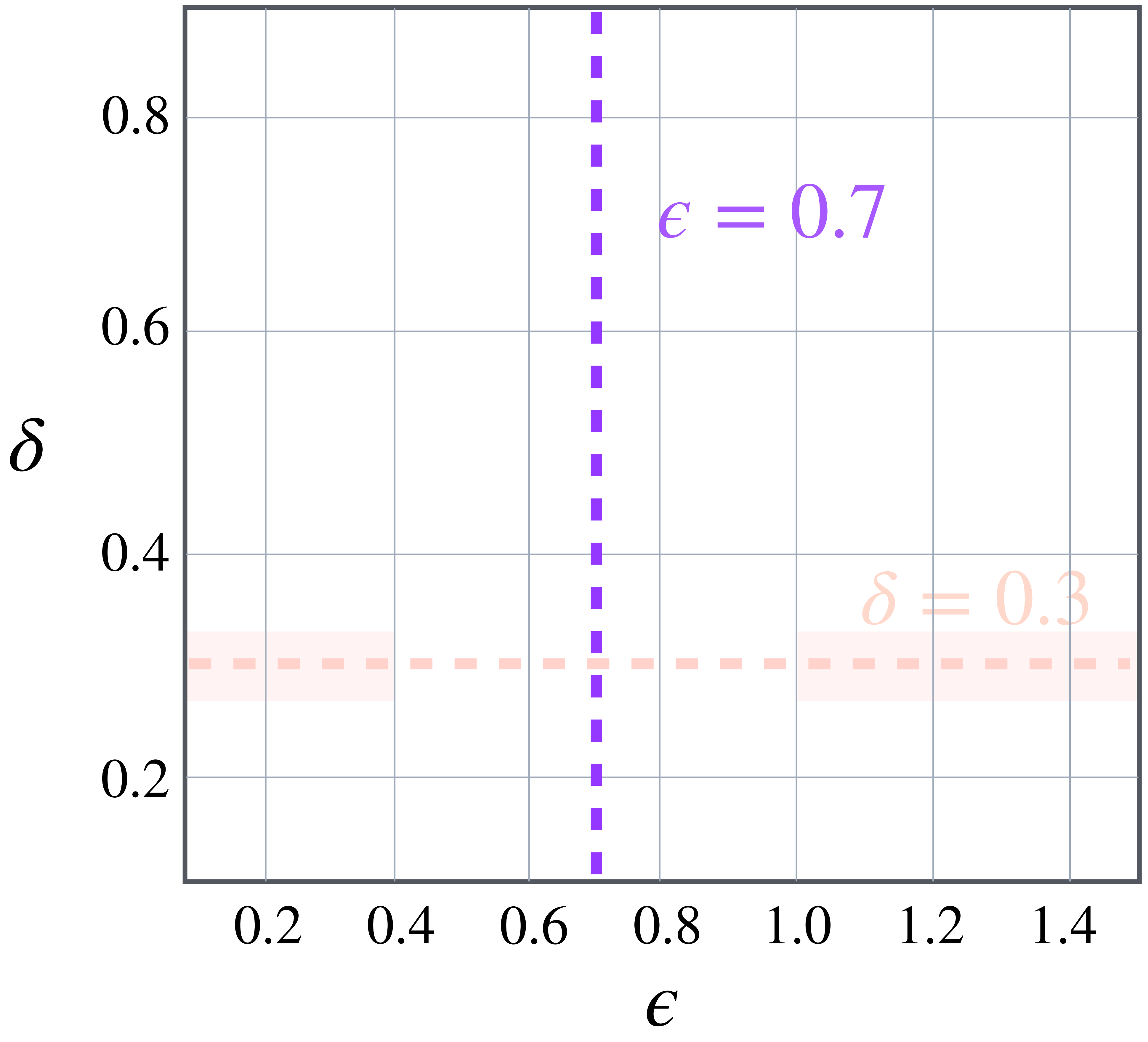

Energy conversion rate

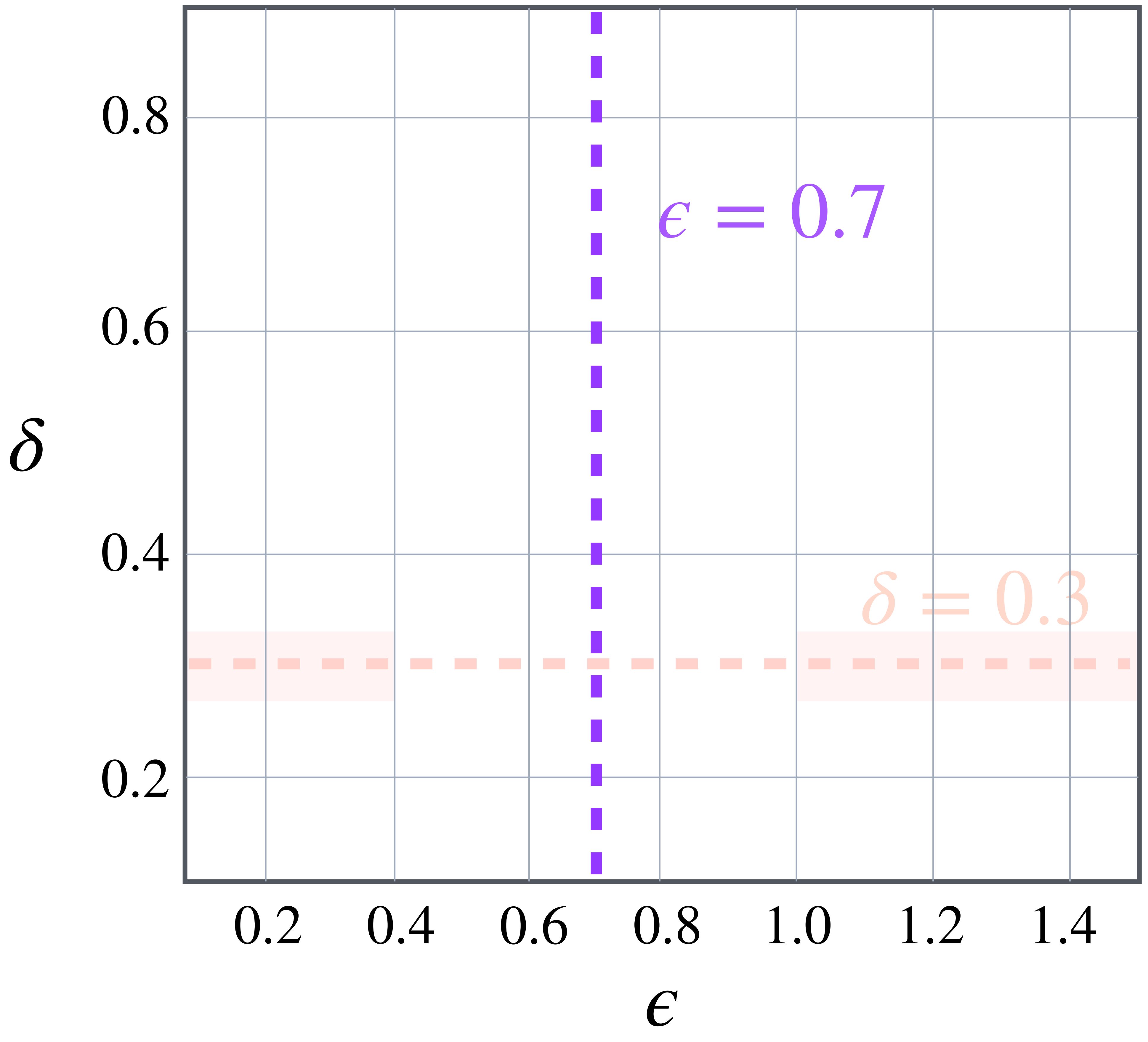

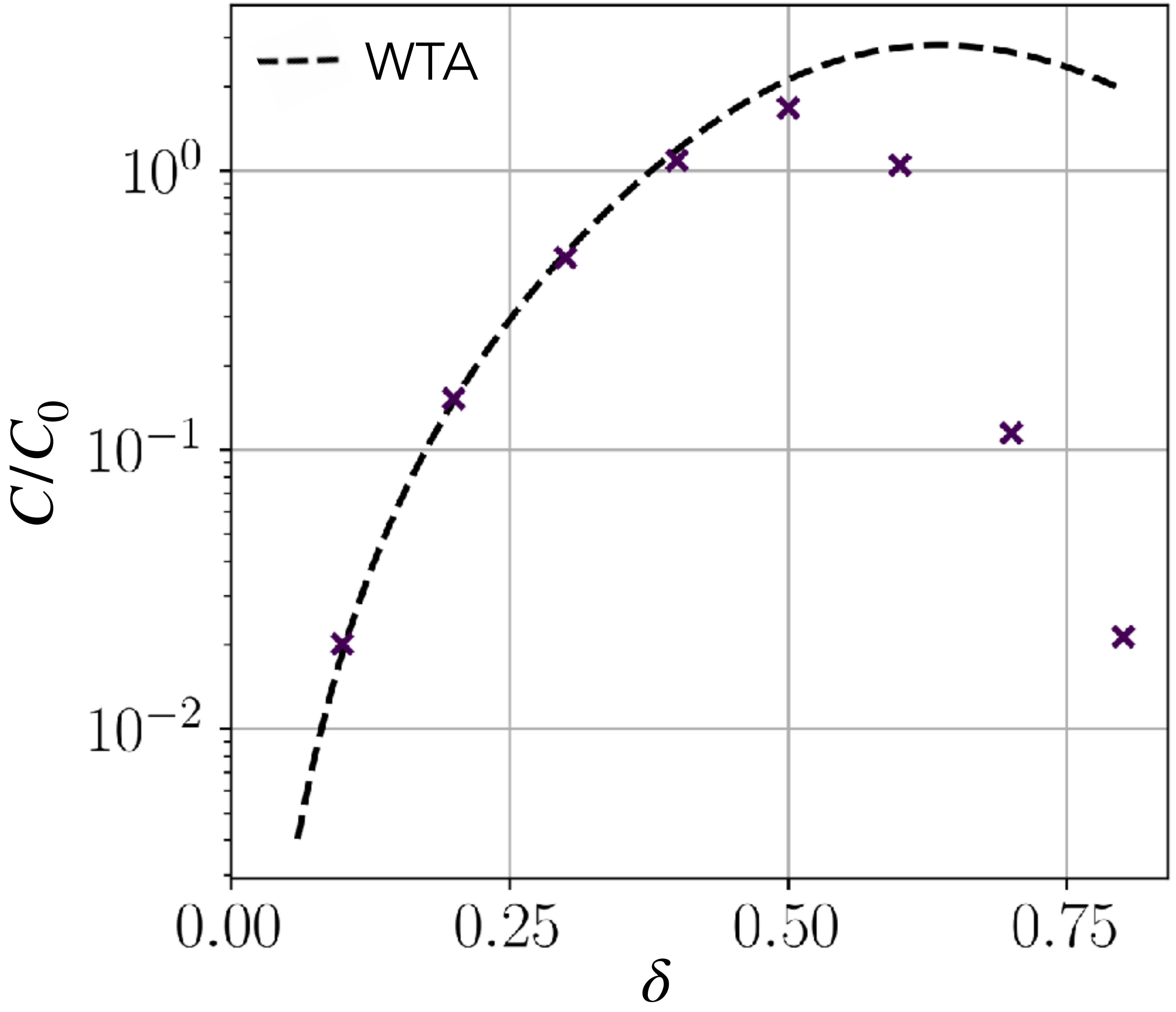

Energy conversion rate

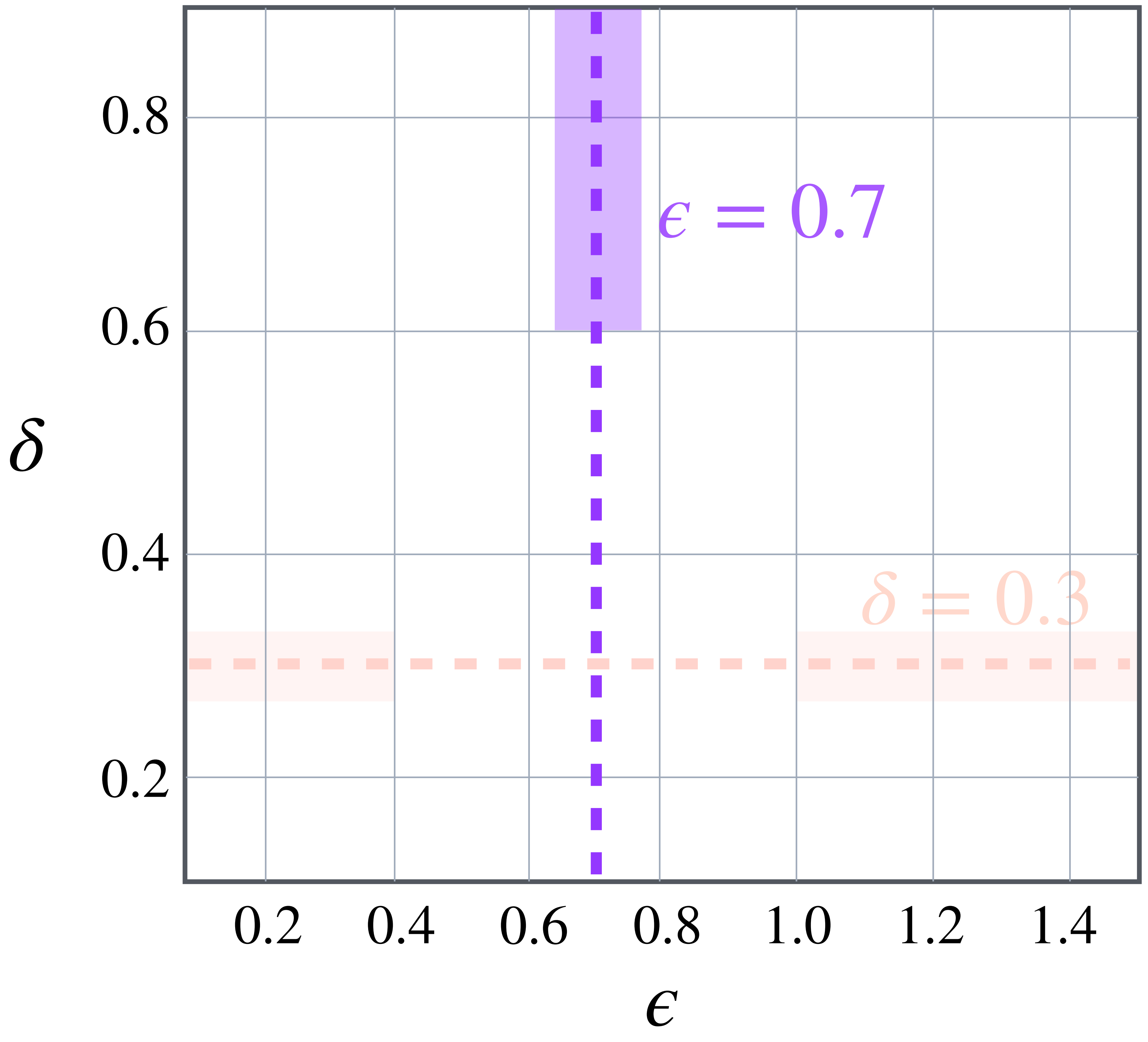

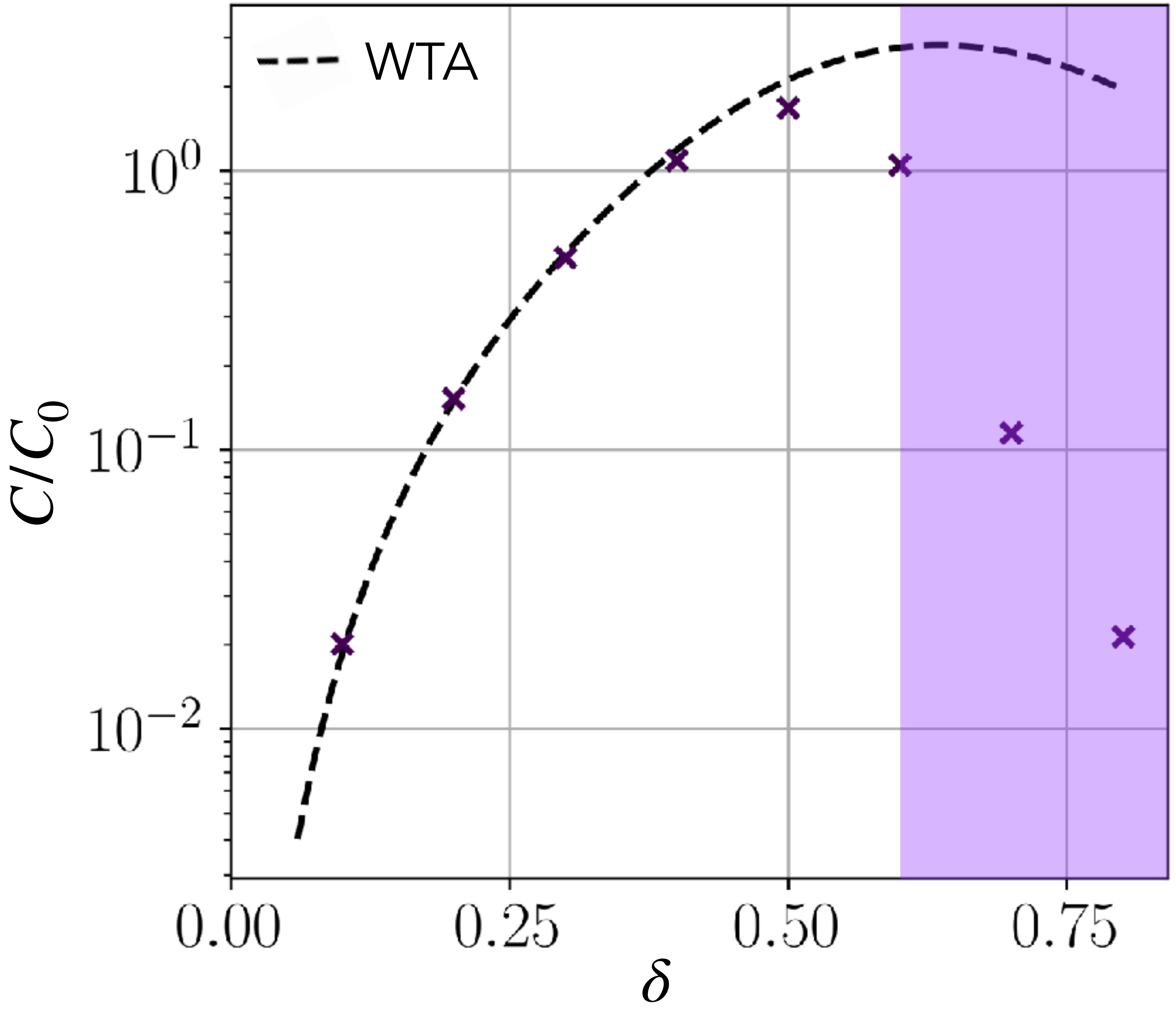

Energy conversion rate

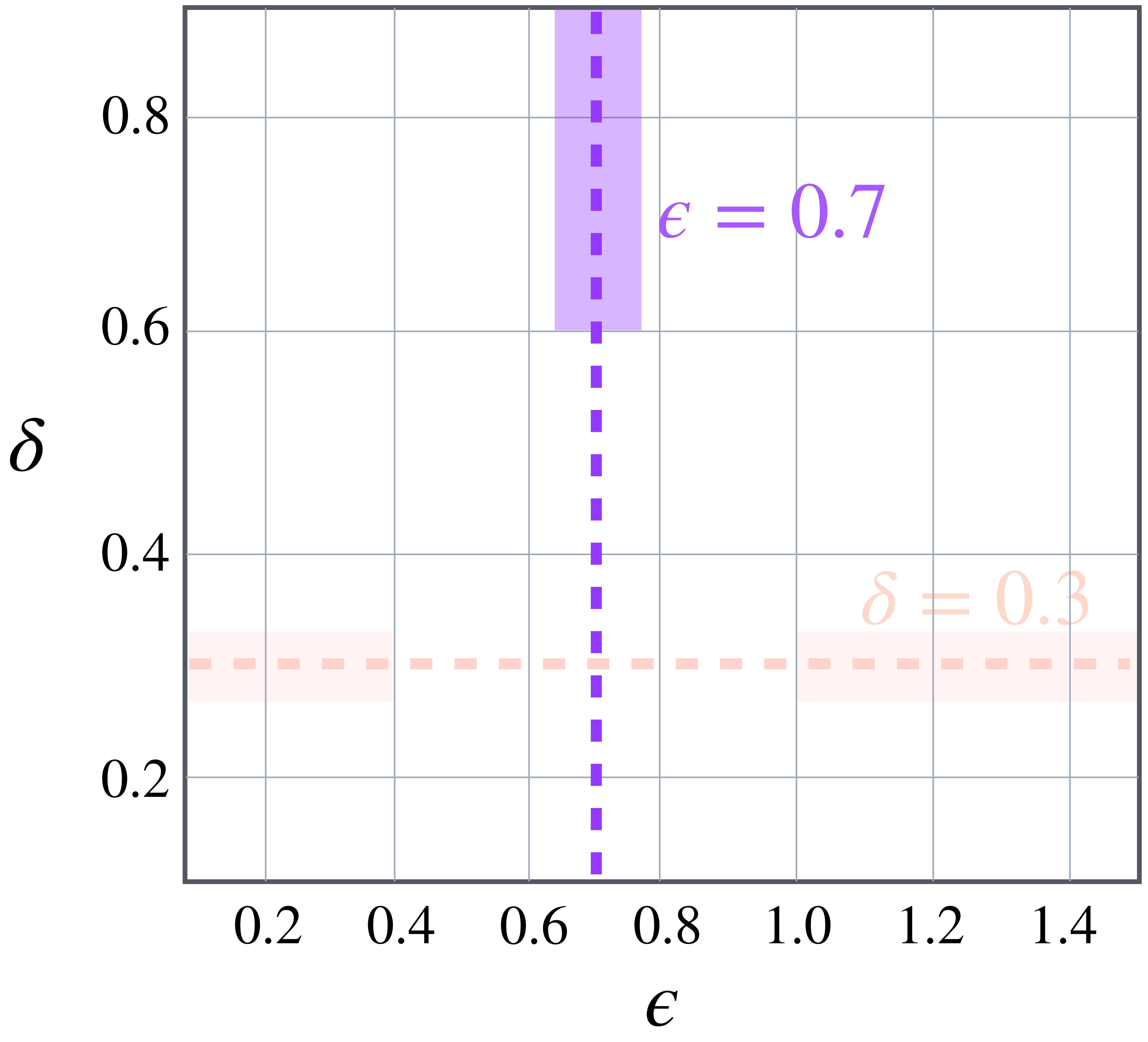

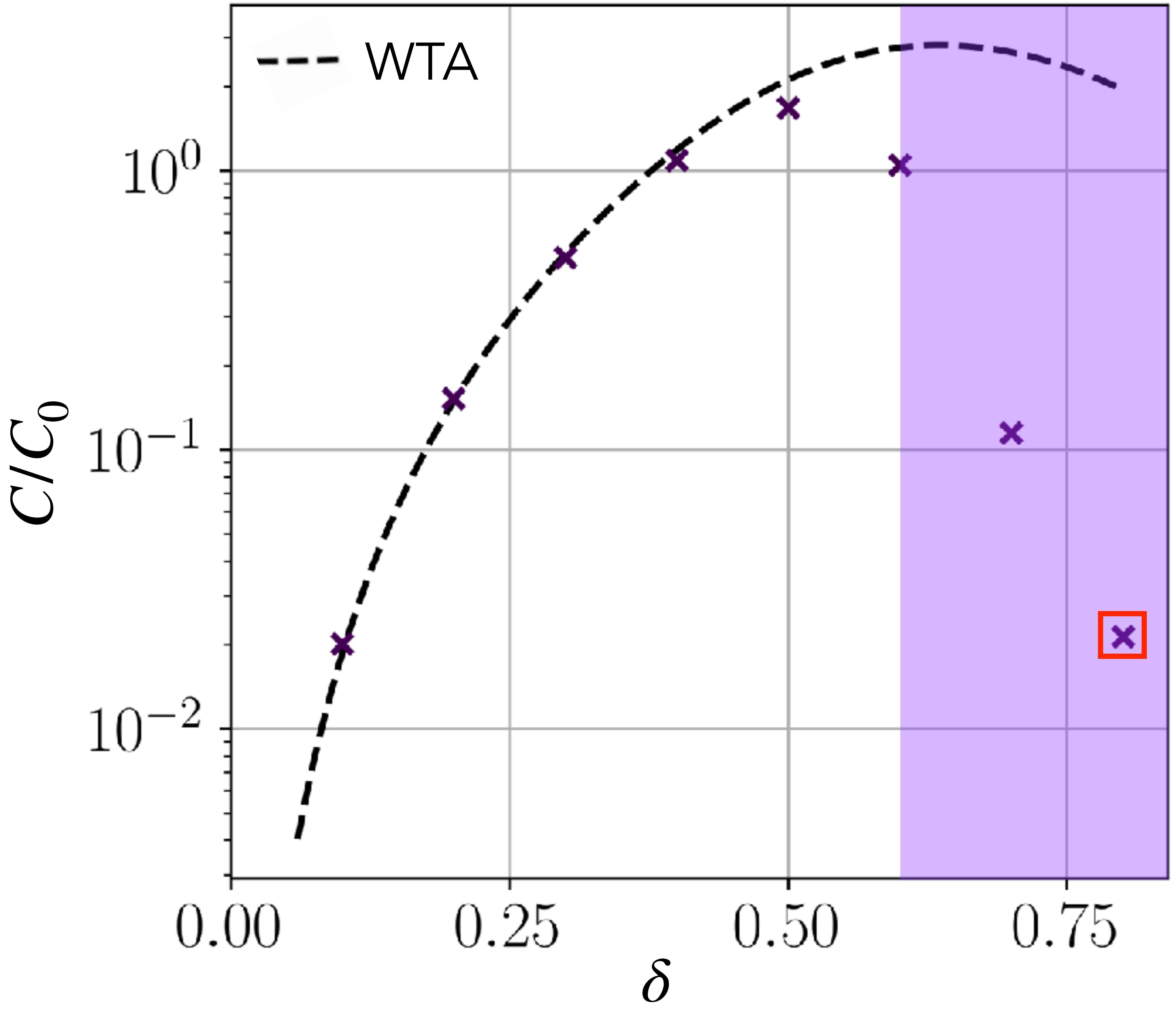

Non-radiating topographies ?

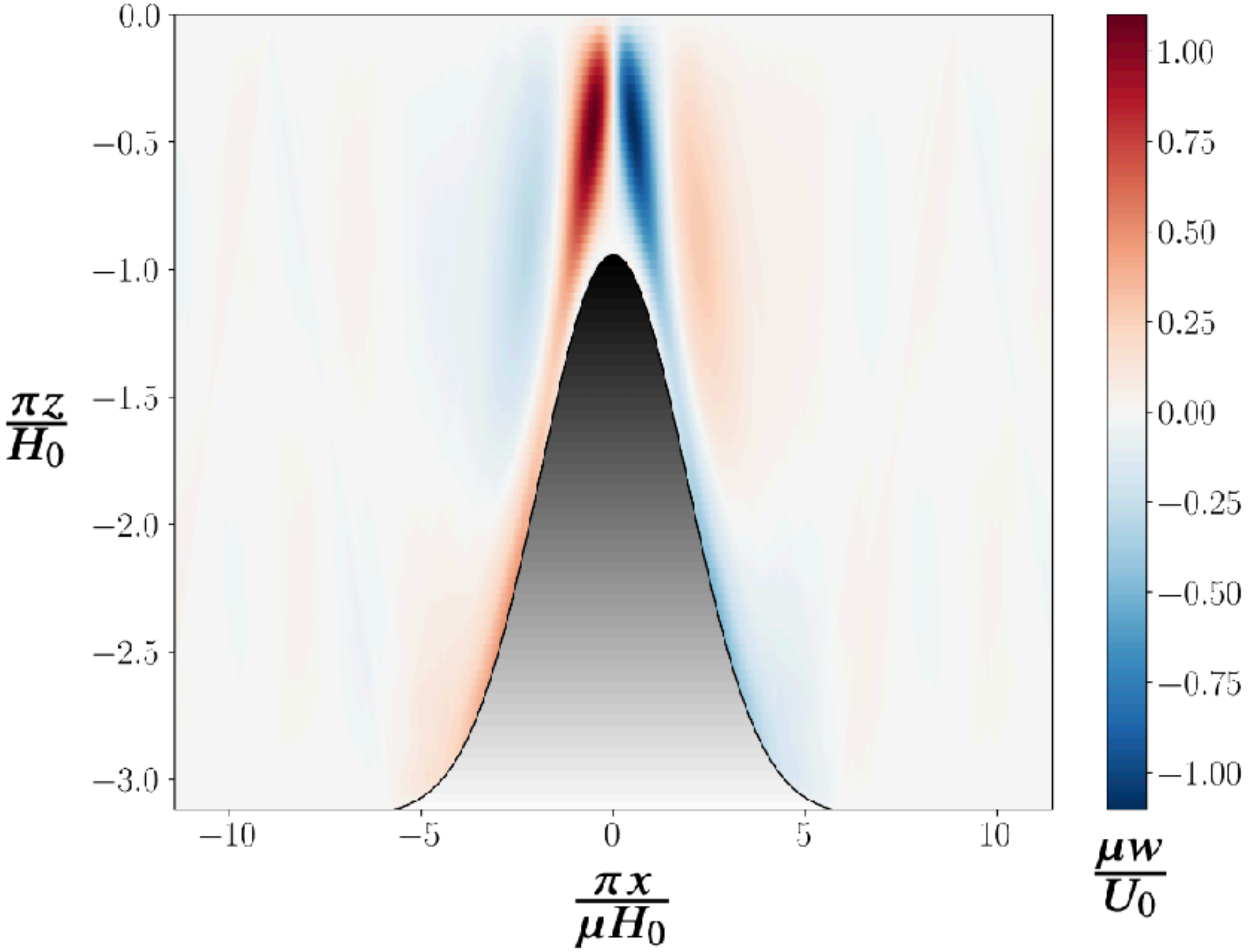

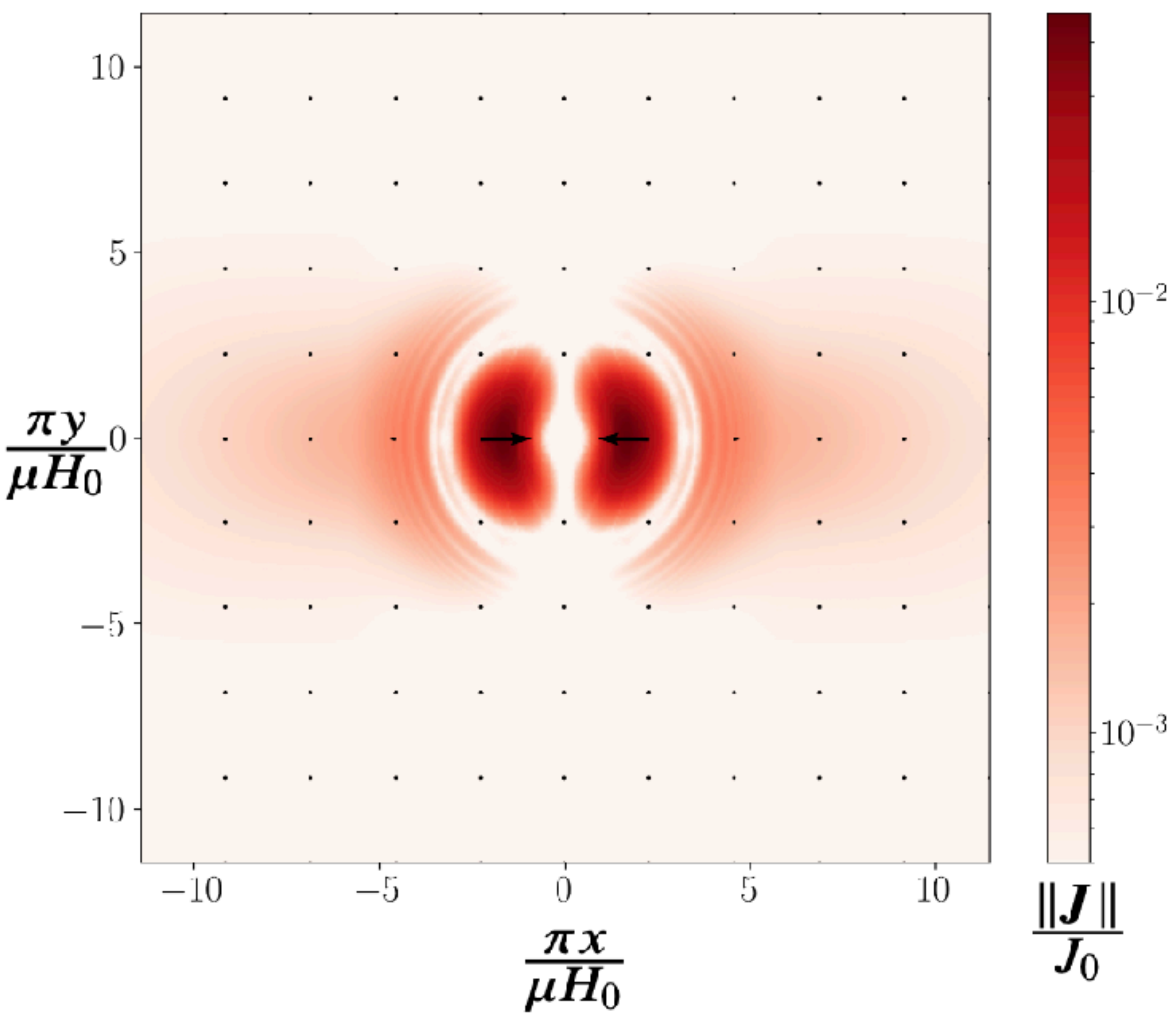

Energy conversion rate

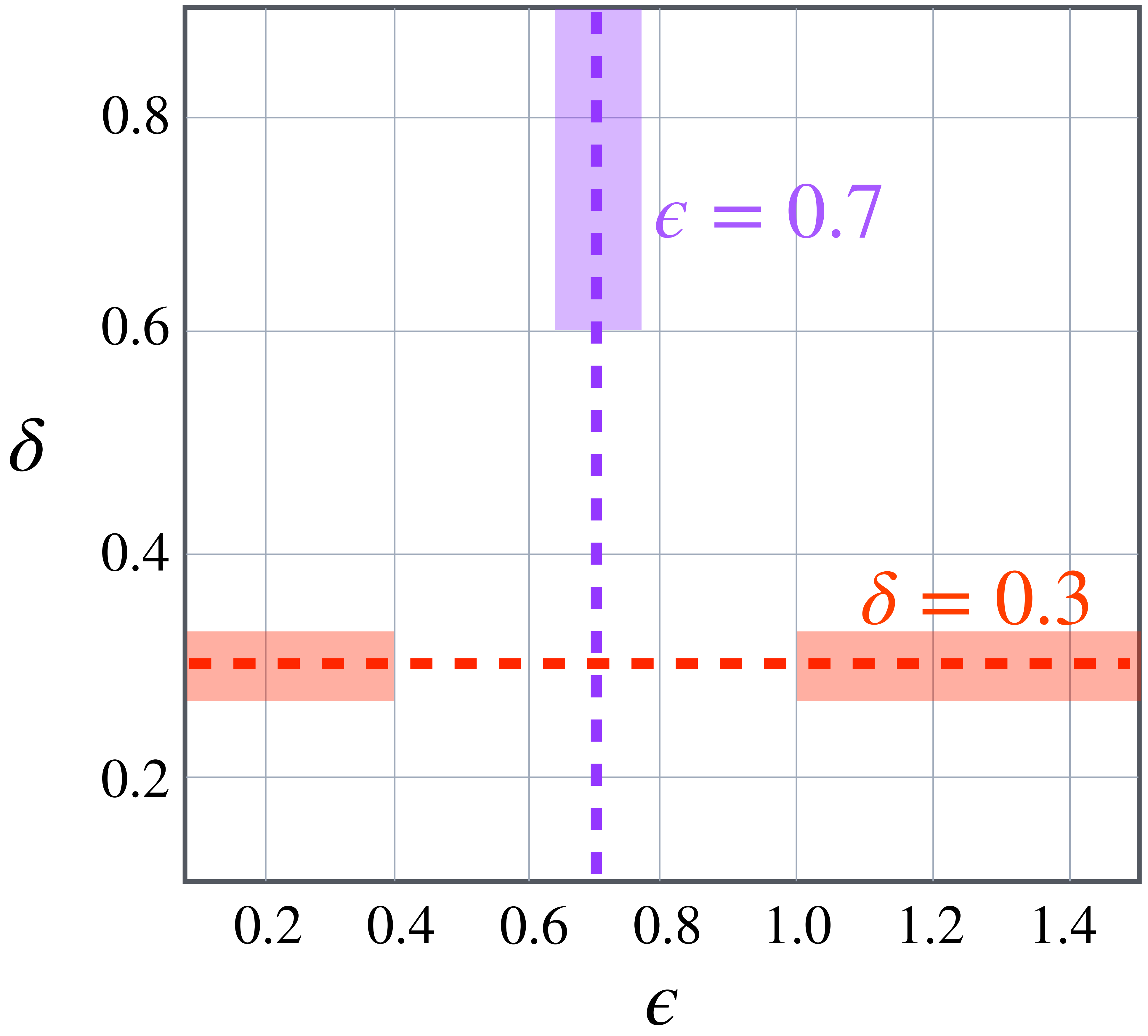

Energy conversion rate

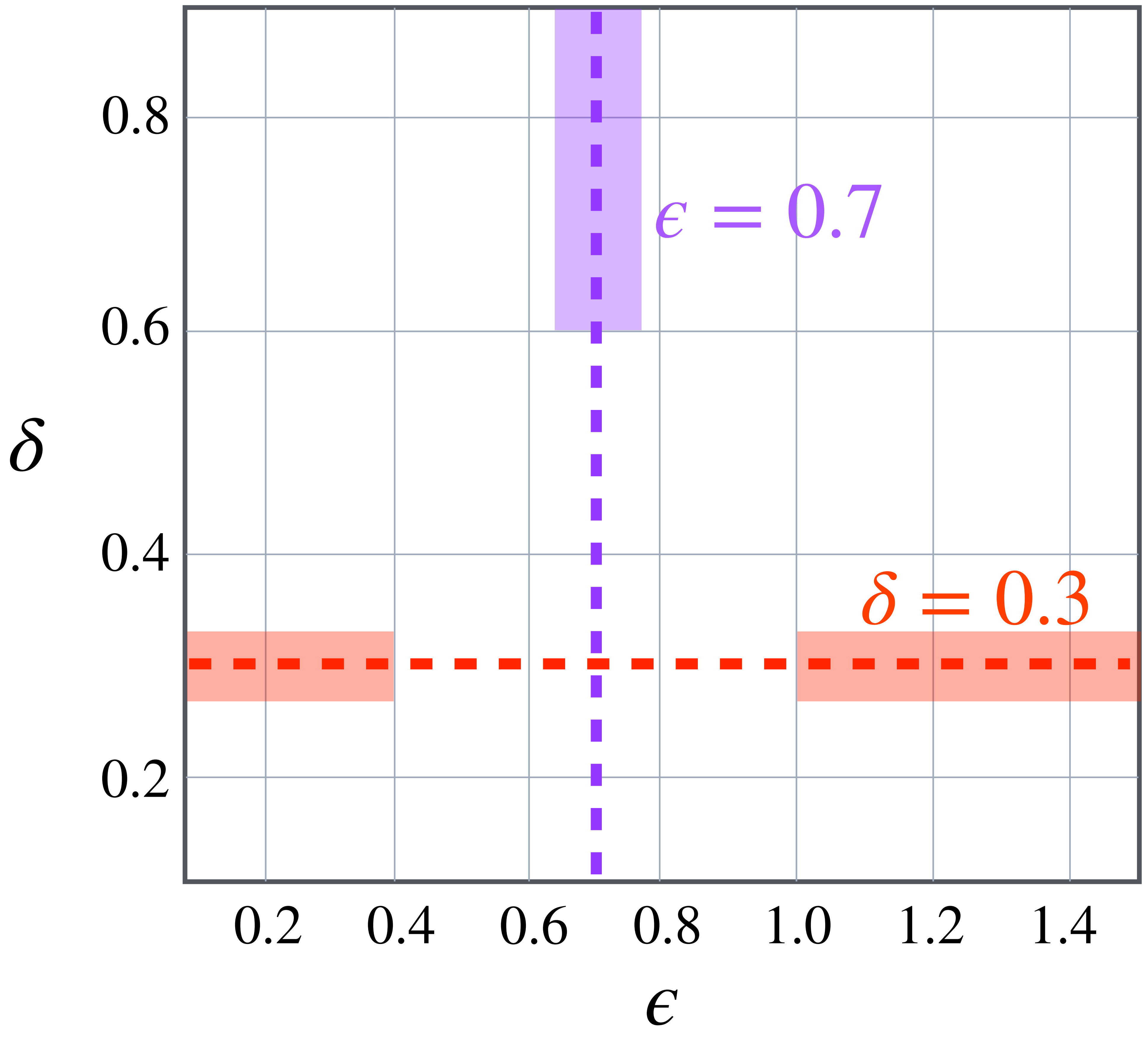

- WTA overestimates the conversion rate in the highlighted regions

Energy conversion rate

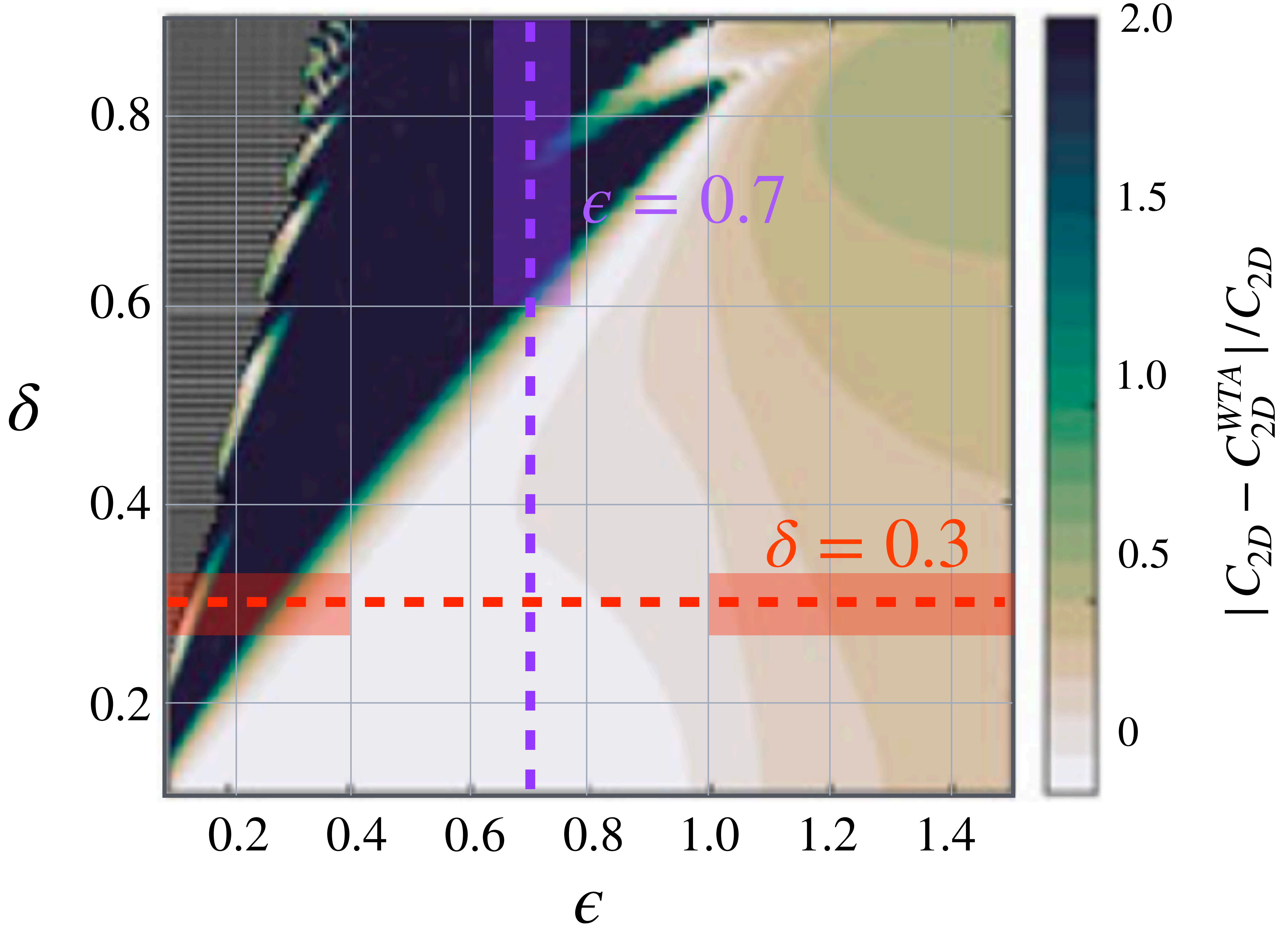

- WTA overestimates the conversion rate in the highlighted regions
- Similar qualitative results observed in 2D by *Papoutsellis et al* (2024)

Generation by a 2D Gaussian (from *Papoutsellis et al* (2024))

Energy conversion rate : influence of $\beta = f/\omega$

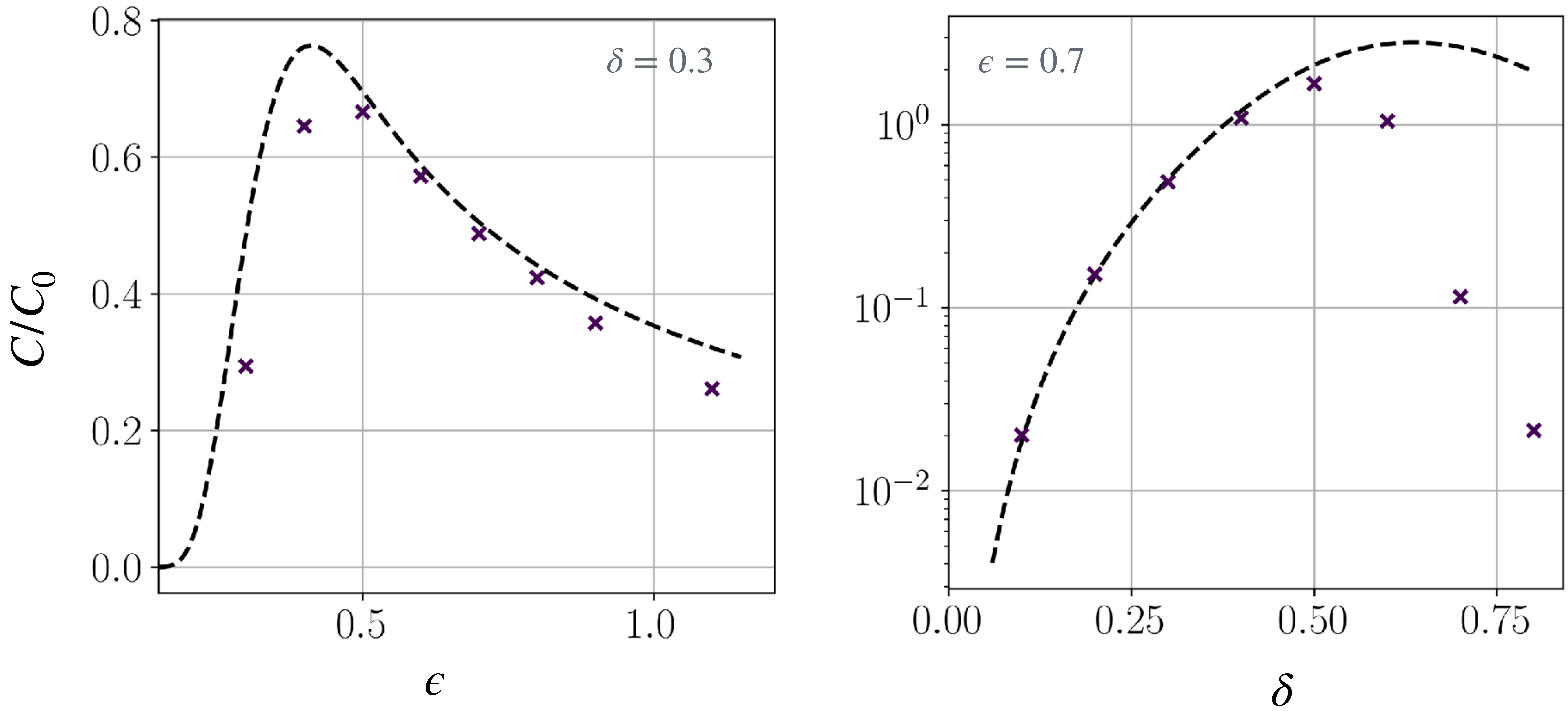

Energy conversion rate : influence of $\beta = f/\omega$

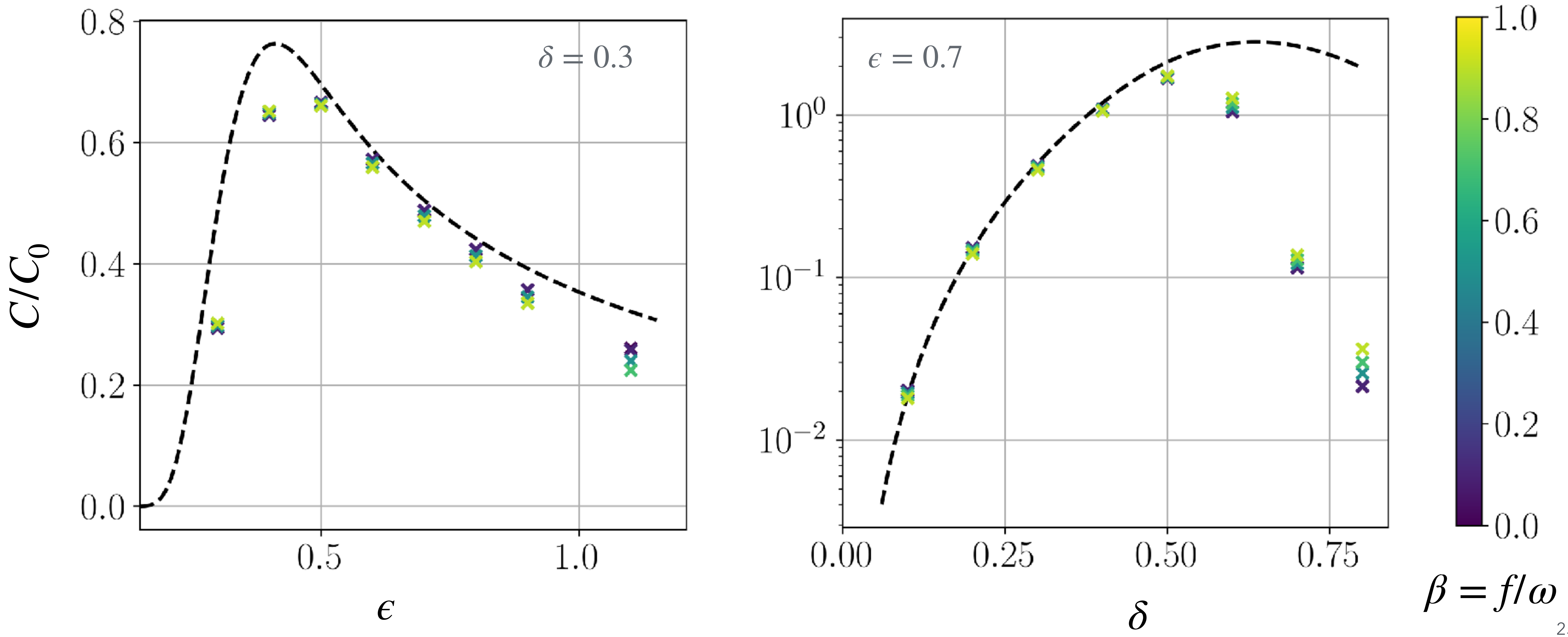

Horizontal cut of vertical velocity w

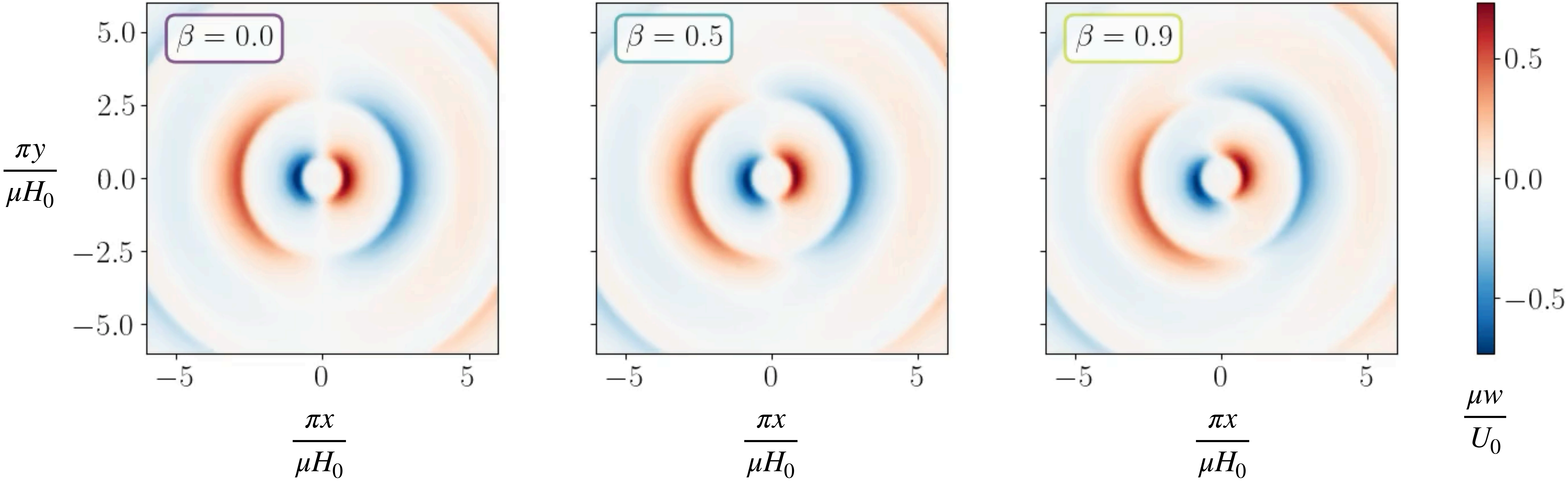

$\delta = 0.3$ and $\epsilon = 0.7$

Horizontal cut of vertical velocity w

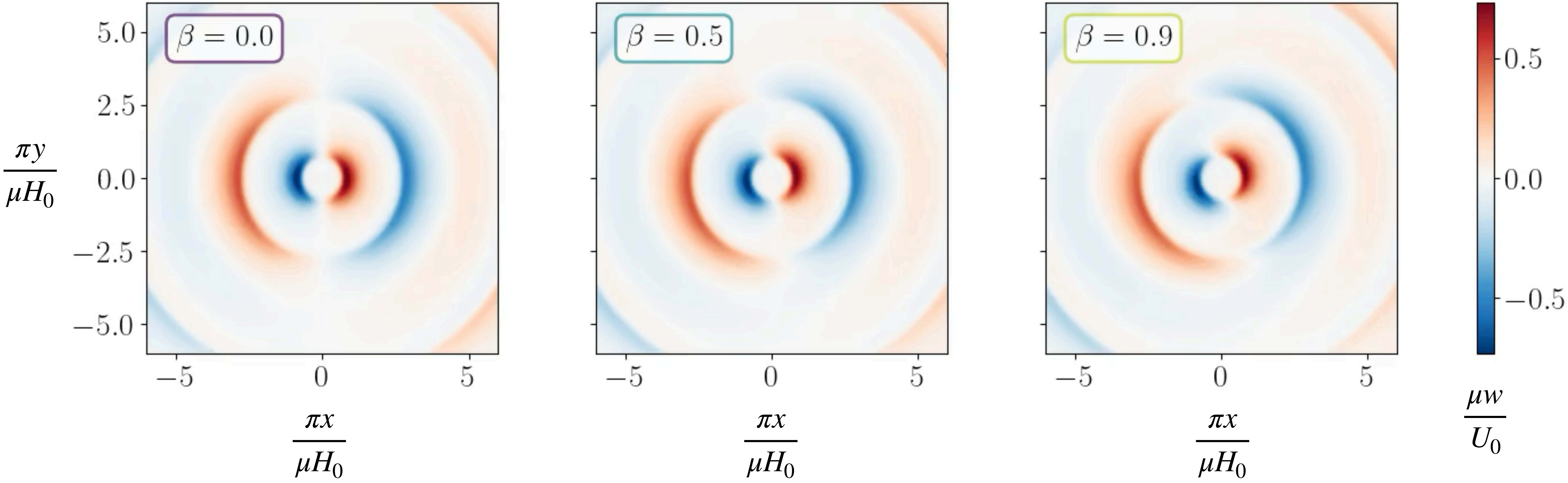

$\delta = 0.3$ and $\epsilon = 0.7$

Horizontal cut of vertical velocity w

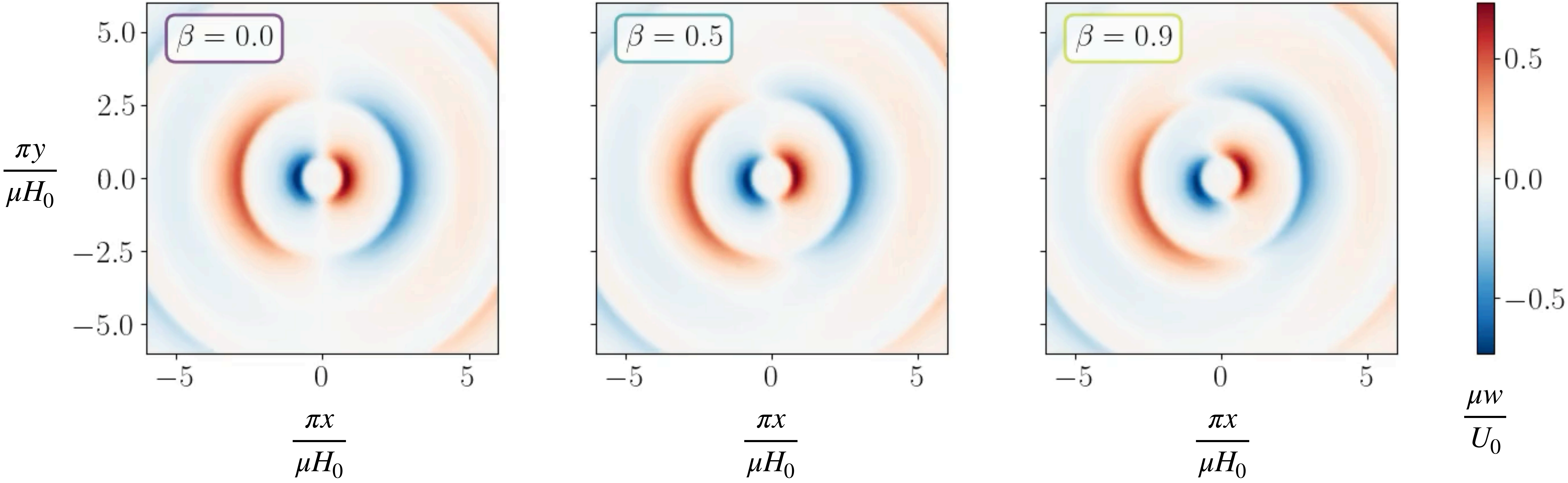

$\delta = 0.3$ and $\epsilon = 0.7$

Horizontal cut of horizontal velocity u

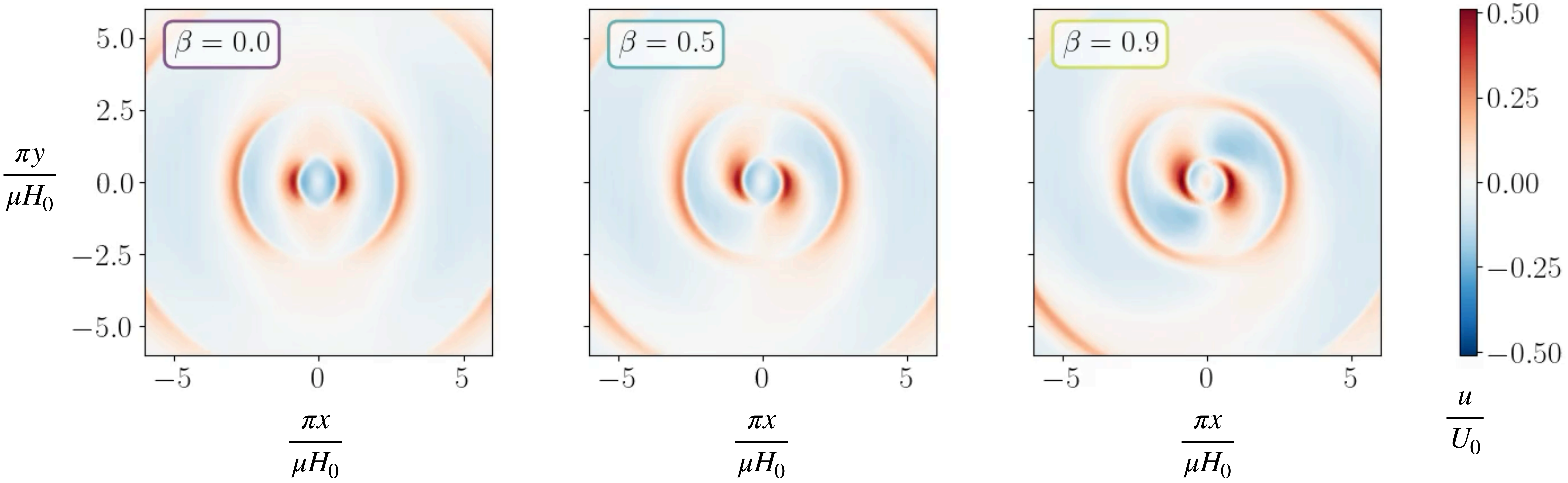

$\delta = 0.3$ and $\epsilon = 0.7$

Horizontal cut of horizontal velocity $\boldsymbol{u}$

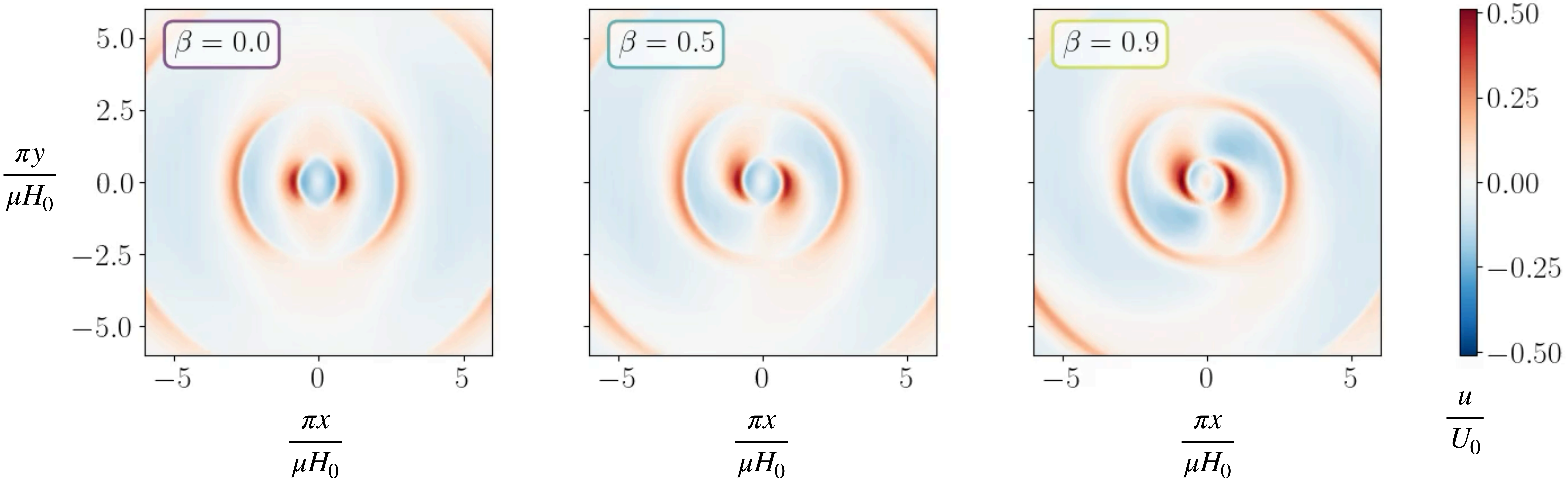

$\delta = 0.3$ and $\epsilon = 0.7$

Horizontal cut of horizontal velocity u

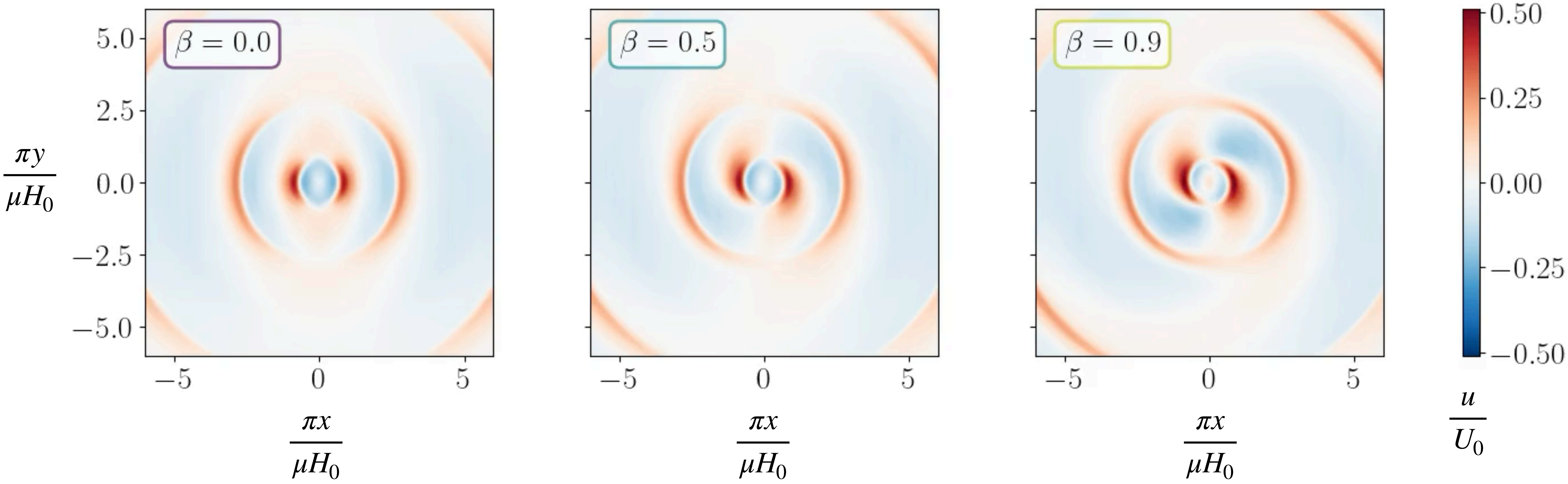

$\delta = 0.3$ and $\epsilon = 0.7$

Horizontal cut of horizontal velocity v

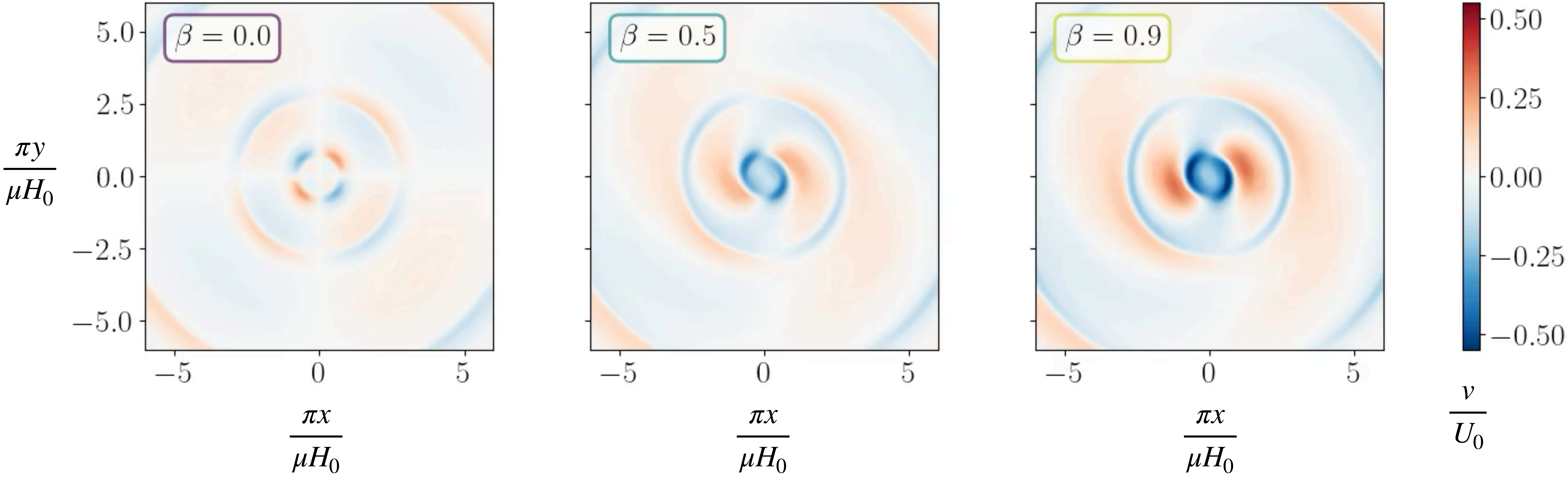

$\delta = 0.3$ and $\epsilon = 0.7$

Horizontal cut of horizontal velocity v

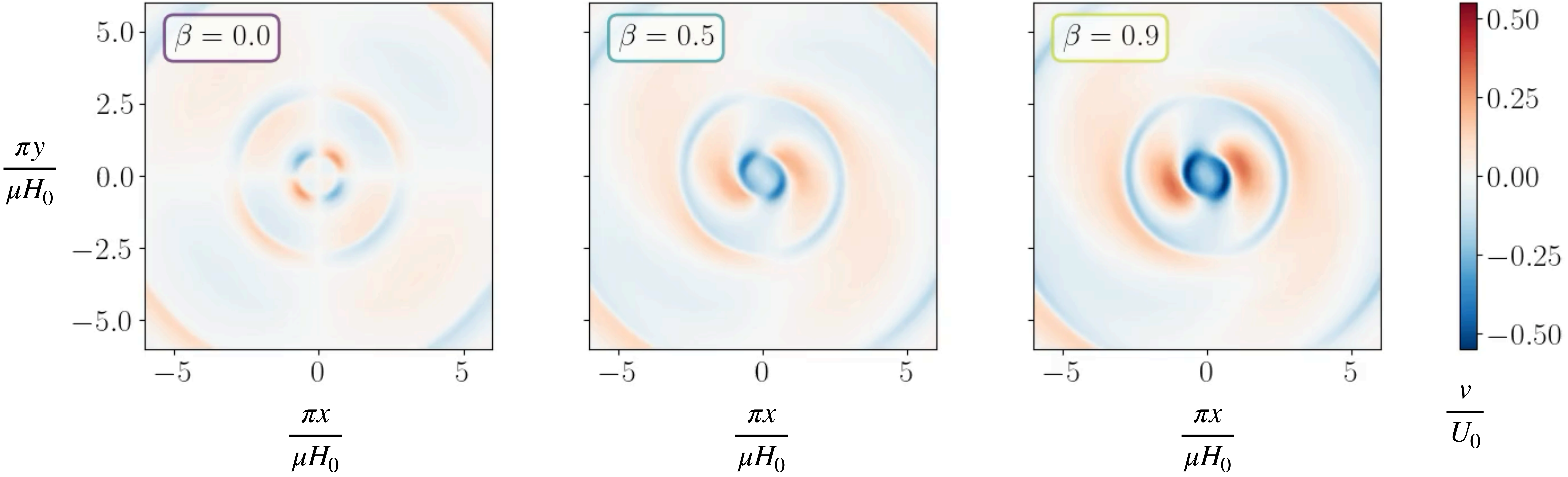

$\delta = 0.3$ and $\epsilon = 0.7$

Horizontal cut of horizontal velocity v

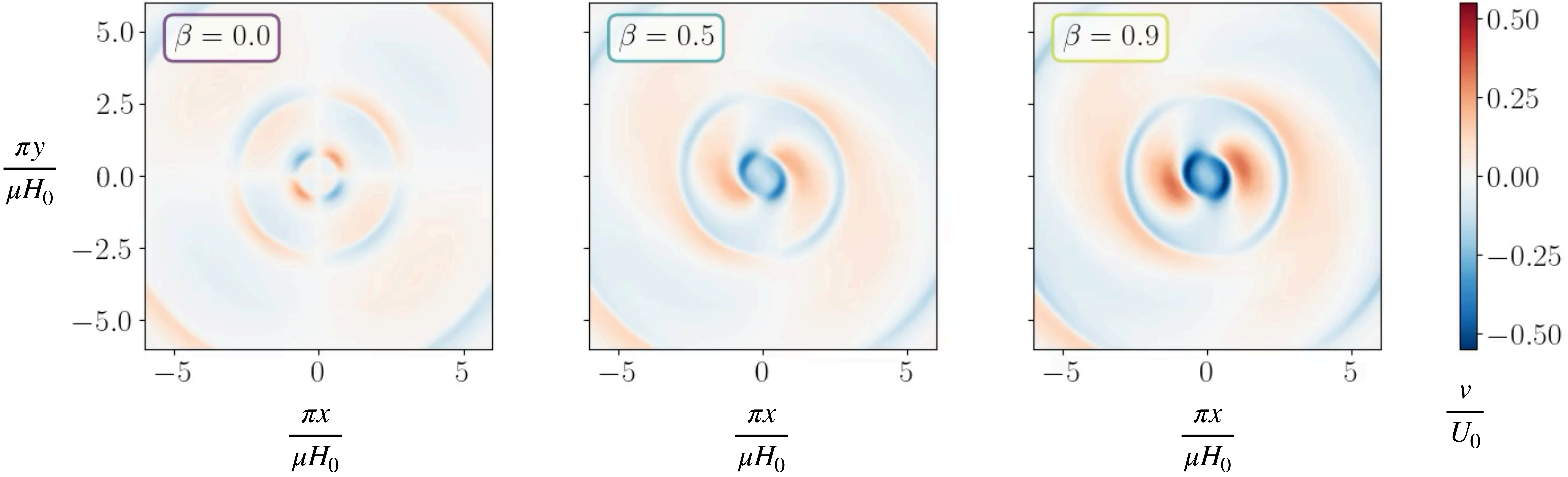

$\delta = 0.3$ and $\epsilon = 0.7$

Energy flux direction

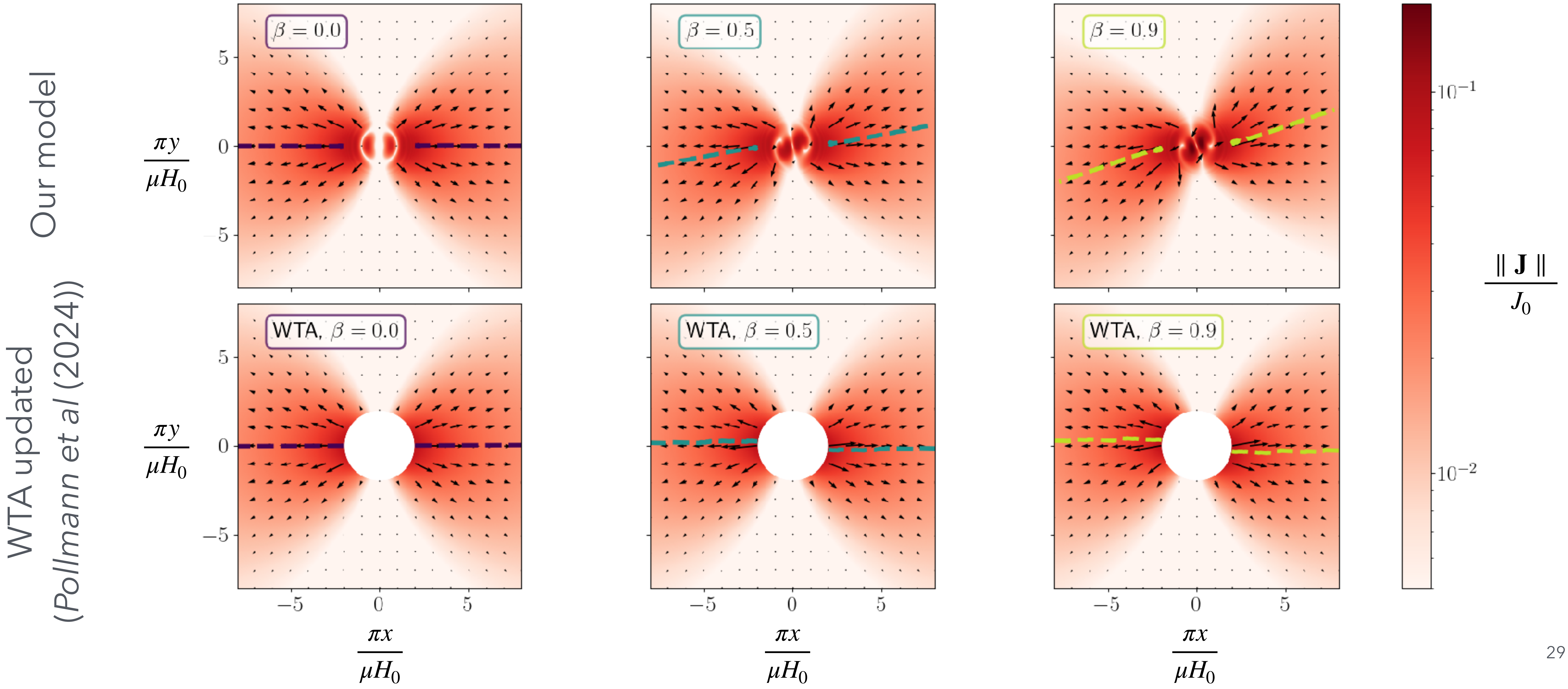

Energy flux direction

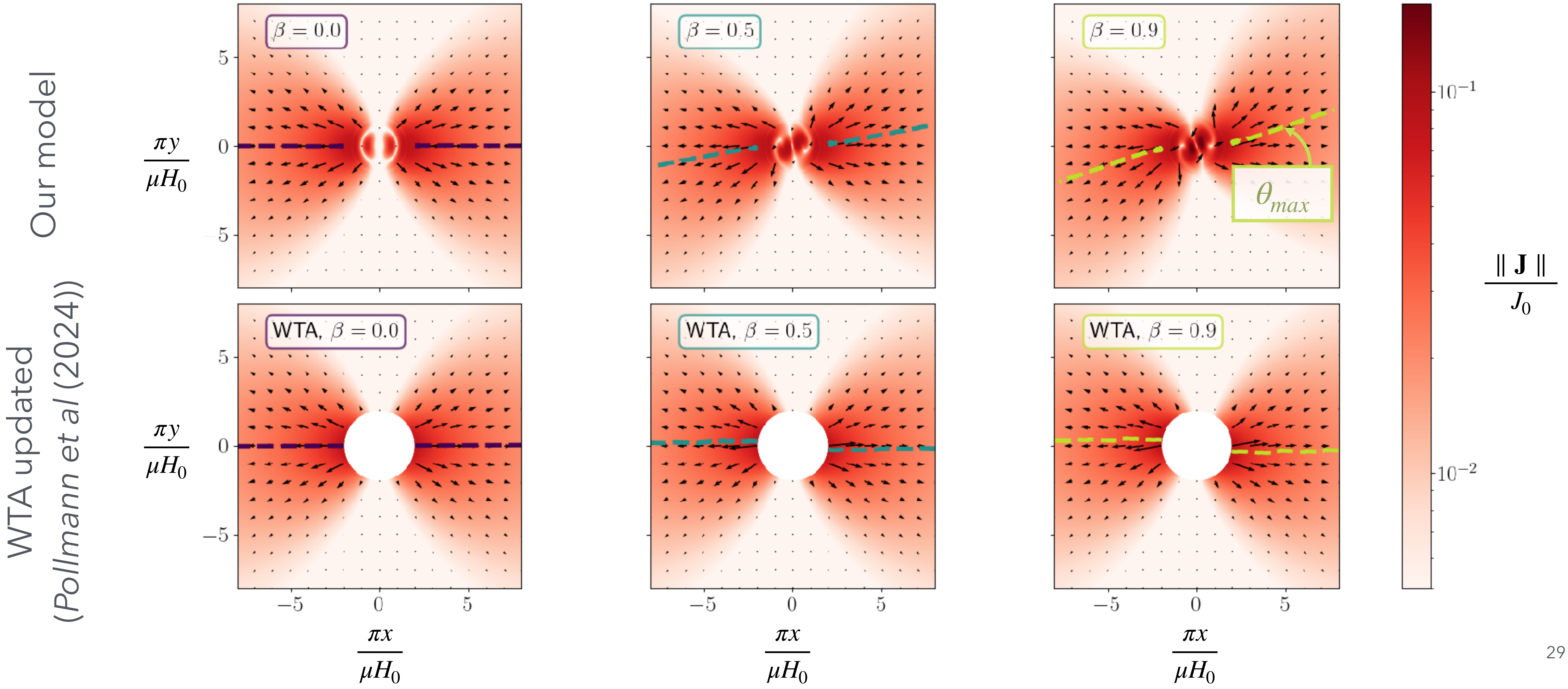

Energy flux direction

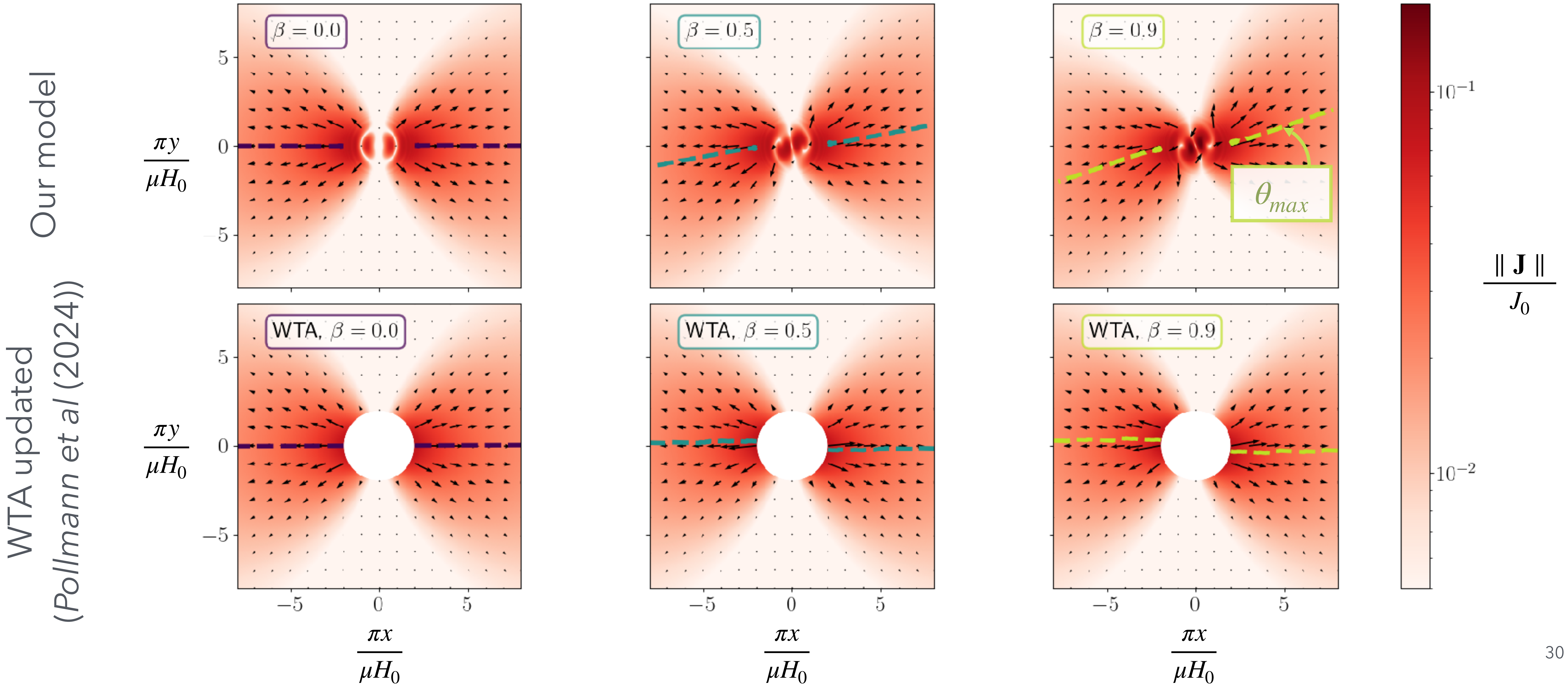

Energy flux direction

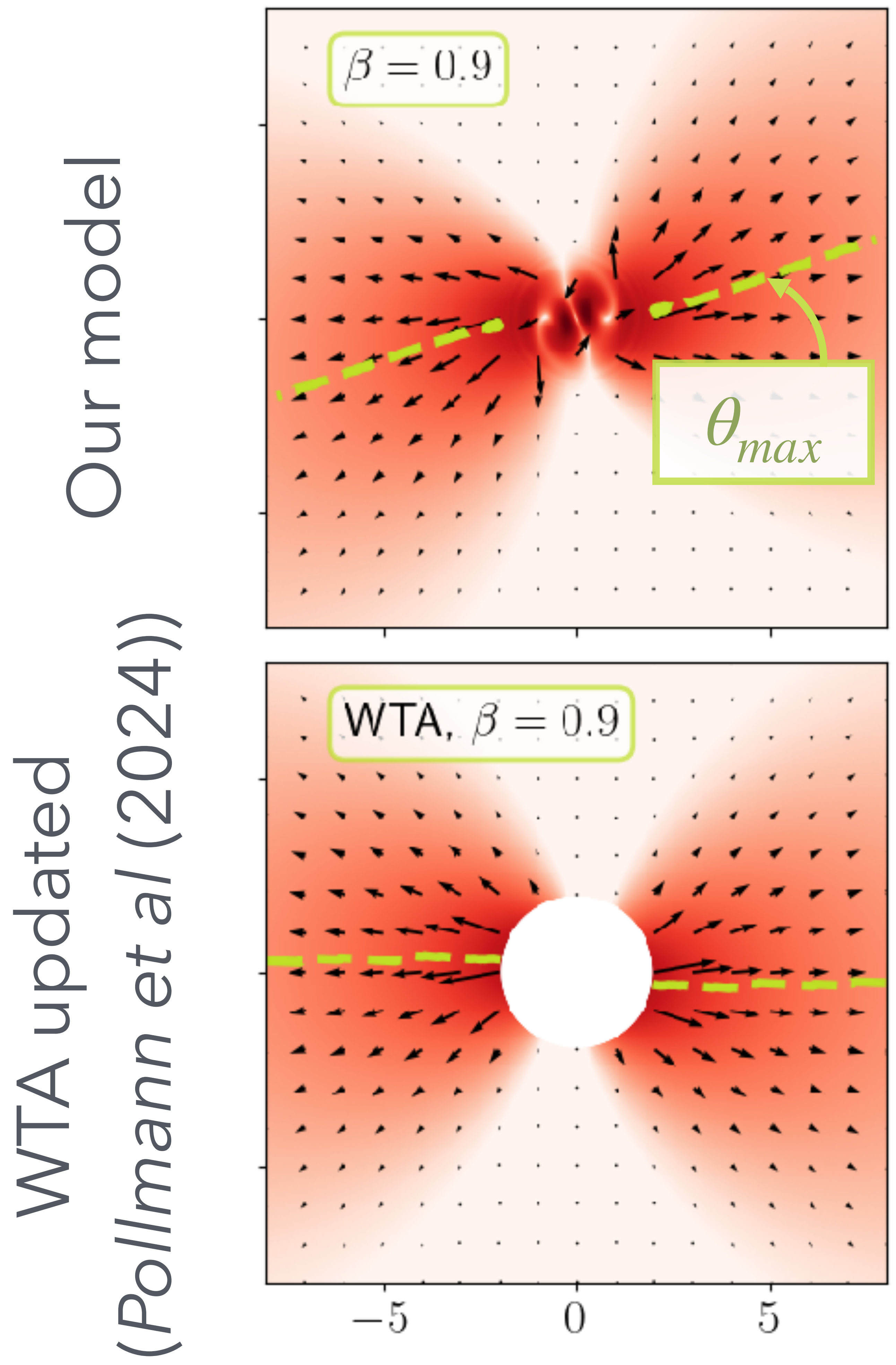

Energy flux direction

Our model

WTA updated (*Pollmann et al* (2024))

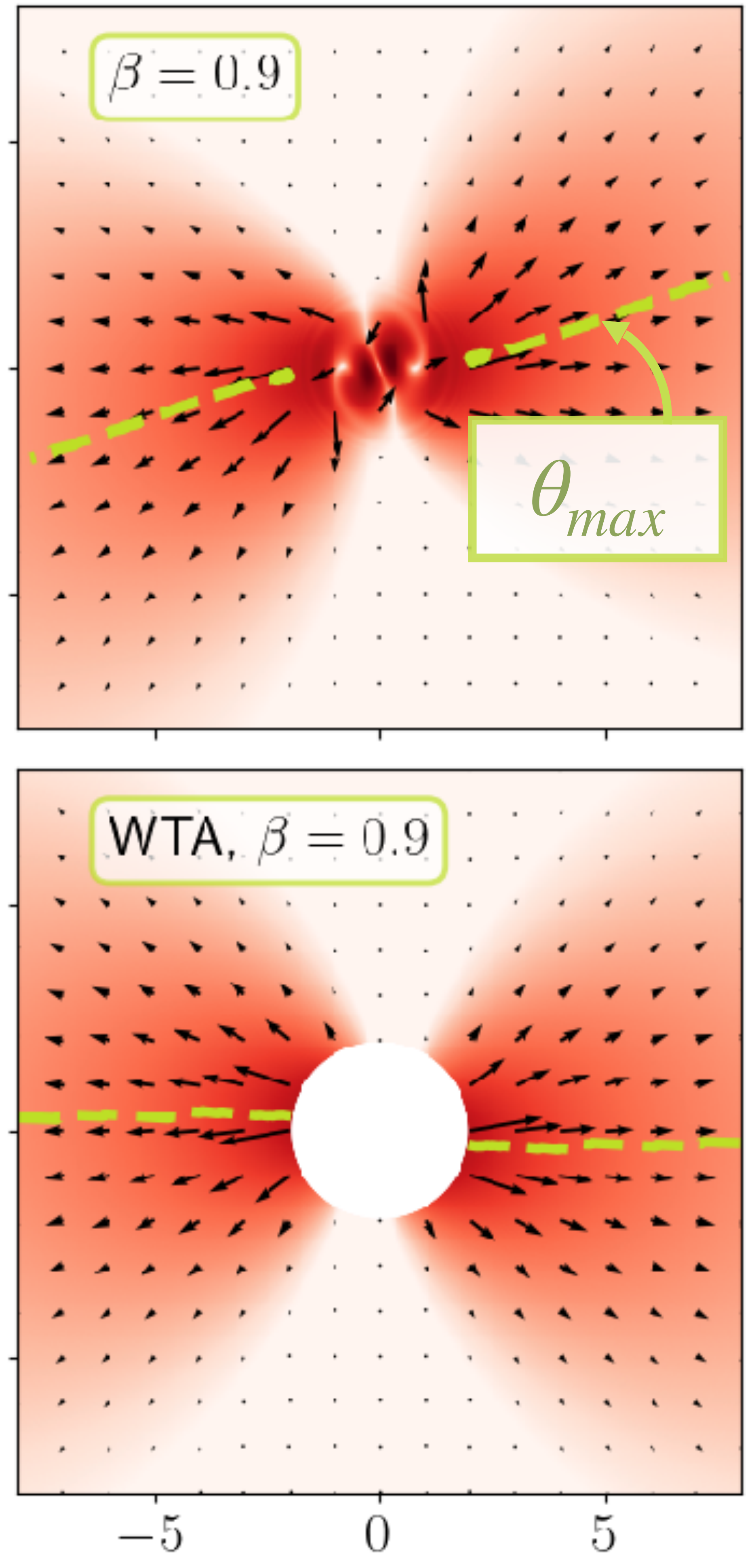

- Flux deviated by positive angles θ_{max} (counterclockwise)
- θ_{max} increases with β and with the distance up to a non-zero value θ_∞

- Direction of maximal radial flux given by $\theta_{max} \sim -C\beta/r$
- No deviation at ∞

Direction of the maximum radial flux at ∞

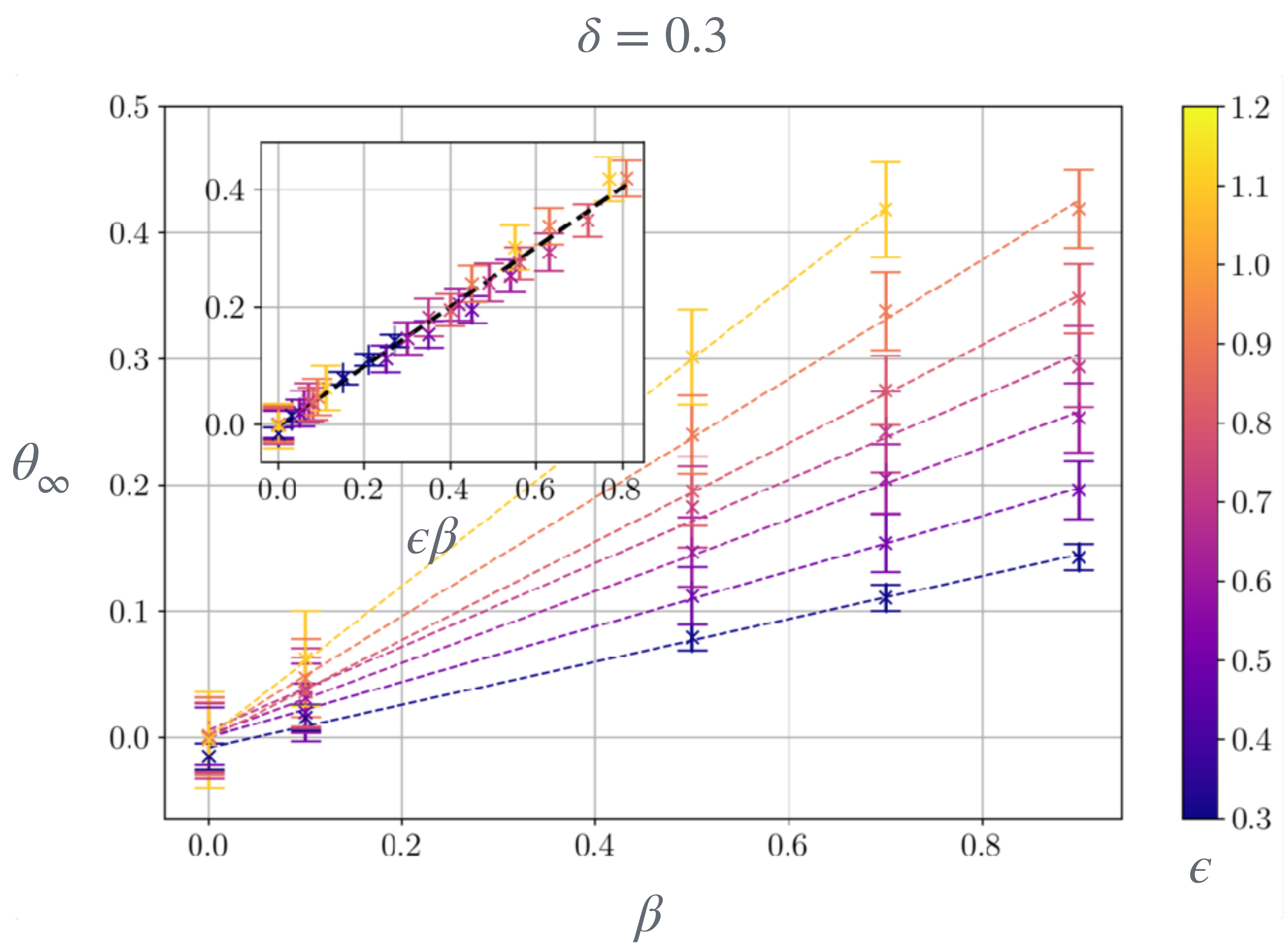

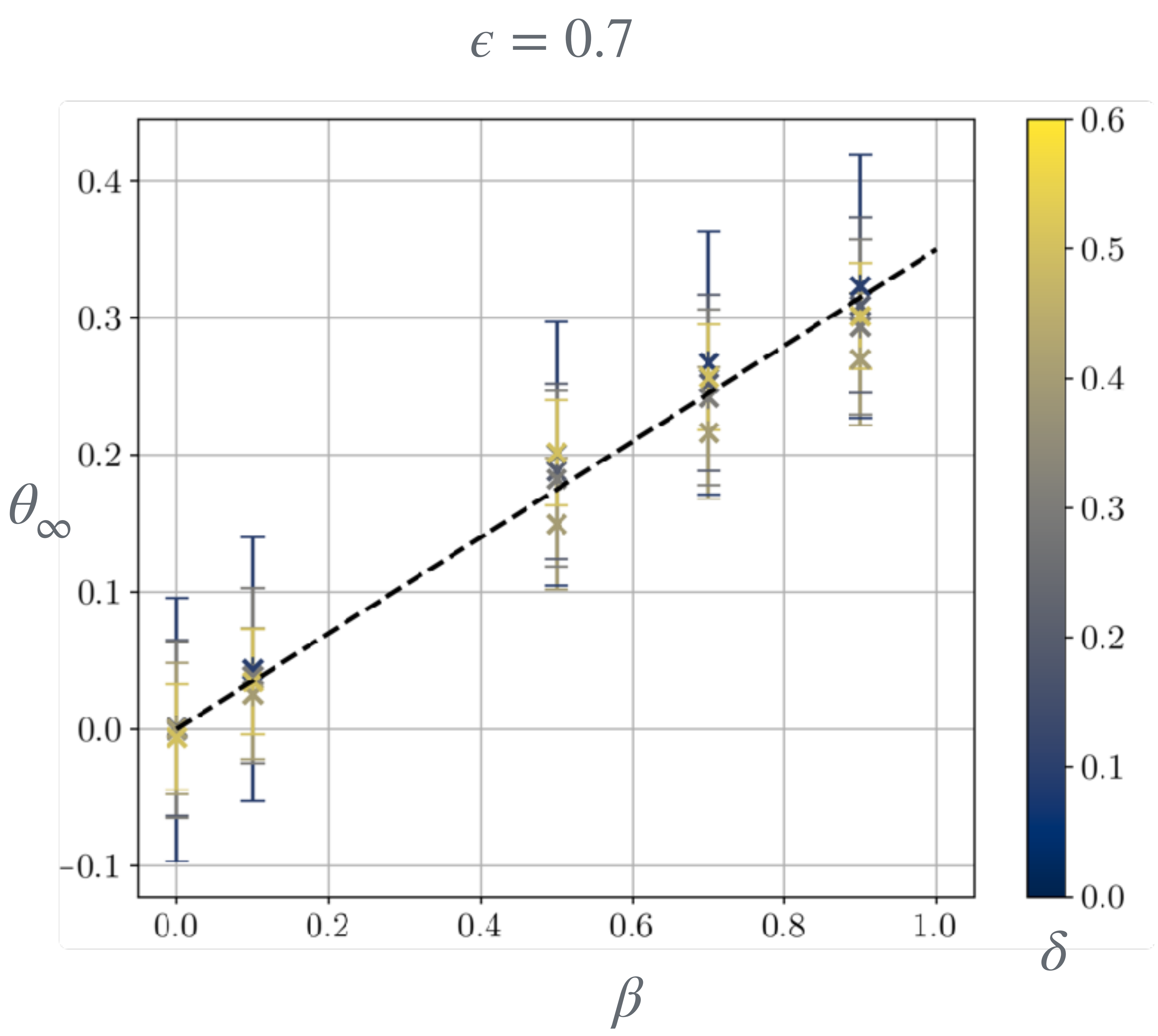

Direction of the maximum radial flux at ∞

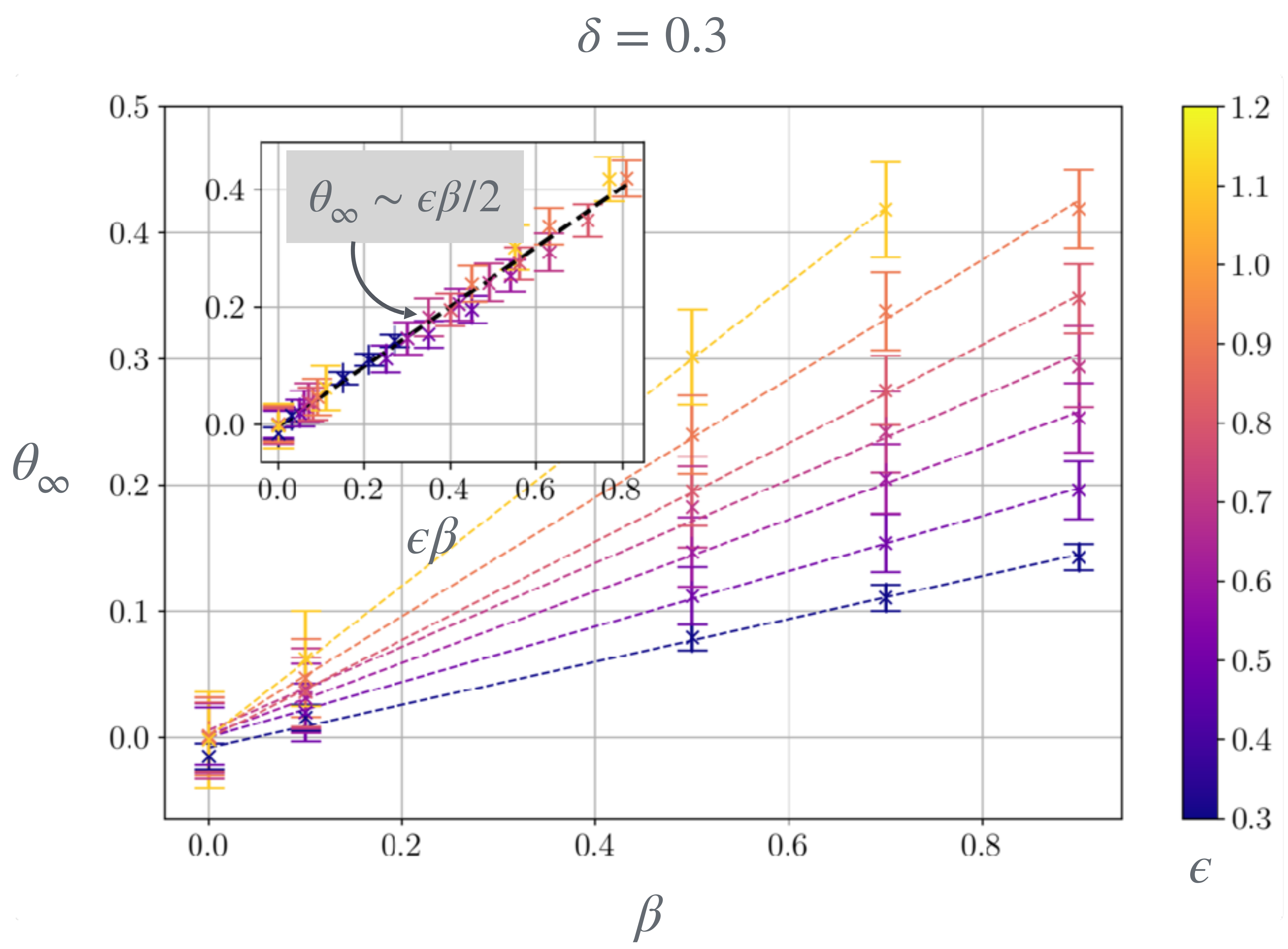

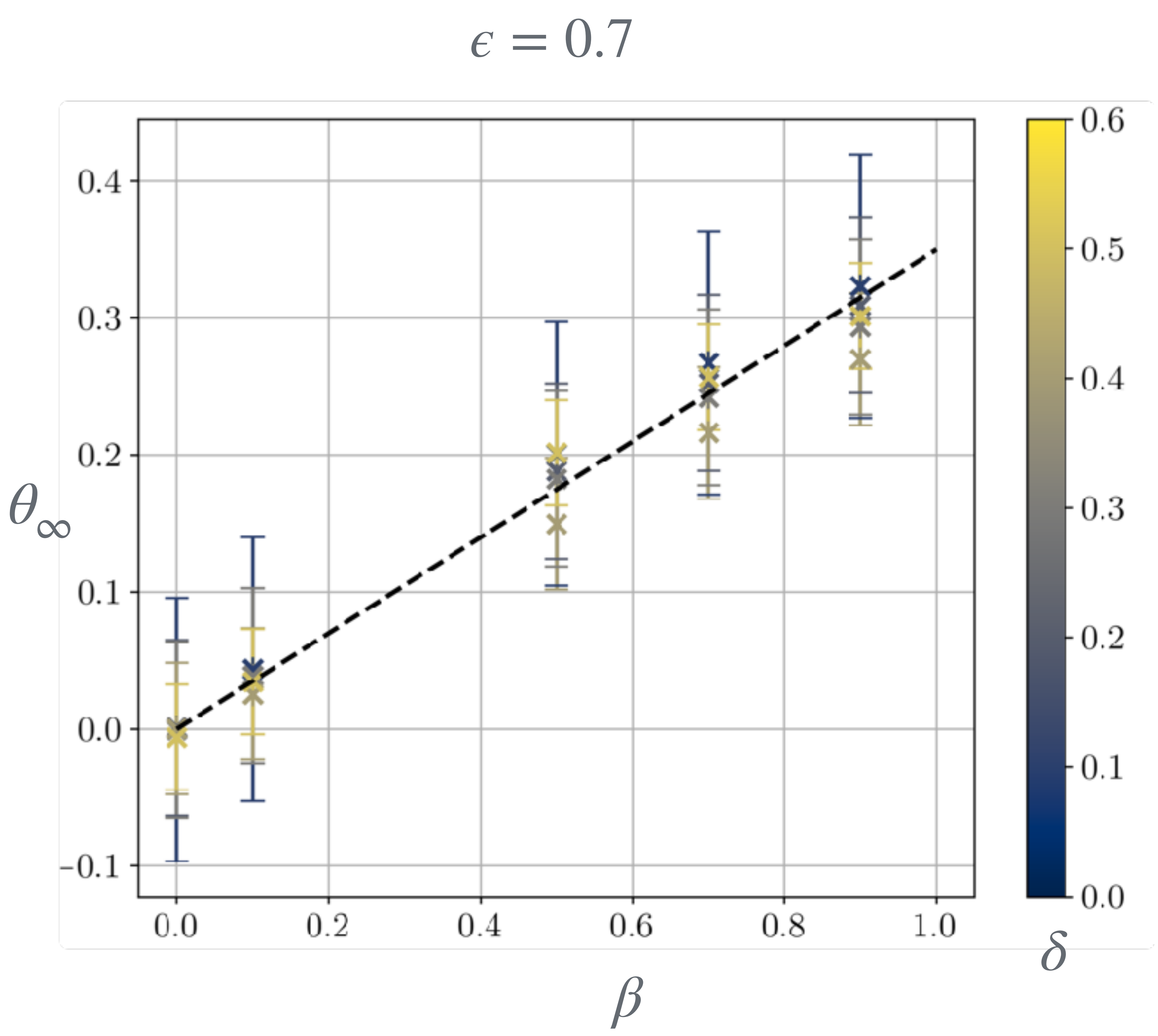

Conclusion

- New 3D semi-analytical method for arbitrary topographies
- Energy conversion rates over-estimated by WTA for a large portion of the parameter set
- Influence of rotation
  - Spiral waves in the velocity fields
  - Flux deviated counterclockwise in the far-field by an angle $\theta_\infty = \frac{\epsilon\beta}{2}$.